DEVELOPMENT OF CELLULOSE-BASED SUPERABSORBENT HYDROGELS FROM COCONUT FIBER

JOYLINE GICHUKI

MASTER OF SCIENCE

(Chemistry)

JOMO KENYATTA UNIVERSITY OF

AGRICULTURE AND TECHNOLOGY

2021

Development of Cellulose-Based Superabsorbent Hydrogels from Coconut Fiber

Joyline Gichuki

A Thesis Submitted in Partial Fulfillment of the Requirements for the Degree of Master of Science in Chemistry of the Jomo Kenyatta University of Agriculture and Technology

2021

DECLARATION

This thesis is my original work and has not been presented for a degree or any other University.

Signature…………………………… Date……………………………….

    Joyline Gichuki

This thesis has been submitted for examination with our approval as supervisors

Signature …………………………………. Date………………………………

    Prof. Patrick Gachoki Kareru, PhD

    JKUAT, Kenya

Signature ………………………………… Date………………………………

    Prof. Anthony Ngure Gachanja, PhD

    JKUAT, Kenya

Signature ………………………………… Date………………………………

    Dr. Catherine Nyambura Ngamau, PhD

    JKUAT, Kenya

DEDICATION

I dedicate this work to my entire family, to my mum Ms. Anne Chepkong'a, Mr. and Mrs. Akong'a, and my cousins Mr. and Mrs. Boniface, Winslet, Leroy, Sharleen, Velma, and Gyan.

ACKNOWLEDGEMENTS

TABLE OF CONTENTS

LIST OF TABLES

LIST OF FIGURES

LIST OF APPENDICES

LIST OF PLATES

ABBREVIATIONS AND ACRONYMS

AGU	Anhydroglucose unit
CA	Citric acid
CMC	Carboxymethyl Cellulose
DS	Degree of Substitution
DSC	Differential Scanning Calorimeter
DVS	Divinylsulfone
EC	Ethyl cellulose
FTIR	Fourier Transform Infrared
HEC	Hydroethylcellulose
HPMC	Hydroxylpropylmethyl Cellulose
IR	Infrared
KCDA	Kenya Coconut Development Authority
MC	Methylcellulose
NaCMC	Sodium carboxymethyl cellulose
NEMA	National Environmental Management Authority
SAH	Superabsorbent Hydrogel
SAP	Superabsorbent Polymer
TGA	Thermogravimetric Analysis
XRD	X-ray Diffractometer

ABSTRACT

The upsurge in the global population leads to a rise in agricultural production to meet the growing food demands which in turn results in increased waste generation. Moreover, the rise in water demand for farming purposes necessitates the need to utilize the little we get effectively and prevent water loss. Thus, the use of superabsorbent hydrogels is a possible solution to water conservation. In this study, cellulose-based hydrogels were synthesized from coconut fiber. This was achieved through extraction of cellulose using soda process, then modified to carboxymethyl cellulose (CMC) by esterification, followed by crosslinking with commercial hydroxyethyl cellulose (HEC) using citric acid in a non-polar solvent. The bulk density, tapped density, and swelling capacity of cellulose, CMC and the CMC-HEC were then evaluated. The functional groups, the thermal properties, and degree of crystallinity of cellulose, carboxymethyl cellulose and the hydrogels were evaluated using a Fourier Transform infrared spectrophotometer (FTIR), Thermal Gravimetric Analyzer (TGA), Differential scanning calorimeter (DSC), and an X-ray diffractometer (XRD). The water-holding capacity of the synthesized hydrogel was evaluated by growing tomatoes in hydrogel-modified soils for 54 days at different water regimes. The tomatoes grown in soils without the hydrogels were used as a control group. The statistical analysis showed that the cellulose yield, bulk density, and swelling capacity was 42.1 ±1.5%, 0.08 ±0.0 g/cm^3 and 8.5 ±0.14 g of water per gram of cellulose respectively. Upon introduction of the carboxymethyl groups, the degree of substitution and the swelling capacity of the resulting carboxymethyl cellulose was found to be 1.82 ±0.12 and 11.3 ±0.28 g of water per gram of CMC respectively. This swelling capacity was further enhanced by chemical crosslinking of CMC with commercial HEC using citric acid as a crosslinking agent. An optimum swelling capacity of 30 g of water per gram of hydrogel was obtained when the hydrogel was prepared using 2.75% of citric acid as the crosslinking agent. Infrared spectra of the hydrogels displayed a carbonyl functional group frequency at 1652 cm^{-1}, which was an indication that the crosslinking reaction between CMC and HEC had occurred. Changes in the degree of crystallinity and thermal stability observed from TGA/DSC thermograms, and X-ray diffractograms were a result of reactions that occurred when cellulose was converted to CMC and the hydrogels. Plants grown in soils containing the hydrogel had a higher plant height, leaf length, average number of leaves, moisture content, and higher root density as compared to the controls at the different water regimes. In conclusion, the cellulose-based superabsorbent polymer obtained from coconut fiber improved the water retention of soil mixed with the hydrogels and thereby resulted in improved plant growth and is recommended.

CHAPTER ONE

INTRODUCTION

1.1 Background of the Study

The rising global population has seen an increase in demand for food crops to meet the demand which in turn leads to an increase in waste production associated with agricultural activities (Hüttermann *et al*., 2009). The development of new biodegradable materials from such agricultural residues for applications in food packaging, agriculture, hygiene products, medicine, and other areas has attracted attention in research and manufacturing. A biodegradable polymer is a material that can easily decompose which is an important factor in limiting environmental contamination and problems associated with waste disposal of synthetic polymers. Biodegradability, affordability, and greater availability of natural polymers make them advantageous over their synthetic counterparts (Zhou *et al*., 2007). One such application is in the development of superabsorbent polymers which can retain water for longer periods and thus can find application in agriculture as hydrogels (Cannazza *et al*., 2014).

These polymers have been reported to reduce the percolation rates that necessitate water uptake by plants and in response to this, cellulose-based superabsorbent polymers have become the focus of research. Commercially available superabsorbent polymers (SAPs) such as sodium polyacrylates are known to be successful in their absorbance. However, they are non-biodegradable hence the need to develop environmentally friendly biodegradable polymers (Madeleine and Ruffinegngo, 2013). Superabsorbent hydrogels (SAHs) have a desirable characteristic in that they can be able to absorb and retain large quantities of liquids, which can be evaluated in terms of mass difference before and after liquid absorption (Mcgraw *et al*., 2004).

A hydrogel is a composition of polymer networks that form a three-dimension structure that can swell in solution and retain water or fluids while maintaining their structure (Zohuriaan-mehr and Kabiri, 2008). They can either be synthetic or natural depending on

1

their source material but both originate from chemical crosslinking reactions of either synthetic polymers such as polyacrylic acid or natural-forming polysaccharides such as gelatins, cellulose derivatives, and proteins respectively (del Valle *et al*., 2017). Hydrogels are a class of gels obtained by crosslinking hydrophilic polymers that are insoluble in water but can absorb liquids through a swelling process. Considering these features, SAHs have been utilized in areas such as drug delivery in pharmaceuticals, catalysis, bio-sensing, diapers, hygiene products, and in agriculture as smart delivery devices and water reservoirs (Kiatkamjornwong, 2007).

To date, a change in climatic conditions and unfavorable weather patterns have necessitated the need to shift to new farming methods such as the application of superabsorbent polymers as water and mineral reservoirs. The amount of water in the soil determines plant growth and health, as excess water causes root rot and limited water leads to low nutrient supply. Large pore soil sizes hinder water retention potential thus leaching of nutrients and water for growth is higher (Bhardwaj *et al*., 2007). In arid and semi-arid areas, rapid fertilizer and water infiltration rates have led to low crop production due to the loss of fundamental needs for plant growth. These can be remediated by the application of cellulose-based hydrogels which are biodegradable and environmentally friendly as compared to their synthetic counterparts that are commercially available (Sannino *et al*., 2009).

1.2 Statement of the Problem

The rise in the global population translates to increased demand for food, water, and other resources. Water scarcity and unpredictable climatic changes have become prevalent. In the case of commercial irrigation water loss to the ground aquifer has led to economic losses because of shallow layers of soil. Most regions experience short rains insufficient for good crop harvest. However, the use of synthetic polymers for water retention has not been made possible due to slow biodegradability. One of the most common scenes of the Kenyan Coastline is the waste accumulation from coconut shells and husks produced from the consumption of tender coconut water or other coconut products. Generally, coconut

shell and husk wastes are used as fuel in some cases or allowed to decay naturally or are burnt. The husk contains cellulose which can be used to make useful products such as hydrogels. These hydrogels have water retention capacities and are from natural polymers, which are environmentally friendly, and biodegradable. Hence, this project investigated the use of coconut fiber that may be used to synthesize hydrogels for use in various applications in health and agriculture, and are biodegradable.

1.3 Justification

Superabsorbent polymers have been employed to curb the effects of degraded soils which has a direct impact on demand for food and energy production. Water-soluble polymers have been in use in ancient times as they are effective soil conditioners. The polymers and soil contain hydrophilic groups that bind to water molecules hence maintain the soil moisture for long period. Polymers have more enhanced hydrophilicity, which promotes water retention of the soil and improves the drought resistance of the plant. Thus, the value addition of agricultural wastes rich in cellulose is ideal due to their availability and ability to degrade easily. The coconut fiber biomass can be utilized in the production of biodegradable superabsorbent polymers. The natural polymer hydrogels do not have negative effects on the soil as they enhance water retention thereby influencing plant growth.

1.4 Hypothesis

Cellulose-based superabsorbent hydrogels synthesized from coconut fibers do not have adequate water retention capacity for application in crop production.

1.5 Objectives

1.5.1 General Objective

To develop cellulose-based superabsorbent hydrogels from coconut fibers for optimal water absorbance in crop production.

1.5.2 Specific Objectives

i. To extract cellulose from coconut fibers and determine the moisture, bulk density, tapped density, and swelling capacity.

ii. To synthesize carboxymethyl cellulose (CMC) and determine the degree of substitution, bulk density, tapped density, and swelling capacity.

iii. To synthesize hydrogels using commercial hydroxyethyl cellulose - carboxymethyl cellulose (HEC-CMC) through chemical crosslinking using citric acid.

iv. To characterize cellulose, CMC, and HEC-CMC hydrogel using Fourier Transform Infrared (FT-IR), Thermogravimetric analysis (TGA), degree of crystallinity using Differential scanning calorimetry (DSC) and X-ray diffraction (XRD).

v. To determine the swelling capacity, degradation, and effects of different ratios of HEC-CMC hydrogels and CMC on the growth of tomatoes in a greenhouse.

1.6 Significance of the Study

The study seeks to add value to coconut fiber in the extraction of cellulose, which through surface modification can be use as raw material for the synthesis of hydrogels.

1.7 Limitations of the Study

The study only focuses on the use of coconut (coir) fiber. This study did not include a control sample for swelling studies for the extracted cellulose, CMC and synthesized CMC-HEC hydrogels. The application studies were carried out in a greenhouse for a single season for 54 days.

CHAPTER TWO
LITERATURE REVIEW

2.1 Cellulose Biomass from Agriculture Waste

According to Khalil *et al.* (2006) cellulose biomass produced in the world in a year is estimated to be 2×10^{11} tons over the synthetic polymer production which is 1.5×10^{8} tons hence an abundant polymer. Cellulosic fibers are a major component of the plant materials hence they can be utilized for the production of cellulose (Shogren *et al.*, 2011). Cellulose is a profuse polysaccharide that has attracted much attention in both academic and industrial fields, due to its handiness and low cost of production (Hubbe *et al.*, 2007). The utilization of lignocellulose biomass in the development of value-added products is an interesting area of research for industrial productions of biocompatible materials (Poletto *et al.*, 2014). Murigi *et al.*, (2014) quantified the amount of cellulose in some selected biomass such as banana peels (18.35%) and rice straws (19.62%), which seem under-utilized. Several studies have been carried out on the utilization of cellulose-rich agricultural wastes. For instance, fiber sludge waste is an essential material for bacterial cellulose production through the fermentation process (Cavka *et al.*, 2013). Moreover, technological advancements have also seen cellulose being utilized in the development of biometric sensors that are characterized by low power consumption coupled with increased bending displacement (Kim and Yun, 2006).

The ability of cellulose to decompose and degrade easily has also led to the development of biodegradable products that are viable and ecologically friendly thus, adherence to the principles of Green Chemistry Technology. One such application is in the development of hydrogels in which surface modification of hydroxyl groups present in cellulosic polymers aid in water absorption and retention, as the water molecules can form hydrogen bonds with the polymer network. Liquid uptake by fibrous structures is influenced by the porosity of the material, whereas the rate of liquid diffusion is affected by the capillary shape and structure permeability. Hence further modification of the cellulose networks leads to the formation of more hydrophilic groups thus increased water absorption.

5

2.2 Coconut Shells and Husks

Heaps of wasted coconut shells and husks are a common sight across the Coastal region thus an environmental hazard. According to Lomemeli-Ramirez and colleagues coconut, green husk pollution in Brazil has been on the rise due to the high consumption of tender coconut water that leads to more waste production that takes about eight to ten years to degrade (Lomelí-Ramírez *et al*., 2018). Currently, the predominant use of coconut husks is in direct combustion to make charcoal; otherwise, husks are simply thrown away. In this case, the coconut husk is transformed into a value-added energy source that can replace wood and on the other hand utilize the amount of waste biomass produced. Currently, there is no documented data on the quantity of coconut waste in Kenya.

Coconut fiber is also referred to as coir. The white fiber spun to the yarn is used in making rope and fishing nets as it is strong and resistant to saltwater. Brown fiber is majorly used in making mattresses, sacking, brushes, composites, and in agriculture (Ferreira *et al*., 2006; Sen and Reddy, 2011). The automobile industry in Europe uses brown fiber bonded with rubber latex for car upholstery. The ability to resist sunlight, absorb water, durability, and biodegradability makes it suitable for use in the geotextile industry for portable seed or flower germination (Beena, 2013). The building technology textiles have utilized the coir wood to manufacture articles such as false ceiling boards, roofs, furniture, windows, and wall panels (Verma *et al*., 2013). This coir wood is made from coir fiber in presence of phenol-formaldehyde resin and converted to board.

According to Khalil *et al*. (2006) the brown fiber is rich in cellulose with a yield of 44.2%, whereas the white fibers are 35.1%. The brown coconut fibers as shown in Plate 2.2 (d), obtained through the dehusking process, involves the separation of the coconut fruit and the husk. This is achieved by soaking in water for a given period to soften the husk. The husk contains the coco peat and fiber, during processing coco peat is removed as dust (Ogali *et al*., 2011). Plate 2.1 (a) shows the coconut tree of which there are several varieties of the coconut, which can be tall or dwarf variety. Plate 2.1 (b) shows the mature coconut fruit harvested from the palm, which is composed of three layers; the endocarp, mesocarp,

6

and exocarp. The mesocarp and exocarp make up the coir, which also contains coco peat. The endocarp forms the coconut stone as shown in Plate 2.2 (c), which is the fruit that contains the fleshy part and the coconut water (KCDA, 2013).
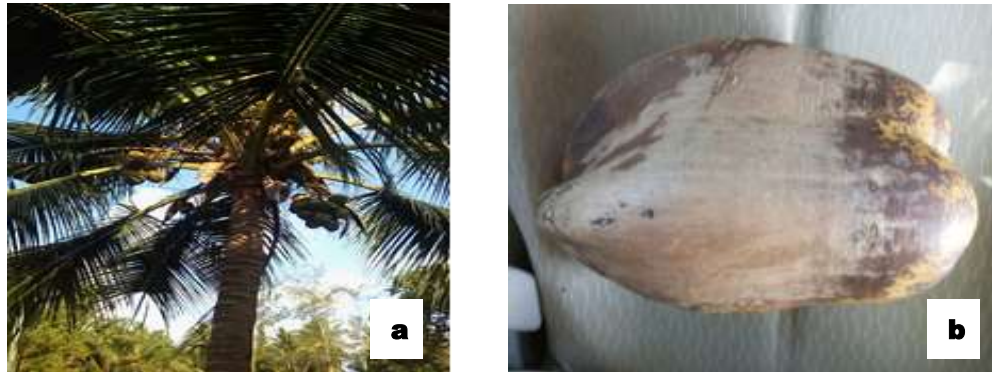
Plate 2.1: Coconut tree (a) and coconut fruit (b) (Author, 2018)

Plate 2.2: Dehusked coconut fruit (c) and coconut fiber (d) (Author, 2018)

2.3 Coconut Fiber Properties

Several researchers have tested the physical and mechanical properties of coir for instance, Nazeer evaluated the density and tensile strength of the coir and established that modifying the length of the fibers alters the mechanical property of the fibres. Increasing the length of the fiber increases the mechanical property (Nazeer, 2014). Waifielate and Abiola, (2008) carried out a test on the mechanical properties of the inner and outer coir and found out that the inner coir had higher mechanical strength thus, can withstand the

high stretching. According to Ferdus, (2014) the physical properties are as shown in Table 2.1.

Table 2.1: Physical properties of coconut fiber (Ferdus, 2014)

Physical property	Quantity /(Units)
Length	0.15-0.2 m
Density	1400 Kg/m^3
Tenacity	10.0 g/Tex
Breaking elongation	30%
Diameter	0.1-0.5mm
Modulus	0.19 Pa
Swelling in water	5%
Moisture at 65% RH	10.50%

Typically a coconut fruit comprises 40% coconut husk that is made up of 30% fiber and dust volume taking up the rest (Tooy *et al*., 2014). The chemical composition of coconut fiber consists of cellulose, lignin, pyroligneous acid, gas, charcoal, tar, and tannin, with high lignin and cellulose content. According to Ferdus (2014), the chemical composition is as shown in Table 2.2.

Table **2.2: Chemical composition of coconut fiber (Ferdus, 2014)**

Compound	Percentage composition (%)
Lignin	45.84
Cellulose	43.44
Hemicellulose	0.25
Pectin and related compounds	3.00
Water-soluble	5.25
Ash	2.22

2.3.1 Cellulose

Cellulose is one of the most abundant and biodegradable polymers that has a promising future in the production of various materials used for a variety of applications. In the recent history of cellulose-based materials have found use in the absorption of water and other aqueous fluids and these materials include paper towels, tissue papers, diapers, and feminine hygiene products (Beuther *et al*., 2010; Gigac and Fišerová, 2008). Demetri and colleagues carried out studies on the use of cellulose-based superabsorbent polymers (SAPs) in optimizing water use in agriculture and it proved to be efficient in providing good absorption capabilities that suited its application for that purpose unlike the acrylate-based SAPs (Demitri *et al*., 2008). The introduction of acrylate-based superabsorbent polymers products led to a decline in the use of cellulose over time as they have high absorption rates (Yang *et al*., 2021).

However, cellulose is currently receiving much attention because it is a renewable resource, biodegradable and has a low cost of availability from a wide range of materials such as agricultural waste biomass. These cellulosic sources include plant wastes such as rice straw, maize cobs, coconut fiber, coffee husk, sugarcane bagasse, cotton and groundnut husks, and fibrous remnants of forages such as grass, among others (UNEP, 2009). On a global scale, the quantity of cellulosic wastes available varies with the predominantly agricultural and industrial crops produced in a given society. Although agricultural biomass wastes have found significant applications as sources of heat and electric energy (Ahorsu *et al*., 2018; Gupta and Prakash, 2015), enzymes production (Martins *et al*., 2011), value addition can be achieved through utilization of these wastes for the production of cellulose derivatives that have significant economic value, renewable and environmentally friendly. Cellulose extraction from the plant biomass can be achieved using several extraction techniques which include solvent extraction, distillation method, pressing and sublimation based on different principles. The extraction efficiency is determined by the solvent choice, raw material particle size, the ratio of solvent to the

material and temperature hence these factors should be considered in before choosing a extraction method(Zhang *et al*., 2018).

Cellulose is a linear homopolymer of D glucopyranose units linked together by β-(1, 4)-glycosidic bonds formed between C-1 and C-4 of adjacent glucose units as in Figure 2.1.
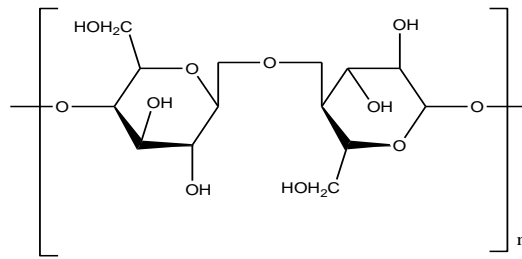
Figure 2.1: Structure of cellulose

Cellulose occurs in the form of long, slender chains, a polymer of glucopyranose units. Hydroxyl groups in each unit contribute to the formation of various kinds of inter and intra-molecular hydrogen bonds (Sethi *et al*., 2019). The intermolecular H-bonding is between each glucopyranose unit and the intramolecular bonding is between the -OH group of fiber and -OH group of the matrix. The formation of inter and intra-molecular hydrogen bonds in the cellulose has a strong influence on the physical properties of cellulose, solubility, hydroxyl reactivity, and crystallinity also has an impact on the mechanical properties of cellulose-based composites (Shen and Gnanakaran, 2009).

The presence of hydroxyl groups throughout the cellulose structure enables its chemical modification, which improves its properties such as solubility and water uptake. The amorphous regions and spaces occupied by the non-crystalline hemicellulose have been observed to swell and retain water (Kocherbitov *et al.*, 2008) while the outer surface that is crystalline interacts with water but these crystalline domains do not absorb any water molecules. Vitta *et al*. (1989) carried out some studies and concluded that treatment of cellulose with zinc chloride solution disrupted the crystallinity to an extent and this resulted in a high amount of water absorption capacity.

2.3.2 Hemicellulose

Hemicellulose is a branched polymer of pentose and hexose sugars, found in the plant cell wall. Generally, in almost all plant cell walls, hemicellulose is present along with cellulose, and the swelling of cellulose fibers is attributed to the proportion of hemicellulose (Berglund *et al*., 2020). Cellulose is crystalline, strong, and resistant to hydrolysis. On the other hand, hemicellulose has a random amorphous structure with little strength. The irregular structure, side groups present, and branching enhance the swelling of hemicellulose. Despite being highly hydrophilic due to the acid groups, hemicellulose extraction from kraft fibers with alkaline solutions was found to increase the water absorptivity of the fibers. This is due to the conversion of other ionic forms of remaining hemicellulose to the sodium form that enhances swelling (Strunk, 2012).

Unlike cellulose, hemicellulose is a heteropolymer constituted by 5-carbon sugars such as arabinose and xylose, and 6-carbon sugars including galactose and mannose, which are 500-3,000 sugar units as opposed to 7,000-15,000 glucose molecules per polymer seen in cellulose. Pentose and hexose sugars mostly known as cellulose are released from the hemicellulose structure utilizing some chemical or enzymatic pretreatment (Mussatto and Roberto, 2004).

2.3.3 Lignin

Lignin is present in almost all vascular plants between the cells and the cell walls. The firm and crunchy nature of vegetables are due to lignin which makes up the food fiber. Lignin is embedded in the cellulose and hemicellulose structure, which helps to strengthen the cell walls' rigidity. It represents thirty percent of lignocellulose biomass; however, it is under-utilized though researchers have carried several studies. Amen-Chen *et al*., (2001) found out that lignin can prevent the penetration of chemicals that can destroy the cell wall as well as offering protection to the plant against microbial attack.

Lignin has been extracted as a by-product in the cellulose extraction process with sodium hydroxide while boiling under pressure from selected biomass or wood pulp. The by-product accumulates in form of black liquor. However, its composition, molecular weight and amount present differ from plant to plant (Azadfar *et al*., 2015). The precise chemical structure of lignin remains unknown, because of its complex polymeric nature and due to the degree of random coupling involved in the arrangement of the macromolecule.

2.4 Synthesis of Hydrogels

Hydrogel's development history date back to 1950 when the first absorbent polymer was synthesized (Zohuriaan-mehr and Kabiri, 2008). Hydrogels consist of a polymer network chain-linked either through chemical or physical processes forming a three-dimensional network structure, which is insoluble in water. Chemical or physical crosslinking is required to avoid the dissolution of the hydrophilic polymer into an aqueous phase. According to Hashem and colleagues, polymer crosslink can be formed through covalent, electrostatic, hydrophobic bonds, or dipole-dipole interactions (Hashem *et al*., 2013). Polymer hydrogels are swiftly developing a set of resources providing a solution in many areas such as medical, packaging, and agriculture. Traditional biodegradable hydrogels have been replaced by acrylic-based and synthetic hydrogels which can absorb water up to three hundred times their weight but have a major drawback in that they are not biodegradable and have been associated with environmental degradation (Hubbe *et al*., 2007).

Negative environmental impacts of synthetic polyelectrolytes such as poly sodium acrylate have led to the development of natural polymers, and hydrogels in this case have attracted more researches due to their ability to degrade easily (Ahmed, 2015). Synthetic hydrogels are prepared using acrylic acid and acrylamide monomers coupled with a suitable crosslinking agent. The degree of crosslinking is an important parameter that influences the quality and properties of the hydrogel such as degradation, mechanical properties, and the degree of swelling (Sannino *et al*., 2003). Therefore, this makes it possible to synthesize hydrogels design for specific use depending on the crosslinking

agent. Demitri *et al*. (2008) prepared a biodegradable cellulose-based hydrogel from cellulose derivatives hence cellulose can be regarded as a precursor in the synthesis of hydrogels. Hydrogels can maintain their structure under different environmental conditions depending on the nature of the linking bond (Saini, 2017). The development of fluorescent hydrogels has also been on the rise due to their biocompatibility, flexibility and luminescent properties (Su *et al*., 2020). According to Sikdar *et al*. (2021) injectable hydrogels recently have sparked the interest of researchers due to their numerous advantages, including non-invasive administration, high permeability, configurable mechanical properties, cytocompatibility, adjustable degradability, and injectability. These hydrogels can also be utilized for tissue regeneration or carriers of therapeutic agents such as drugs, proteins, and cells.

2.5 Classification of Hydrogels

Hydrogels can be either natural or synthetic, but this classification depends on the origin. Natural forming hydrogels have the characteristic of being biocompatible and biodegradable, though they are highly fragile due to their structure (Sethi *et al*., 2019). On the other hand, synthetic hydrogels are stable at high temperatures thus do not degrade easily (Ahmed, 2015). Hydrogels can also be classified according to their crosslinking method, either physical or chemical. Physical crosslinking has temporary and weak bonds as they result from the entanglement of the polymer species. Chen and colleagues synthesized starch hydrogels through baking with gamma radiation and further did agricultural application analysis (Chen *et al*., 2004). Chemical crosslinking results in permanent bonds that are strong. According to Kaith *et al*. (2010) hydrogels can be classified according to their sensitivity and response to their environment. Hydrogels can respond to changes in pH, temperature, light, and electric field. Akar and Altınıs (2012) developed reversible pH-dependent hydrogels by crosslinking sodium-carboxymethyl cellulose (NaCMC) with fumaric acid, which can be exploited in bioengineering applications.

2.6 Cellulose Derivatives

Simončič and Rozman, (2007) have suggested that cellulose and cellulose derivatives are environmentally friendly since they can degrade producing specific enzymes through bacteria and fungi that are present in the air, water, and soil. Plant cellulose requires purification and chemical modification which involves either esterification or etherification of hydroxyl groups to produce cellulose derivatives that are easily processed and utilized for industrial applications.

Cellulose ethers are high molecular weight compounds that are produced by substituting the hydrogen atoms of hydroxyl groups with alkyl or substituted alkyl groups. The stability against biodegradation, heat, hydrolysis, oxidation, and solubility are useful properties of cellulose ethers derived by molecular weights, chemical structure and distribution of the substituent groups, degree of substitution, and molar substitution. These derivatives include methylcellulose (MC), hydroxylpropylmethyl cellulose (HPMC), ethyl cellulose (EC), hydroxyethyl cellulose (HEC), and sodium carboxymethyl cellulose (NaCMC) (Strunk, 2012). In order to achieve improved absorbance of these derivatives, it is possible to crosslink link two or more polymers using suitable crosslinking agents though it is not recommended to crosslink monomer derivatives. A representation of this cellulose derivative structure is shown in Figure 2.2.
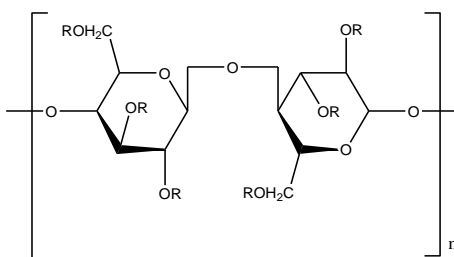
Figure 2.2: Cellulose ether derivatives structure

Where; R group =H or MC -CH_3, EC -CH_2CH_3, HEC -CH_2CH_2OH, CMCNa-CH_2COONa, HPMC -$CH_2CH(OH)CH_3$

Cellulose esters are categorized into organic and inorganic groups. Various types of organic cellulose esters are used in commercial products or pharmaceutical investigations such as cellulose acetate, cellulose acetate phthalate, cellulose acetate butyrate, cellulose acetate trimelitate, hydroxylpropylmethyl cellulose phthalate (HPMCP). Cellulose esters are widely used in pharmaceutical controlled release preparations such as osmotic and enteric-coated drug delivery systems. This is due to their ability to form good film and water-insoluble nature (Shokri and Adibkia, 2013).

2.7 Cellulose Based Hydrogels

The abundant hydroxyl groups present in cellulose enhances hydrogel preparation. These hydrogels are synthesized from cellulose by crosslinking the various derivatives of cellulose, such as carboxymethyl cellulose, hydroxyethylcellulose, ethylcellulose, and methylcellulose with a suitable crosslinking reagent. Sannino *et al*. (2003) carried out studies on cellulose-based superabsorbent polymer for imbibing body fluids in the treatment of oedemas. The hydrogels prepared using CMC and HEC cross-linked with divinyl sulphone were found to be sensitive to ionic strength and pH of the external solution (Astrini *et al*., 2012). To develop cellulose-based hydrogel single or more monomers need to be combined through the functional groups present using a bond. These functional groups have binding sites that allow bond formation and breaking (Ahmed, 2015). This can be achieved through a chemical or physical process and the use of inorganic solvent is ideal since it inhibits swelling.

2.8 Crosslinking of Cellulose Derivatives

The choice of crosslinking technique depends on the nature of the polymer and the cellulose derivatives used. It can occur through polymerization of monomers by condensation or covalent bonding between polymeric chains via irradiation, sulphur vulcanization, or chemical reactions by adding different chemicals under heat or pressure. Common cellulose cross-linkers include epichlorhydrin, aldehydes, aldehydes-based reagents, urea derivatives, carbodiimides, and multifunctional carboxylic acids (Saini,

15

2017). Biocompatibility of the hydrogel is an important aspect to consider, hence crosslinker such as aldehydes known to be toxic thus not recommended.

Demitri *et al*. (2008) carried out studies on novel superabsorbent cellulose-based hydrogels crosslinked with citric acid and found out that they displayed good swelling properties, enhanced by their biodegradability and absolute safety of the production process. On the other hand, Astrini and colleagues reported that crosslinking of NaCMC and HEC with divinyl sulfone (DVS) resulted in high swelling capacity and retention capability of the hydrogel under influence of temperature, time, and the composition ratio of the derivatives (Astrini *et al*., 2012). The resultant polymer crosslink has better properties as compared to individual cellulose derivatives since they become mechanically stronger, resistant to heat, wear, and attack by solvents (Maitra and Shukla, 2014).

2.9 Applications of Hydrogels

2.9.1 Wound Dressing

The wound healing process entails some stages such as inflammation, autolytic debridement, granulation tissue formation, and re-epithelialization. A suitable wound dressing tool is desired to enhance healing and protection from other infections. Hydrogels employed as a wound dressing can maintain the moisture balance in the wound bed, by absorbing wound exudates or by hydrating the wound. Several studies on hydrogels as wound dressing materials have been done and some products are available in the market (Ghadi *et al.*, 2016). Several investigations are ongoing on hydrogel performance as a novel wound dressing.

2.9.2 Water Treatment Hydrogels

Hydrogels can absorb water, aqueous solution, cationic dyes, and metals. As such, they can be used as an alternative way of water treatment in the removal of heavy metal ions. The ionic three-dimensional network of superabsorbent polymers enables uptake of

molecular and ionic species. The elimination of negatively charged anion contaminants from water sources has been a great challenge. However, researchers have come up with hydrogel that can remove anions and then be plucked out of the water, rinsed, and reused (Ji *et al*., 2018).

2.9.3 Utilization of Hydrogels as Hygiene Products

Development and innovation of hygiene products began in western countries a long time ago and a gradual product improvement has been seen over time. In the early 1920s, a section of the women in America produced hand-made napkins from cotton, gauze, flannel, or rags that were pinned to undergarments and later washed for reuse. In the 1890's Johnson and Johnson, set up an industry that produced a large volume of disposable gauze-covered towels (Bharadwaj and Patkar, 2004). Hydrophilic wood pulp and rayon are slow to absorb fluids hence cannot be used on their own. Recently, an advent of cross-linked polymers known as superabsorbent polymers (SAPs) that can swell and retain water when wet. This has led to the development of non-woven pads containing SAP and they absorb fluid faster and are small compared to traditional methods (Zohuriaan-mehr and Kabiri, 2008). Improvement on the design, structure and nature of the absorbing material made to achieve the quick and maximum capacity of liquids. In developing countries, substantial work is ongoing to improve menstrual hygiene among women especially in regions where the commercially available hygiene products are inaccessible.

2.9.4 Hydrogels as Smart Delivery Devices and Water Reservoir in Agriculture

Agriculture is an important sector in the development and growth of a country. Following changes in climatic conditions leading to prolonged droughts and consequently reduced crop production, a substantial gap exists between the demand for food and the ability of production in most regions. The need to reduce water consumption and optimize utilization of water resources in all agricultural practices brings about a culture and habit

to save unnecessary water use. Storing water in soil decreases the negative impacts of droughts. Different soils have varying water holding capacity hence the type of crop production is influenced by such factors. However, there is a need for soil amendment to improve the water holding capacity and supply of nutrients of soils (Mudgal *et al*., 2014).

There are many ways in which this can be achieved such as the use of hydrogels such as polyacrylamide and its copolymers which are non-biodegradable and have low salt tolerance or the use of biodegradable hydrogels such as starch-based, chitosan-based, and cellulose-based. Hydrogels absorb a large amount of water causing them to swell to a rubber-like structure, hence store water. These swollen hydrogels can release the water slowly through diffusion. In arid and desert regions dry hydrogels are mixed with soil in the area surrounding the plant roots due to water scarcity, upon watering, the hydrogel absorbs the water and later release as needed thus keep the soil humid for a longer period. Hydrogels can be packed together with nutrients and plant drugs. Agaba *et al*. (2011) carried out some studies that found out that there was a dense network and aggregation of roots with improved water efficiency of hydrogel amended soil.

Hydrogels have great value in agriculture such as reduced irrigation water consumption and plant death, reduced evapotranspiration rates of plants, reduced compaction tendency, and increased soil aeration, mitigating the effect of soil salinity, bonding heavy metals, and mitigating action on plants (Hüttermann *et al*., 2009). Thus, hydrogels enhance plant growth by improving the soil properties through absorption, storage of water, and nutrients for longer periods in the soil matrix.

Cellulose-based hydrogels conform to the current trend of developing eco-friendly alternatives to superabsorbent material that are acrylate-based. Cannazza and colleagues (2014) carried out studies on the use of cellulose-based superabsorbent polymers (SAPs) in optimizing water use in agriculture. In this study, the developed hydrogels proved to be efficient in providing good absorption capabilities that suited its application for that purpose unlike the acrylate-based SAPs (Cannazza *et al*., 2014). Cellulose from agricultural residues is biodegradable, thus hydrogels from this cellulose can be utilized

in some applications. Sannino *et al*. (2000) carried out studies and developed a novel class of cellulose-based hydrogel that was biodegradable and biocompatible and was able to absorb up to one litre per gram of dry material.

2.10 Methods of Analysis

2.10.1 Extraction Process

Extraction is a principle method carried out when isolating or purifying natural products, usually the first step (Kargarzadeh *et al*., 2017). There are several extraction techniques these include solvent extraction, distillation method, pressing and sublimation and they all have different principles. The extraction efficiency is determined by the solvent choice, raw material particle size, the ratio of solvent to the material and temperature hence should be factored in before choosing a method to use (Zhang *et al*., 2018).

2.10.2 Degree of Substitution

The degree of substitution (DS) of a polymer refers to the average number of substituent groups attached to the monomeric unit. This facilitates the elimination and substitution mechanism for electrophiles in case steric hindrance is a limitation (Hadi *et al*., 2020). It has a direct correlation to its capacity to hold water, which is one the most important parameters especially when dealing with hydrogels as it is the overall measure of its performance in the field. In this study DS of the modified product was determined by a titration method. All ester linkages were saponified with NaOH and the amount of remaining excess NaOH was determined by titration with HCl.

2.10.3 Fourier Transform Infrared Technique

To better understand changes that occur when cellulose is subjected to different modifications such as esterification, there is a need to observe the introduction of new functional groups in its structure. Through infrared analysis one can be able to observe these changes and conclude whether the chemical modifications were successful as the

presence of new groups can be visualized (Chen *et al*., 2015). The amount of infrared radiation absorbed in a given frequency similar to the vibration bond energy of a particular functional group.

2.10.4 Differential Scanning Calorimetry Technique

Calorimetry is a primary method used to determine the thermal behaviour of polymers in order to establish a link between temperature and particular physical properties of the materials, and it is the only method for determining the enthalpy involved in the process of interest directly (Gill *et al*., 2010). The difference in the amount of heat required to raise the temperature of a sample and a reference is measured as a function of temperature. The thermal changes in the cellulose and the cellulose-based products can be monitored using differential scanning calorimetry (DSC). This technique helps in the observation of fusion and crystallization as well as glass transition temperatures, through heating or cooling of the material alongside an inert reference (Allen *et al*., 2012).

2.10.5 Thermogravimetric Analysis Technique

Thermogravimetry is a measure of frequency and quantity of sample weight variation as a function of time and temperature in a controlled environment, which involve the purging of nitrogen gas. used mostly in evaluation of the thermal, oxidative stability and compositional properties of samples (Ng *et al*., 2018). Bond breaking and formation in cellulose and cellulose-based products can be expressed as a thermal factor. This technique provides a comparative measure of heat flow, which provides insight into molecular motion. In this case, the sample is subjected to a controlled temperature program resulting in a change in mass as temperature increases (Agrawal *et al*., 2019; Astrini *et al*., 2012).

2.10.6 Powder X-ray Diffractometer Technique

Powder X-ray diffraction (XRD) is a popular technique used to identify nanoscale materials. Powder X-ray diffraction analysis of a sample provides essential information that supplements multiple microscopic and spectroscopic techniques, such as phase identification, crystal size and sample purity (Holder & Schaak, 2019). The possible structural changes in the cellulose and modified derivatives can be observed using XRD. They generate patterns that display the structural orientation of atoms of a compound. This provides information such as the crystallinity, strain, and crystal defects.

2.10.7 Application Studies

Soil quality determination involves physical, chemical, and biological properties. In order to use soil for planting it is important to know its composition, as some may inhibit or favor plant growth (Salve *et al*., 2018). The retention ability of hydrogels in the soil can be demonstrated in a controlled environment such as a greenhouse since a known amount of water can be used and all other factors are constant. Different set up of control and hydrogel composition help in the evaluation on whether this can be a solution to irrigation and water conservation (Astrini *et al*., 2012). The roots play an important role in the growth of plants in that it aids in nutrient and water acquisition. The development of lateral roots increases the strength of roots (Ogbuehi *et al*., 2014). In the growth of plants, moisture is required hence plants do not wilt and dry up. This moisture can vary depending on the amount of water present in the soil. Hydrogel's ability to retain and release water can be evaluated with the amount of moisture loss in terms of dry weight analysis. This is a destructive process hence carried out the end of the experiment (Golzarian *et al*., 2011).

CHAPTER THREE

MATERIALS AND METHODS

3.1 Study Area

The coconut fiber samples collected were from a local processing miller Kocos Kenya Limited, Kilifi County (0°39'24.4"S 39°18'10.3"E) as shown in Figure 3.1.
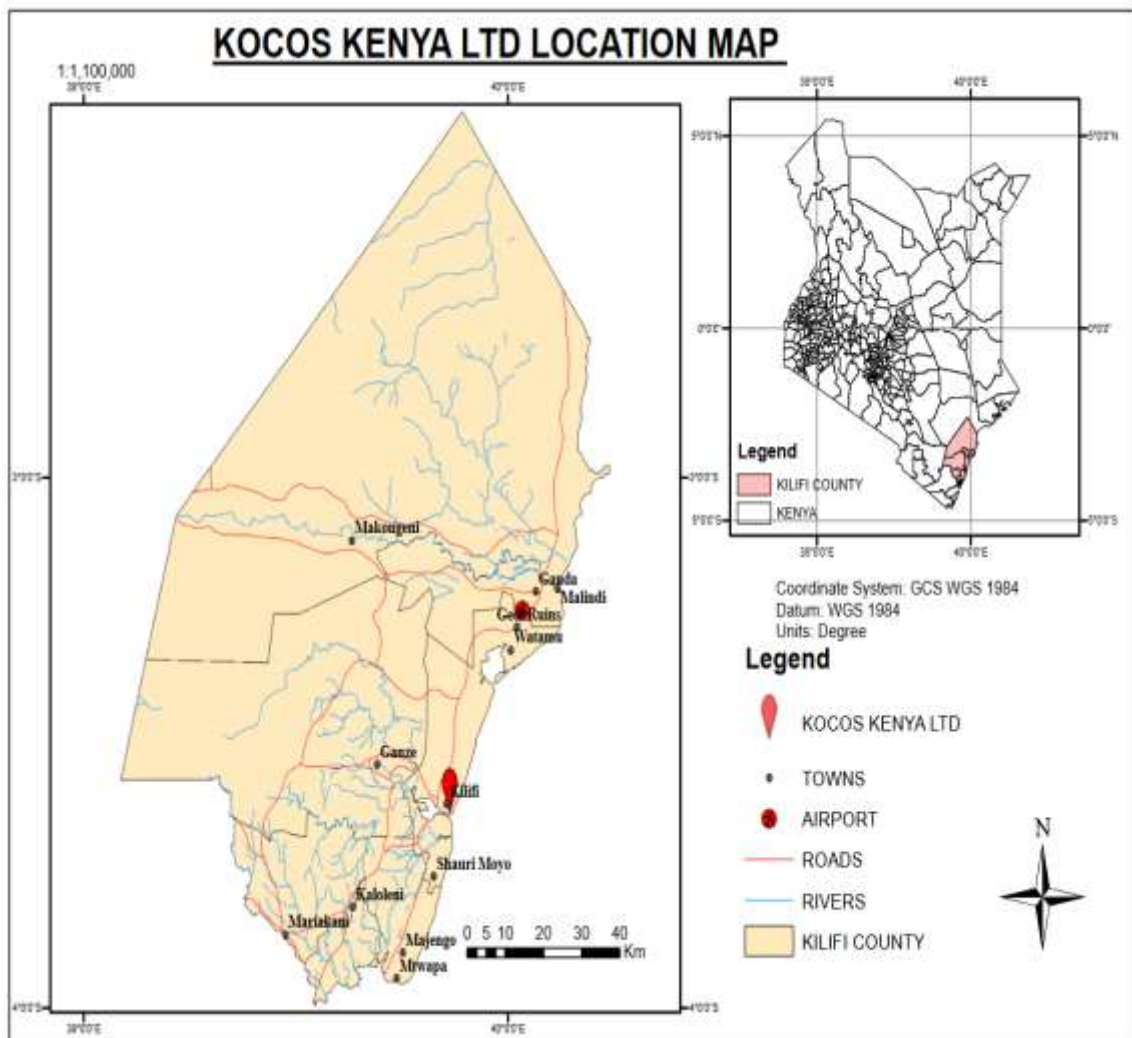
mend

Figure 3.1: Kocos Kenya, coconut (coir) fiber sampling site (Geocon Surveys Limited, 2021)

3.2 Sampling and Pretreatment

The coconut fiber samples (10 kg) collected were from Kocos Kenya Limited, Kilifi County. It was then transported to the JKUAT laboratory where it was sorted to remove any coco peat, present cleaned, and stored. The coconut fiber samples were air-dried, washed with water to remove particulates, and then oven-dried overnight at 105°C. Before extraction of cellulose, the dried sample was chopped into small pieces,1 cm in length.

3.3 Extraction of Cellulose

In this study, 200 g of dried biomass was mixed with 2.5 M aqueous NaOH solution in a ratio of 1:10 biomass to alkali ratio and the mixture stirred using a mechanical stirrer for 3 hours at 100°C, followed by filtration and then washing with 10% ethanol and distilled water repeatedly to remove the base. The hemicellulose-free biomass cake was dried in an oven at 100°C to constant mass followed by treatment with peracetic acid in a ratio of 1:5 of the recovery mass while stirring at 80°C for 2 hours. The residue was filtered and washed with distilled water repeatedly and oven-dried at 105°C to constant mass (Murigi *et al*., 2014).

3.4 Determination of Moisture Content of Cellulose

The cellulose was weighed into a pre-weighed petri-dish with cover and placed in an oven at 105°C for 2 hours. The petri-dish with the sample was cooled to room temperature and reweighed. The sample was then heated at intervals of 30 minutes till a constant mass was obtained (Okon *et al*., 2012). The moisture content was then determined according to Equation 3.1.

$$\%Moisture = \frac{W_2 - W_1}{W_1} \ldots\ldots\ldots\ldots \text{Equation 3.1}$$

where W_1 is the initial mass of cellulose before drying and W_2 is the final mass of cellulose after drying.

3.5 Determination of Degree of Substitution

The degree of substitution (DS) of CMC was determined by a titration method as described by Kimani and colleagues, (2016). All ester linkages were saponified with 0.1 M NaOH and the amount of remaining excess NaOH was determined by titration with 0.1 M HCl. The 0.2 g of the CMC sample was weighed accurately and placed in a 500 mL plastic flask. Then 50 mL of distilled water was added to the flask and the mixture stirred overnight at room temperature. 30 mL of 0.1 M NaOH was added and the mixture heated at 50°C for 3 hours. After cooling it to room temperature, titration was conducted with 0.1 M hydrochloric acid with phenolphthalein as an indicator. A molar quantity of the ester linkages was determined and the concentration of ester linkages per repeated unhydroglucose unit calculated as DS according to Equation 3.2 (Asl *et al*., 2017; Kimani *et al*., 2016).

$$DS = \frac{162 \times \%CM}{(100 \times 58 - (58-1) \times \%CM)} \; \dots \text{ Equation 3.2}$$

$$\%CM = \frac{(Vo - Vn) \times A \times \frac{58}{1000}}{M} \times 100 \; \dots \text{ Equation 3.3}$$

Where, A is the normality of HCl used, Vo and Vn volume to titrate blank and sample respectively, M mass of the sample, 162 is the molecular weight of anhydroglucose and 58 is the molecular weight of cellulose content (CM) group.

3.6 Synthesis of Carboxymethyl Cellulose

The CMC was synthesized according to a method described by (Haleem *et al.,* 2014; Latif *et al*., 2006). The extracted cellulose was converted to CMC in two steps; alkalization and esterification of cellulose under heterogeneous conditions. In alkalization pretreatment, 5 g of prepared cellulose was weighed and added to 100 mL of isopropanol. Aqueous Sodium hydroxide (5 M) was then added dropwise while stirring for an hour at 30°C. Esterification reaction was accomplished by adding 7.5 g of sodium monochloroacetic acid (SMCA) and the reaction mixture heated for 2 hours at 50°C. After the first

esterification process, the sample was washed with 90% ethanol, filtered, and dried. The esterification process was carried repeated five times (Latif *et al*., 2006).

3.7 Determination of Bulk and Tapped Density of Cellulose and Synthesized CMC

Each of the 10 g of sample was poured at an angle of 45°C into a 50 mL glass-measuring cylinder. Before determining the tapped density, the bulk density was first determined by measuring the initial volume V_0. The tapped density was determined by measuring the final volume V_1, after 40 taps. Determination of Carr's index and Hausner ratio for cellulose were calculated from bulk density and tapped density as in Equations 3.4 to 3.7 (Azubuike *et al*., 2012).

$$Bulk\ density = \frac{mass}{untapped\ volume}………Equation\ 3.4$$

$$Tapped\ density = \frac{mass}{tapped\ volume}………Equation\ 3.5$$

$$Hausner's\ ratio = \frac{tapped\ density}{bulk\ density}………\ Equation\ 3.6$$

$$Carr's\ Index = \frac{tapped\ density - bulk\ density}{tapped\ density} * 100…Equation\ 3.7$$

3.8 Synthesis of HEC-CMC Hydrogel

This study used commercial HEC and synthesized CMC from coir cellulose. First HEC was added to petroleum ether for 5 minutes, a clear solution was obtained with a slight increase of viscosity and then CMCNa was added while stirring for 2 hours. Finally, different concentrations of citric acid were added (2.75%, 3.75%, 10%, and 20% w/w polymer) to obtain samples with various crosslinking degrees. All samples were first pre-dried at 30°C for 24 hours to remove absorbed water and then kept at 80°C for the crosslinking reaction for 24 hours with or without initiator(Demitri *et al*., 2008).

3.9 Determination of Swelling Capacity

The water absorbency of the HEC-CMC hydrogels was measured by the tea bag method (Japanese Industrial Standard (JIS) K 7223). Tea bags, 200 x 100 mm containing 1 g of cellulose, CMC, and HEC-CMC hydrogels were immersed in water at 25°C. After 1 hour of treatment in water, the tea bag was picked up from the water, and excess water was drained for 10 minutes. The mass of the tea bag and sample (W_t) was measured and the absorbency calculated as in Equation 3.8:

$$\text{Absorbency} = \frac{Wt - Wb - Wp}{Wp} \dots\dots\dots \text{Equation 3.8}$$

Where; W_b is the mass of the empty tea bag after the water treatment and W_p is the mass of the dry sample.

Again, the tea bag was dipped for 1 hour and picked up for 5 minutes to evaluate the absorbency (total treatment time 2 hours). The absorbency after 24 hours was evaluated in the same way. Further, the absorbency in an aqueous sodium chloride solution (0.9 and 3.5% concentrations) was investigated similarly (Astrini *et al*., 2012). These concentrations corresponded to those of physiological saline and seawater, respectively. After 24 hours of swelling the hydrogels were monitored for degradation. The mass of the degraded hydrogels and empty tea bags were taken every 24 hours for 10 days (Mcbath and Shipp, 2010).

3.10 Characterization of Cellulose, CMC, HEC-CMC Hydrogels

3.10.1 Fourier Transform Infrared Protocol

The infrared (IR) vibration frequency represented in the spectrum is a representation of the amount of IR absorbed for a particular functional group. Characterization of the cellulose, CMC, and synthesized hydrogels was carried out using a Shimadzu Fourier Transform Infrared spectrophotometer (Shimadzu, Japan, Model FTS-8000). 10 mg of cellulose, CMC and hydrogel sample, finely ground, was mixed with 300 mg of potassium

bromide (KBr) and pressed into a pellet using a Shimadzu hand press. The spectra were recorded between 4000 - 400 cm^{-1} by placing each pellet in the beam of the FT-IR spectrophotometer (Hadi *et al.*, 2020; Kimani *et al.*, 2016).

3.10.2 Thermogravimetric Analysis Protocol

The mass 10 mg of cellulose, CMC and hydrogel sample was subjected to a controlled temperature program resulting in a change in mass as temperature increases as described by (Agrawal *et al.*, 2019; Astrini *et al.*, 2012). The TGA thermograms were obtained using a Mettler Tolledo DSC/TGA 3+ system (Mettler-Toledo GmbH, Switzerland) at a heating rate of 10°C/min between 25°C and 600°C. Nitrogen was used as an inert purge gas to displace air in the pyrolysis zone, thus avoiding unwanted oxidation of the sample.

3.10.3 Differential Scanning Calorimetry Protocol

The degree of crystallinity was determined as described by Allen *et al.* (2012). This analysis was carried out using a DSC (Mettler-Toledo GmbH, Switzerland). All the samples (10 mg) were heated from 25 - 400°C at 10 °C/min (Ponce *et al.*, 2013). The degree of crystallinity (α) was estimated from the peak area using Equation 3.9:

$$\propto = \frac{\Delta h}{\Delta h_c} * 100 \ldots\ldots\ldots\ldots\ldots\ldots\ldots\ldots\ldots\text{Equation 3.9}$$

Where Δh is the specific enthalpy of fusion (in J/g) of the sample determined from the peak area and Δhc is the enthalpy of fusion of a 100% crystalline material, in this case, the value of polyethylene of 290 J/g was used for Δh_c.

3.10.4 Powder X-ray Diffractometer Protocol

The crystallinity phase of the nanoparticles was identified using STOE STADIP P X-ray Powder Diffraction System (STOE and Cie GmbH, Darmstadt, Germany). The X-ray

generator was equipped with a copper tube operating at 40 kV and 26 mA and irradiating the sample with monochromatic CuKα radiation with a wavelength of 1.5409 nm. X-ray diffractograms were recorded at room temperature between the 2θ range of 2 - 90° at 0.05° intervals with a measurement time of 1 second per 2θ intervals (Katata-seru *et al.*, 2017). The crystallinity index was calculated using Equation 3.10 (Segal equation) and the d-spacing values obtained by use of Equation 3.11 (Bragg's equation).

$$\text{Cr. I.} = \frac{I_{200} - I_{am}}{I_{200}} * 100 \ \text{………Equation 3.10}$$

$$n\lambda = 2d\sin\theta \ \text{…………….…Equation 3.11}$$

3.11 Application of Hydrogels in Agriculture

3.11.1 Soil Quality Determination

Soil properties were determined as explained by Salve *et al*. (2018). The soil samples were analyzed for pH, available phosphorous, potassium, and total nitrogen at the Phytotechnology Laboratory - JKUAT. Soil pH was measured in a 1:5 soil-water ratio using a glass electrode pH meter (Debnath and Pachauri, 2014). The total nitrogen was determined by the modified Kjeldahl digestion and distillation procedure (Bista *et al*., 2020). Soil sample of 0.3 g was weighed into a digestion tube, 6 g of digestion mixture was added then 15 mL concentrated sulphuric acid. The sample was placed into the digester at 400°C for 2 hours and allowed to stand for 30 minutes to eliminate fumes. Then 10 mL of the digested sample was measured and 15 mL of NaOH added and placed on the distiller. Then 10 mL of 1% boric acid and 5 drops of the colored indicator were added (Yimer and Chimdi, 2019). The amount of phosphorus present was determined through Olsen's method (Salve *et al*., 2018). The available potassium was determined by the ammonia acetate method. A sample, 1 g, was placed in a shaking bottle then, 10 mL of ammonium acetate was added and shaken for 30 minutes. The sample was filtered and 5 mL of it placed in a sampling tube and 15 mL of distilled water was added. A photometric

instrument was used to take the measurements with standards already prepared in the range blank, 1, 2, 3, 4, and 5 ppm (Debnath and Pachauri, 2014).

3.11.2 Tomato Growth in Hydrogel Modified Soil

Ready tomato seedlings (Anna F1 variety) that were pest and disease-free were obtained from the Horticulture nursery at JKUAT. The seedlings were of almost uniform height, girth, and number of leaves. The seedlings were transplanted in pots in a greenhouse. The pots were filled with soil and this was split into three for the different water regimes, that is, after two days, twice a week, and once a week labeled as x, y, and z respectively as displayed in Appendix S. The pots had five treatments comprising of 1% hydrogel, 2% hydrogel, control (soil only), 1% CMC with 1% hydrogels, and 1% CMC given the label A, B, C, D, and E respectively. The hydrogel and CMC were added and mixed with the soil at the plant root level. The treatments had four replicates each including the control (Demitri, *et al*., 2013). The amount of water for irrigation was 250 mL and later 300 mL for all the treatments. The experimental setup was a complete random design. The plant growth and measurement of the leave length, plant height, number of leaves, and number of branches was observed over eight weeks (Takase *et al*., 2010).

3.11.3 Determination of the Tomato Root Score

The number of root hairs was examined by scoring on a scale since there were numerous hairs thus, counting was tedious. The roots were evaluated and scored on a scale of 1, 3, and 5 representing less dense, dense, and highly dense root systems (Pearson *et al*., 2007).

3.11.4 Tomato Dry Mass Analysis

This is a destructive process hence carried out at the end of the experiment as described by (Golzarian *et al*., 2011). This was carried out on the 54th day as it involved the total destruction of the plant. The plants were removed from the soil and loose soil was washed off, then the root and stem were separated by cutting. The plants were then blotted to

remove free surface moisture. Drying was carried out in an oven, EYELA windy oven, WFO-100ND, (Tokyo Rikakikai Co. Ltd) set to 70°C for 24 hours. It was then cooled to room temperature in a Ziploc bag as plants absorb moisture in a humid environment. Once the plants had cooled, they were weighed using, KERN PLS weighing scale (Kern and Sohn GmbH, D-72336) Balingen, Germany. The root-to-shoot ratio was calculated according to Equation 3.12. The plant mass was calculated as per Equation 3.13 (Basirat *et al.*, 2011).

$$\frac{Root}{Shoot} = \frac{Root\ dry\ weight}{Shoot\ dry\ weight} \ldots\ldots\ldots\ldots\ldots \text{Equation 3.12}$$

$$Plant\ Moisture = Plant\ fresh\ mass - Plant\ dry\ mass \ldots \text{Equation 3.13}$$

CHAPTER FOUR

RESULTS AND DISCUSSION

4.1 Extraction of Cellulose from Coir fiber and Synthesis of CMC

The extraction of cellulose was carried in an alkali medium. The cellulose and CMC were analysed for physical properties, swelling capacity and characterized as described.

4.1.1 Physical Parameters of Cellulose and CMC

Table 4.1 indicates the physical parameters of cellulose obtained from coir fiber and synthesized CMC.

Table 4.1: Physical characteristics of extracted cellulose from coir fibers and synthesized CMC

Physical Parameter	Cellulose (n=5) Mean ±SD	CMC$_1$(n=5) Mean ±SD	CMC$_2$ (n=5) Mean ±SD
Percentage Yield (%)	42.1 ±1.5	8.45 ±0.70	9.45 ±0.76
Moisture (%)	7.3±0.60	-	-
Tapped Density (g/cm^3)	0.12 ±0.00	0.15±0.00	0.84 ±0.00
Bulk Density (g/cm^3)	0.08 ±0.00	0.06±0.00	0.55 ±0.00
Hausner's ratio	1.48 ±0.01	1.40±0.01	1.51 ±0.01
Compressibility Index (%)	32.50 ±0.70	58.39±0.10	33.88 ±0.26

The cellulose extraction process resulted in a 69% recovery of the alkali-treated cellulose (Rosa *et al*., 2012) and a separation of cellulose fibrils from the reinforcing component to give a pale yellow product which was an indication that lignin had been eliminated (Abdel-Halim, 2014). Alkali treatment helps in solubilizing the lignin that is responsible for the brown color while bleaching removed residual lignin. The average percentage yield of cellulose in the coconut fibers was found to be 42.1 ±1.5%. Reaction conditions used during treatment such as reagent concentration, temperatures of the reaction medium, and

the volume ratio of bleaching reagent were optimized to obtain the desired bleaching degree and minimal damage to the cellulose fibers (Ramos *et al*., 2008).

The bulk and tapped density help to understand how well a polymer can be compacted in a given space while the Hausner ratio or Carr's index is used to evaluate powder flow properties. The higher a material's bulk and tapped densities are, the greater its ability to flow and reconfigure under pressure (Murigi *et al*., 2014). According to Azubuike and Esiaba (2012), Carr's index values of 5-11%, 12-17%, 18-22%, and above 23% show excellent, good, fair, and poor flow properties respectively. While the Hausner ratio value of below 1.20 designates good flowability, whereas a value greater than 1.20 suggests poor flow properties of the material. In this study, Carr's index and Hausner ratio (Table 4.1) for the coir fiber indicated poor flow properties. Modification and size reduction of these cellulose will improve these flow properties as they affect the quality of material in terms of uniformity. The moisture content was below 10% this maybe as a result of OH groups present in cellulose absorbing water from the atmosphere. Therefore, an indication that should be stored in dry conditions.

The preparation of CMC from cellulose resulted in an increase in the percent recovery of CMC that can be directly associated with the amount of water it can absorb. When cellulose was esterified once, the CMC had a yield of 8.45 ±0.70 g as compared to a yield of 9.45 ±0.76 g when it was esterified twice. This is attributed to the substitution of the OH group at C_2, C_3, and C_6 by the carboxymethyl group during alkalization and esterification reaction (Chan *et al*., 2017). The bulk and tapped density of CMC_1 were 0.06 ± 0.00 g/cm^3 and 0.15 ± 0.0 g/cm^3 while CMC_2 were 0.55 ± 0.00 g/cm^3 and 0.84 ± 0.0 g/cm^3 respectively as indicated in Table 4.1. These factors are important as they help to determine how well the material can be condensed and packaged in a confined space (Murigi *et al*., 2014). Compressibility index or Carr's index and Hausner ratio are a measure of the propensity of powder to be compressed; the measure of powder flow properties, and were calculated using Equations 3.6 and 3.7 respectively. The Compressibility value of 20% and below indicates the powder is good-flowing while

materials with compressibility above 40% have very poor flow characteristics. Hence, from Table 4.1 CMC had very poor flow properties, a conclusion that was also observed from the Hausner ratio values were greater than 1.25, thus said to have poor flow properties (Azubuike *et al*., 2012).

4.1.2 Degree of Substitution of CMC

Table 4.2 gives the degree of substitution (DS) and carbon content (CM) of the CMC after the first and second esterification; CMC_1 and CMC_2 respectively.

Table 4.2: Degree of substitution and carbon content for esterified CMC_1 and CMC_2

	CMC_1 (n=3) Mean ±SD	CMC_2 (n=3) Mean ±SD
Degree of Substitution (DS)	0.91 ±0.07	**1.82 ±0.12**
Carbon content (CM) %	24.65 ±1.45	**39.63 ±1.67**

From the results obtained, the second esterification process increased the swelling capacity and degree of swelling as compared to cellulose esterified once. The average number of carboxymethyl groups that have replaced OH groups per anhydroglucose unit in the cellulose structure at C_2, C_3, and C_6 is the degree of substitution (Sannino *et al*., 2009). The degree of substitution of CMC is a significant factor that has a direct influence on the hydro-affinity, which determines the solubility of the CMC as a DS of <0.4 implies the polymer is swellable but not soluble. A DS of >0.4 on the other hand implies that the polymer is both swellable and soluble in water. The percentage cellulose content (CM) lied between 24.0 - 40.0 (Table 4.2) with a higher CM value giving a higher degree of substitution of the respective CMC. In a similar study, Chan *et al*., (2017) evaluated the effect of agricultural biomass on the degree of substitution of CMC. He reported that the DS value of CMC is influenced by the agricultural residue used to produce cellulose with coconut fiber cellulose having a DS value between 0.3 - 0.6 and the percentage CM as 10 - 20%. In cases where the DS value was low, this implied that the chemical modification

occurred in the amorphous regions of the cellulose (Barba *et al*., 2002). CMC of the high degree of substitution was utilized for this study.

4.1.3 Swelling Capacity of Cellulose and CMC

The swelling capacity of extracted cellulose and synthesized CMC (CMC1 and CMC2 esterified once and twice respectively) was in both saline and non-saline conditions and the results are depicted in Figure 4.1.
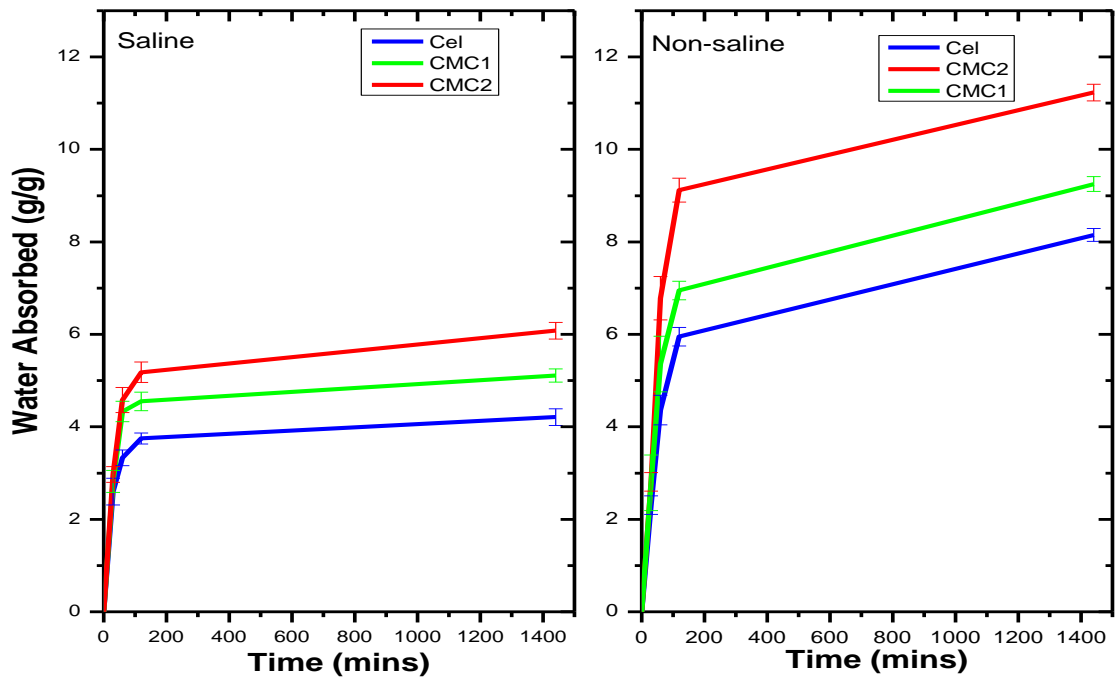
Figure 4.1: The swelling capacity of extracted cellulose and synthesized CMC in saline and non-saline distilled water at room temperature for 1440 minutes

From Figure 4.1, the swelling capacity in distilled water was 8.5 ± 0.14 g of water per gram of cellulose after 24 hours, which was higher as compared to that of 0.9% saline condition (Figure 4.1) of 4.3 ± 0.24 g of water per gram of cellulose. Cellulose has several hydroxyl groups in C_2, C_3, and C_6, which makes it highly hygroscopic (Verma *et al*., 2013). These hydroxyl groups can interact with water molecules through hydrogen bonding to form a network. The water molecules diffuse into the amorphous regions of the cellulose

structure thereby breaking the intermolecular hydrogen bonding, which leads to an upsurge in the inter-molecular distance of the cellulose chains thereby causing swelling. Hence, the swelling behavior of the fibers is an important parameter as it renders cellulose an absorbing material that can retain water for a longer period (Oh *et al*., 2005).

The swelling ratio in saline conditions was lower due to the formation of the anion polymer network unlike the hydrogen bonds formed in non-saline conditions (Figure 4.1). This can be explained by the fact that in saline conditions there is a screening effect that causes the formation of non-uniform electrostatic repulsion that leads to a decline in the osmotic pressure between the cellulose network and the external solution (Hubbe *et al*., 2013). In its natural form, cellulose is unreactive and shows low absorbency, thus modification is usually employed to alter its characteristics such as solubility. These modification reactions are usually carried out on the hydroxyl groups which are susceptible to sulfonation, oxidation, esterification, and derivatization reactions (Shokri and Adibkia, 2013). This forms cellulose derivatives such as carboxymethyl cellulose, hydroxyethyl cellulose among others, which tend to be more hygroscopic and are at times readily soluble in conventional solvents.

From Figure 4.1 it was observed that the swelling capacity in non-saline distilled water after 24 hours was 11.3 ± 0.40 g of water per gram of CMC_2, which was higher as compared to that of cellulose. Cellulose is composed of large hydroxyl groups thus, highly hydrophilic properties when utilized with a hydrophobic material (Verma *et al*., 2013). However, CMC has a higher swelling capacity throughout the range as compared to cellulose due to the esterification process, which introduces carboxymethyl groups within its network thereby making it more hygroscopic. During the esterification process, more carboxylic groups were added to the cellulose thus yielding CMC, the various -OH groups increase the number of the hydrogen bonds with the water molecules as compared to the original cellulose.

Coir cellulose was insoluble in water, after swelling the absorbed water was released on pressing, unlike the CMC that resulted in a gel-like substance in water. The high degree

of substitution of the CMC makes it soluble in water thus good material for superabsorbent polymers (Singanusong *et al.*, 2014). Natural polymers such as cellulose utilized as renewable-based polymeric material due to their availability and biodegradable property (Ogali *et al.*, 2011). Chemical treatment improves the properties of cellulose (Zimmermann *et al.*, 2016). The CMC_2 with high swelling capacity was utilized for the rest of the study.

4.1.4 The FTIR Characterization of Cellulose and CMC

The infrared (IR) spectrum for the raw coir fibers, alkali-treated fibers, and the bleached cellulose and synthesized CMC and CMC standard are depicted in Figure 4.2 and 4.3 respectively.
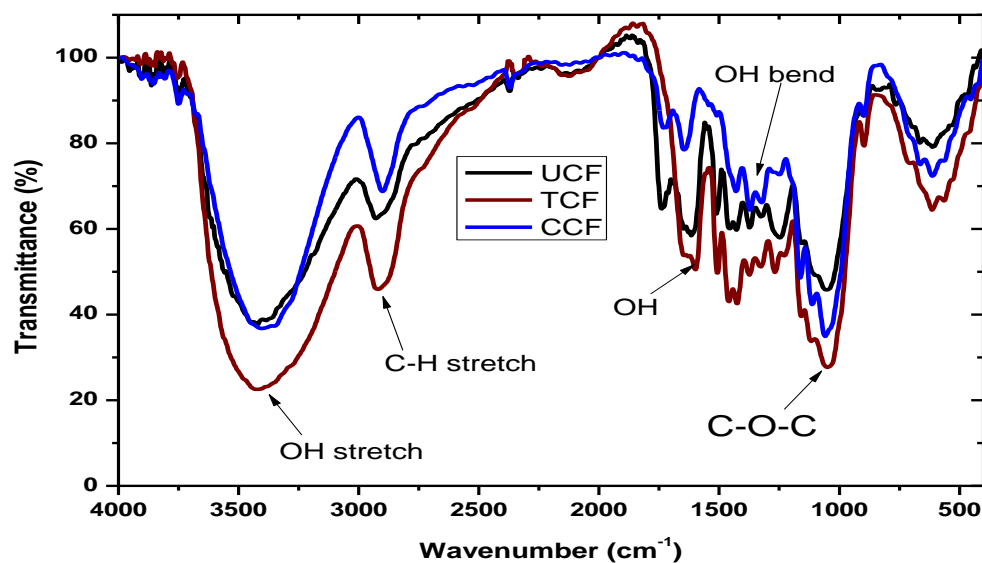
Figure 4.2: FT-IR spectra of coir fiber cellulose (CFC), alkali-treated fiber (TCF), and raw untreated fiber (UCF)

36
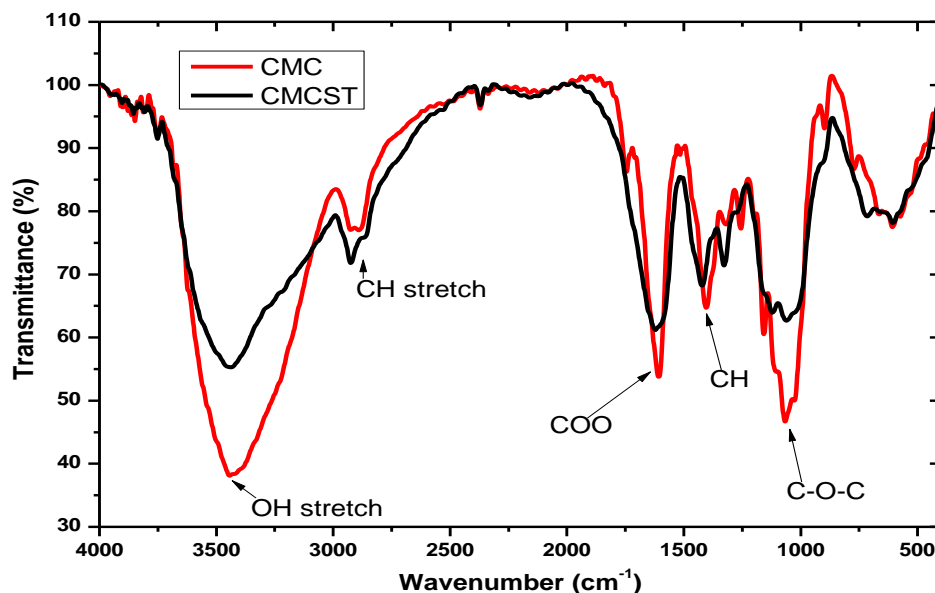
Figure 4.3: The FTIR spectra of synthesized CMC and CMC standard (CMCST)

The treatment steps the raw coconut fibers were subjected to result in minor differences in the infrared spectrum of untreated fiber, the alkali-treated fibers, and bleached cellulose. The broad infrared band observed at 3426 cm^{-1}, 3423 cm^{-1} and 3404 cm^{-1} (Figure 4.2) for raw fibers, alkali-treated and cellulose fibers respectively are characteristic for -OH stretching vibrations. The -OH peaks appear to be broad and narrow intensity as compared to alkali treated and this can be said to be an amorphous OH (Ciolacu *et al.*, 2011). The C-H stretching vibration was observed at 2900 cm^{-1} for cellulose while that of alkali-treated and raw fibers appears at 2930 cm^{-1} and 2925 cm^{-1} respectively and it provides information on the general organic content of the fiber (Poletto *et al.*, 2014). The disappearance of absorption bands at 1510 cm^{-1} and 1244 cm^{-1} in the cellulose spectrum, which is present in alkali-treated and raw fibers is an indication that lignin and hemicellulose were eliminated (Qi *et al.*, 2019). The absorption band at 1622 cm^{-1}, 1616 cm$^{-1,}$ and 1647 cm^{-1} (Figure 4.2) for raw fibers, alkali-treated and cellulose respectively are associated with OH bending vibration of water adsorbed on the surface of cellulose while the absorption bands at 1235 cm^{-1} are associated with a C-OH bond out of a plane (Kia *et al.*, 2017). The bands observed at 1048 cm^{-1}, 1049 cm$^{-1,}$ and 1059 cm^{-1} for raw fibers, alkali-treated and cellulose respectively, are characteristic of -C-O-C- stretching

vibrations respectively. According to Garside and Wyeth, (2003) these bands are attributed to the glycosidic ether band of C-O-C which is a major cellulose characteristic peak.

The total crystallinity index (TCI) (Appendix A) was evaluated from the height of the bands at 1371 cm^{-1} and 2900 cm^{-1} (H1371/H2900). The lateral index order (LOI) in Appendix A was obtained from the ratio of the bands associated with the crystallinity of material at 1430 cm^{-1} and that of the amorphous region of cellulose at 890 cm^{-1} (A1430/A890) (Oh *et al*., 2005; Poletto *et al*., 2014). The degree of intermolecular regularity and crystal system of cellulose has some relation with the mobility of the chain and the bond distance which can be evaluated as the hydrogen bond intensity (HBI); this is the ratio of the band at 3400 cm^{-1} and 1320 cm^{-1} (A3400/A1320) of the OH in cellulose in Appendix A (Khai *et al*., 2017). The hydrogen bond intensity (HBI) of cellulose is closely related to the crystal system, the crystallinity, and the amount of absorbed water. The HBI of cellulose isolated from coconut coir fibers was higher when compared to native fibers which reveals that the extracted fibers had a highly ordered crystalline structure and the crystallinity increased due to the removal of hemicellulose and lignin during treatment (Appendix A). These results were similar to those obtained elsewhere (Oh *et al*., 2005; Poletto *et al*., 2014).

The CMC sample displays a typical FTIR spectrum as that of the CMC standard, major characteristic peaks appear in almost similar wavelengths. The carboxymethyl cellulose IR spectrum displayed a broad peak at 3422 cm^{-1} and a medium peak at 2891 cm^{-1} was attributed to OH group and CH stretching vibrations respectively. The peak at 1600 cm^{-1} (Figure4.3) confirmed the presence of the –COO$^-$ group, which indicates successful carboxymethylation; this peak was absent on the coconut fiber cellulose spectra (Asl *et al*., 2017). The peaks at 1319 cm^{-1} and 1404 cm^{-1} were due to –CH$_2$ scissoring vibration and –OH bending vibration due to water absorbed respectively. The peaks at 1067 cm^{-1} and 1157 cm^{-1} (Figure 4.3) are due to HC-O-CH$_2$ stretching vibrations and there was a slight shift in the peak from that in cellulose that appears at 1059 cm^{-1}. The intensity of

the CH bending vibrations varies between CMC, which appears deep whereas cellulose extract appears shallow.

4.1.5 The TGA and DTGA Curves for Cellulose and CMC

The thermogravimetric analysis (TGA) thermograms and the differential thermogravimetric analysis (DTGA) curves for of cellulose and CMC are displayed in Figure 4.4 and 4.5 respectively.
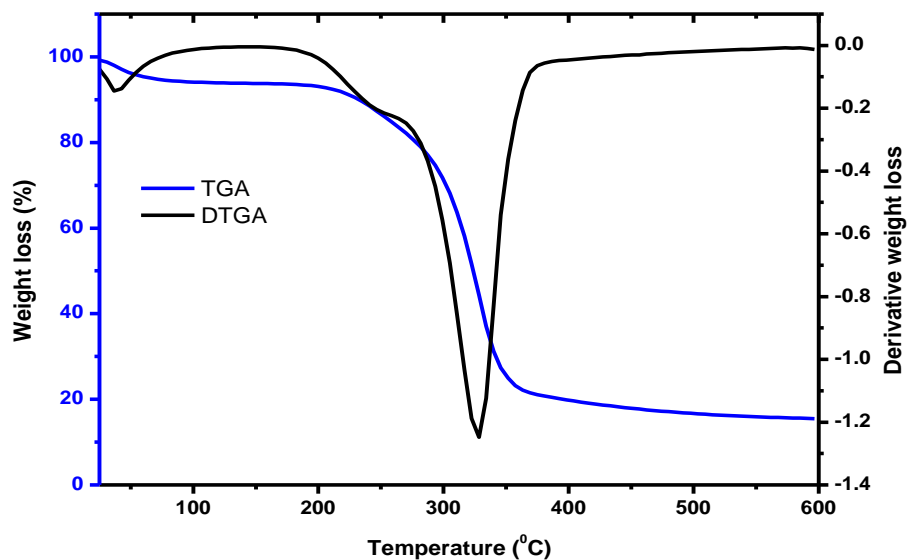
Figure 4.4: TGA curve and DTGA curve for extracted cellulose from coir fiber
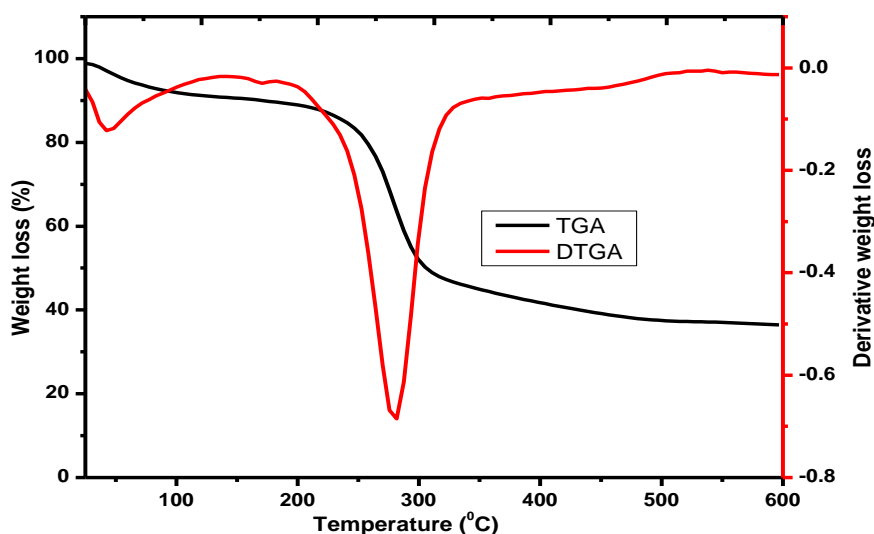
Figure 4.5: TGA and DTGA curve for synthesized carboxymethyl cellulose

From the Thermogravimetric Analysis (TGA) and Differential Thermogravimetric Analysis DTGA thermograms of cellulose (Figure 4.4), the first degradation was observed at 75°C and 48°C for TGA and DTGA respectively, correspond to evaporation water which was trapped inside the isolated cellulose fibers (Astrini *et al*., 2012). The decomposition onset at 196°C and ending at 370°C (Figure 4.4) is associated with the degradation of cellulose and this accounts for about 78% mass loss with only about 12% left as residual ash. The DTGA curves show two minor peaks and a major decomposition peak. The endothermic peak centered at 346°C is due to the decomposition of the cellulose backbone and this is similar to what was reported by Poletto *et al*., (2014). The cellulose, in this case, shows high thermal stability due to the less ordered structure.

The TGA curves for CMC are sigmoid and the significant mass loss occurred at the steep point of the graph (Collazo-bigliardi *et al*., 2018). From the TGA thermograms of CMC, the first degradation was observed at around 50°C, this corresponds to evaporation water (Figure 4.5). Although CMC was dried to a constant mass, there is water trapped in the amorphous region of the cellulose structure (Hubbe *et al*., 2013). According to Capanema *et al*. (2018) increase in hydrogen bonding in the NaCMC is due to the presence of a hydrophilic group (Na^+) hence there is more interaction with water molecules. The

40

decomposition onset at 194°C and ends at 330°C is associated with degradation of CMC, which is at a lower temperature as compared to that of native cellulose. The degradation account for about 53% mass loss with only about 36% left as residual ash for CMC. The ash content in cellulose was lower as compared to that of CMC due to the presence of sodium metal that requires high temperatures to decompose (Capanema *et al*., 2018). The thermal stability of CMC reduced when compared to that of neat cellulose due to bond breaking and new bond making during the carboxymethylation process leading to the interference of the network. The DTGA curve (Figure 4.5) has two peaks and a shoulder peak on the major endothermic peak. The peak below 100°C centered at 47°C is due to loss of water (Astrini *et al*, 2012). The major mass loss for CMC occurred at a temperature range of 200-330°C, centered at 280°C similar to that reported by Astrini *et al*., (2012). Thermal stability of CMC was lower than that of the native cellulose as result oof esterification process leads to the substitution of the -OH groups (Ibrahim *et al*., 2013).

4.1.6 Differential Scanning Calorimetry Profile of Cellulose and CMC

Figure 4.6 illustrates the Differential Scanning Calorimetry (DSC) thermograph of extracted cellulose and synthesized CMC.

41
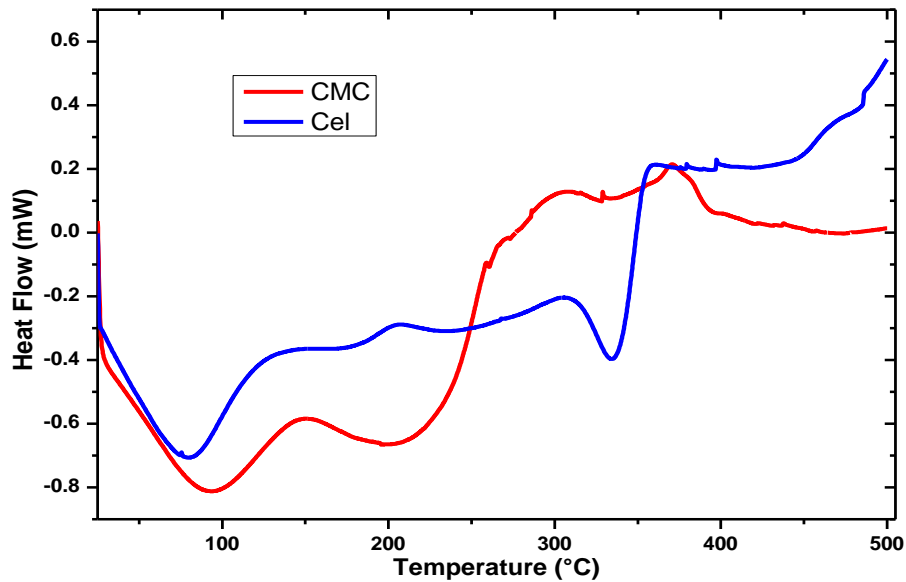
Figure 4.6: The DSC thermograms for extracted cellulose from coir fiber and synthesized CMC

Cellulose is composed of a supramolecular structure that has a direct effect on the thermal degradation of the material. DSC is used to determine the glass transition, melting temperature, and crystallinity of cellulose and hence its structural arrangement depicted. The DSC thermograms show an endothermic degradation at 85°C (Figure 4.6) that is ascribed to water loss caused by heating of the sample (Yang *et al*., 2007). A minor exothermic peak was observed at 206°C, which is the glass transition temperature of cellulose where the ordering of the material occurs. A sharp endothermic peak is also observed centered at 336°C, which correlates to the dissolution of glycosidic bonds and the thermal decomposition of cellulose similar to what was reported by (Rosa *et al*., 2012; Yeng *et al*., 2015). The transition at 336°C can move to lower temperatures depending on factors such as molecular weight, amount of amorphous content, crystallite sizes among others. From Equation 3.9, the degradation of cellulose is used to estimate the crystallinity of the fibers, which in this case was calculated to be 37%. However, cellulose isolated from coir fibers was less crystalline or non-crystalline when compared to other sources such as cotton cellulose which has been reported to have a high degree of crystallinity associated with the high fiber strength (Ciolacu *et al*., 2011).

CMC displayed a broad glass transition temperature as compared to cellulose around 95°C characteristics of water loss (Rosa *et al*., 2012), endotherm melting at around 202°C, and exothermic crystallization transition temperature at 150°C. CMC showed an exothermic reaction at 372°C which is due to its decomposition or degradation (Figure 4.6). Cellulose was stable between 380 – 460°C (Figure 4.6) and above 470°C it shows an increase with increase in temperature and this could be a result of the disintegration of the functional groups (Yang *et al*., 2007). The esterification of cellulose resulted in a derivative with low thermal stability as indicated by a decrease in the melting and crystallization temperature. This effect is due to the formation of CMC, which has a highly ordered structure as compared to cellulose.

4.1.7 The X-ray Diffractograms of Cellulose and CMC

X-ray diffractograms of extracted cellulose and synthesized CMC are shown in Figure 4.7 and 4.8 respectively.
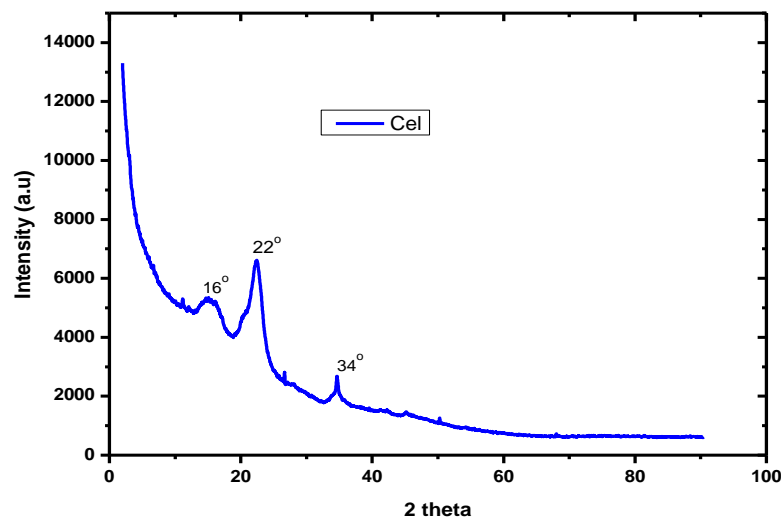
Figure 4.7: The X-ray diffractogram of extracted cellulose from coir fiber
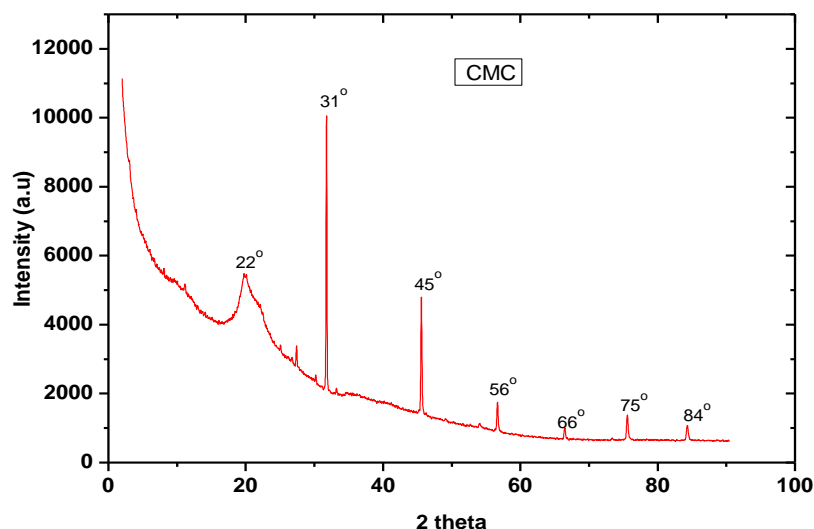
Figure 4.8: X-ray diffractogram of synthesized CMC

The diffractograms in the cellulose sample under study are similar to that of cellulose as reported by Ciolacu *et al*. (2011) and Wei *et al*. (2016). The 2 theta values were found to be 16°, 22°, and 34° (Figure 4.7). The crystallographic planes can be assigned to each of the 2θ values and these values correspond to 110, 200, and 300 for 2θ values 16°, 22°, and 34° respectively (Qi *et al*., 2019). Cellulose comprises an amorphous phase, represented at 2θ value 18° and crystalline phases displayed the peaks. X-ray diffraction pattern of cellulose was carried out to quantify the crystallinity of the structure. The ratio of crystalline and the amorphous region influences the rigidity and flexibility of cellulose fibers which, are affected by the treatment steps (Wei *et al*., 2016). The crystallinity index can be calculated using the Segal method (Equation 3.10), which was found to be 39.5%. The crystallinity of cellulose is ascribed to the presence of the hydroxyl groups that give rise to the intramolecular and intermolecular hydrogen bonding effect. The Bragg's equation (Equation 3.11) was used to evaluate the d-spacing value and were found to be 2θ values 16.3° d_{110} = 5.50 Å, 22.3° d_{200} = 3.99 Å and 34.6° d_{300} = 2.59 Å.

The X-ray diffractograms show well-defined and sharp peaks for CMC. The CMC characterized by 2θ peaks at 20°, 31°, 45°, 66°, 75°, and 84° (Figure 4.8). The 2θ value at 20° and 31° resembles that of cellulose at 22° and 34° (Figure 4.7) indicating a shift in the

peak position, and this could be a result of derivatization reaction. The peak at 20°
indicates the crystallinity of CMC because of the intermolecular and intramolecular
distance between the -OH group forming a hydrogen bond with –COOH group (Sethi *et
al*., 2019). Bragg's equation (Equation 3.11) is used to determine the d-spacing values as
displayed in Table 4.3.

Table 4.3: Parameters obtained from X-ray diffractogram of synthesized CMC

2θ	d-spacing (Å)	Miller indices
20°	4.44	200
31°	2.81	310
45°	1.99	420
56°	1.62	521
66°	1.41	620
75°	1.26	710
84°	1.15	-

Phase matching of the diffractograms achieved by the use of software to determine the
Miller indices (hkl values) as indicated in Table 4.3. The 2θ value at 31°, 45°, 66°, 75°,
and 84° correspond to the characteristic peaks of sodium chloride which result from the
use of sodium monochloroacetic acid during the derivatization process as indicated in the
chemical equation as in Figure 4.9.
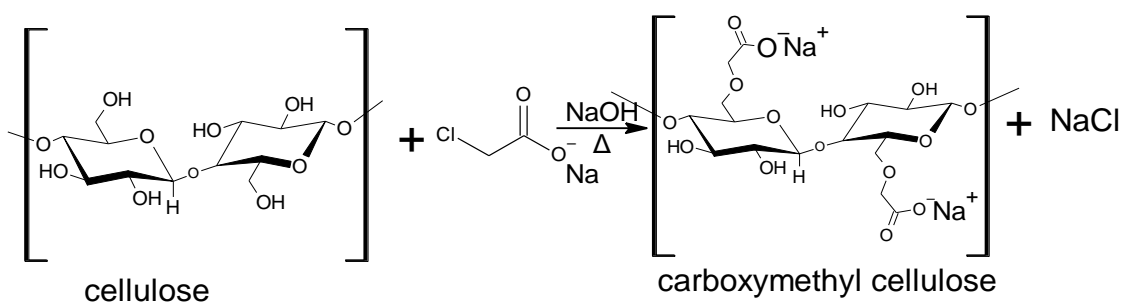
Figure 4.9: Possible reaction during cellulose derivatization

The OH groups in cellulose are that which undergo substitution during the alkalization and esterification process. The modification and widening of the crystalline structure of cellulose using NaOH lead to the breakdown of hydrogen bonds partially thus making AGU accessible to nucleophiles (SMCA) (Massah *et al*., 2007). The choice of solvent is ideal as organic solvent acts as a swelling-restrictive agent and hence, limits the hydration of the cellulose chain CMC was synthesized according to a method described by (Haleem *et al.,* 2014; Latif *et al*., 2006).

4.2 Development of Cellulose-based Hydrogels

The CMC-HEC hydrogels were synthesized in non-polar solvent resulting a powdered hydrogel sample. Synthesized hydrogel resulted in increased yield by 50% of the starting material. The water retention and permeability of hydrogel is a vital characteristic feature, this was evaluated as described.

4.2.1 Functional Group Analysis of Hydrogels

Figure 4.10 displays a plausible structure of the resultant CMC-HEC synthesized hydrogel.
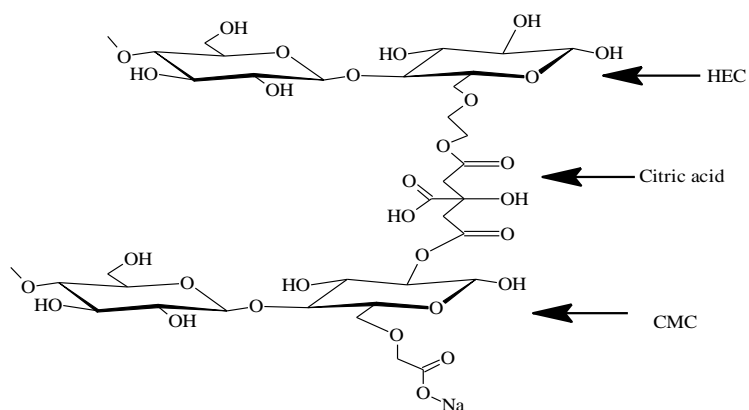
Figure 4.10: Plausible structure of HEC-CMC citric acid cross-linked hydrogel

The IR spectra of hydrogel synthesized through chemical crosslinking of CMC-HEC is depicted in Figure 4.11.
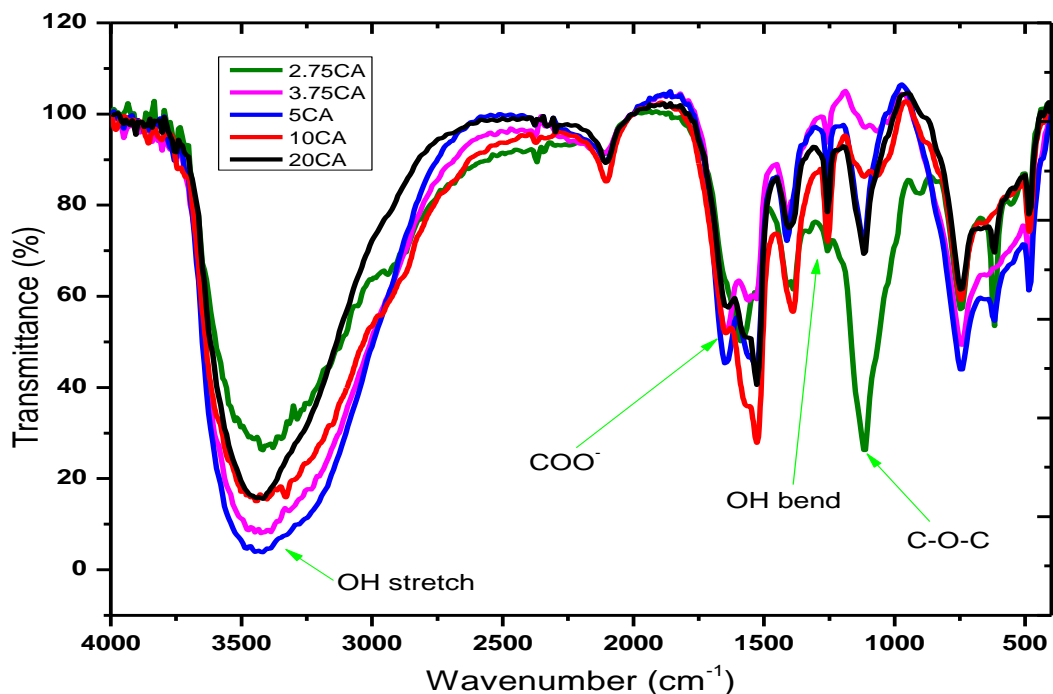
Figure 4.11: The FTIR spectrum for hydrogels synthesized with different citric acid concentrations

The spectra of all the hydrogel films showed characteristic peaks at 1651 cm^{-1} and 1586 cm^{-1} representing C=O stretching of carboxylic acid and ester groups (Figure 4.11. The ester and acid carbonyl peak corresponded with the peak at 1651 cm^{-1} which could result from crosslinking (Ghorpade *et al*., 2017). This new peak appears as a shoulder on the spectrum of the various citric acid concentrations. The peak at around 2939 cm^{-1} (Figure 4.11) was attributed to C-H stretching although as the concentration of citric acid increases the peak disappears and is thus not observed at high concentrations. The broad absorption peak centered at 3424 cm^{-1} is a result of OH stretching in the hydrogel network. This peak is sharp and broad as compared to that of CMC due to the increase in the concentration of OH groups. The C-O vibrations, in this case, could be due to primary or secondary alcohols of the hydrogel formed and this is displayed by absorption peaks at 1112 cm^{-1}, 1065 cm^{-1}, and 980 cm^{-1} for C_2, C_3, and C_6 OH groups (Capanema *et al*., 2018). The

intensity of these peaks is lower than that in cellulose and individual derivatives because the C_6 OH takes part in most crosslinking reactions forming the ester bond.

The HEC-CMC hydrogel crosslinked with citric acid at different concentrations, resulting in ester bond formation as evident by the peak at around 1651 cm^{-1} (Figure 4.11). The cellulose backbone, however, remains the major block due to the presence of C-O-C ring peaks at 1065 cm^{-1}. Sodium carboxymethyl cellulose is characterized by numerous hydroxyl and carboxyl groups in their structure hence can form ester linkage with citric acid (Akar and Altınıs, 2012; Chan *et al*., 2017; Demitri *et al*., 2008). Hydroxyethyl cellulose also forms an ester link with citric acid due to the reactive hydroxyl groups present (Seki *et al*., 2014). According to Ahmed, (2015) these hydrogels can be classified as a copolymer and chemically cross-linked hydrogel due to the permanent ester linkage formed. Hydrogel prepared may be created in several forms such as films, membranes, rods, particles, and emulsion (Bouhendi and Bagheri-marandi, 2010; Joshi *et al*., 2016; Ghorpade *et al*., 2017).

4.2.2 The TGA Thermograms of Hydrogels

The thermal stability of HEC-CMC synthesized hydrogels investigated by TGA and DTGA and the results depicted in Figure 4.12 and 4.13 respectively.
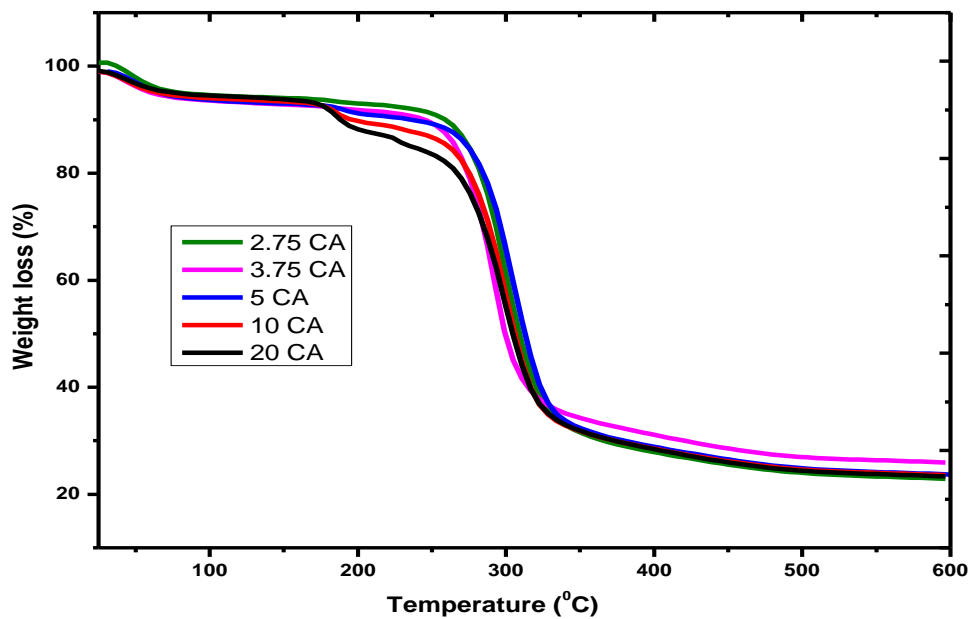
Figure 4.12: The TGA thermograms of hydrogels synthesized with an increasing percentage of citric acid concentrations
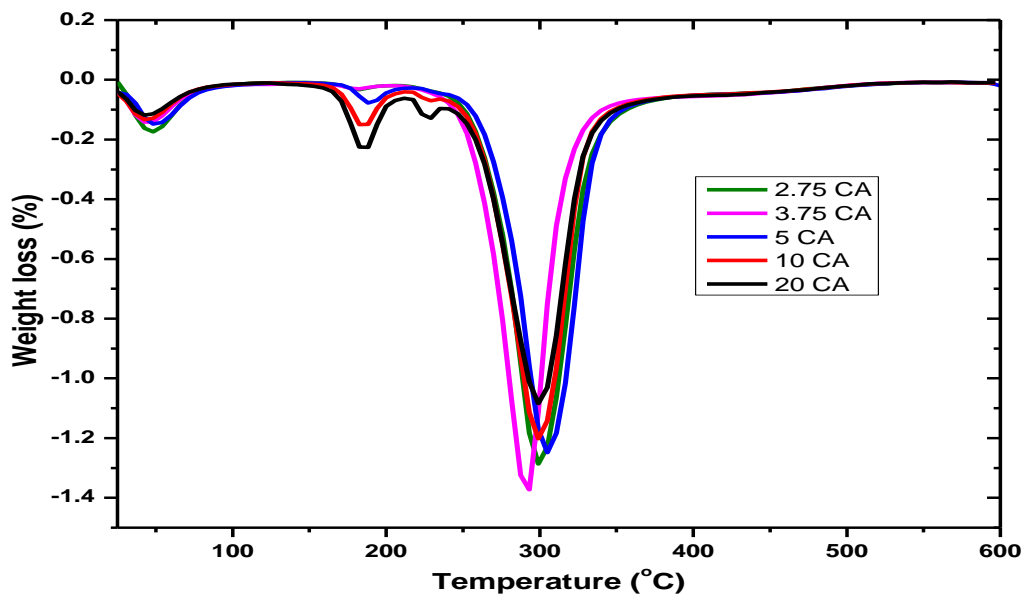
Figure 4.13: The DTGA thermograms for hydrogels synthesized with increasing citric acid concentrations

The influence of citric acid concentration on the thermal behavior of the hydrogels revealed that with an increase in the citric acid concentration, the hydrogels had three

degradation stages as compared to lower citric acid concentration. In Figure 4.12 the first decomposition which occurred between 40 - 140°C was associated with the loss of moisture (Ghorpade *et al*., 2017) while hydrogel degradation was observed to occur between 220 - 360°C irrespective of the citric acid content used during crosslinking of CMC and HEC.

However, at a higher citric acid concentration ($<$ 5%) a second decomposition cycle was observed between 170 - 220°C and it is associated with decomposition of residual citric acid that remains after crosslinking had occurred, which is about 10% associated citric acid degradation (Ghorpade *et al*., 2017). The third range (220 - 370°C) shows a major mass loss of hydrogel, which translates to a 61% loss. The residual mass or ash content for all hydrogels appears to be similar to 2.75% while 3.75% citric acid was 26%. In comparison to the CMC thermograms (Figure 4.5), onset degradation temperatures of hydrogel (Figure 4.12) were higher but lower than that of respective cellulose (Figure 4.4). Capanema *et al*. (2018) concluded that during the carboxymethylation process the supramolecular structure of cellulose undergoes interference due to steric hindrance and electrostatic repulsion. Furthermore, crosslinking reaction affects stability due to the reduction of the hydrogen bonds. The DTGA thermograph display two peaks for low CA and three for higher concentration. The major endothermic peak centered at 300°C and 293°C are characteristic of the decomposition of the hydrogel (Figure 4.13), while that at 45°C is due to loss of bound water. The peak area for DTGA curves is proportional to the amount of mass loss that occurs during the reaction as in Appendix B.

4.2.3 Differential Scanning Calorimetry Thermograms of Hydrogels

The DSC thermograms of the HEC-CMC synthesized hydrogel powder shown in Figure 4.14.
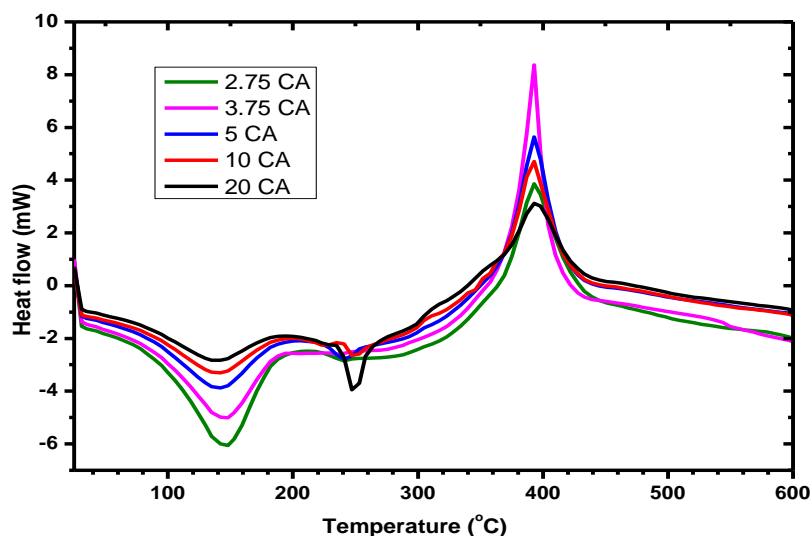
Figure 4.14: The DSC thermograms of synthesized hydrogels with varying citric acid concentrations

The DSC thermograms display an increase in heat flow with the rise in temperature characterized by two endothermic peaks and one exothermic peak. The endothermic peak at 140°C is due to water loss from the hydrogels and this water is from the anhydrification process during the crosslinking with citric acid (Demitri *et al*., 2008; Kia *et al*., 2017). However, the peak decreases with increase in citric acid concentration, a similar trend is displayed in the swelling ratio of these hydrogels and it can be attributed to numerous polymer entanglements. Furthermore, after hydrogel formation, the glass transition temperatures were found to be 245°C (Figure 4.14) as compared to CMC, which was 150°C (Figure 4.6). As the citric acid ratio is increased the transition temperature increases due to the restricted mobility of the polymer, as several short polymer chains are formed (Agrawal *et al*., 2019). The intensity of the endothermic peak at 245°C increases with an increase in citric acid concentration > 5 %, and is associated with the degradation of citric acid (Ghorpade *et al*., 2017). The exothermic peak centered at 393°C crystallization of the hydrogel attributed to the decomposition of the hydrogel. After the glass transition, the polymer gains the energy that induces mobility of the chains thus results in an ordered structure.

4.2.4 The X-ray Diffractograms of the Hydrogels

The X-ray diffractograms of HEC-CMC synthesized hydrogels using different citric acid concentrations is shown in Figure 4.15. Table 4.4 display the diffractogram parameters.
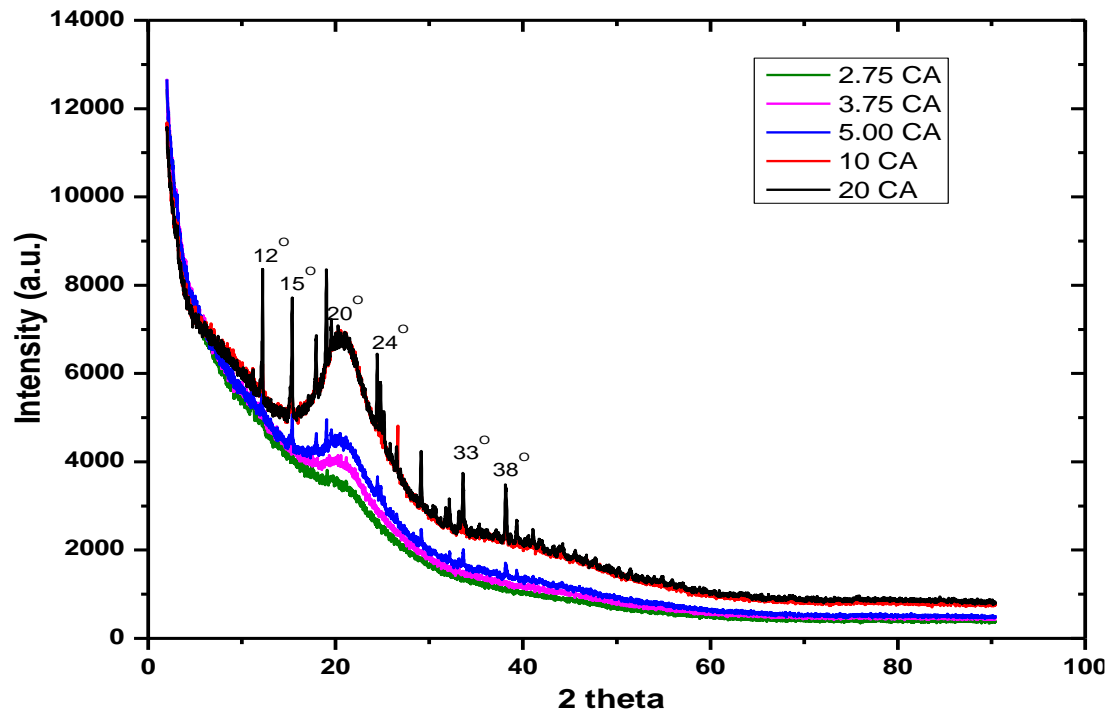
Figure 4.15: X-ray diffractogram for hydrogel synthesized using citric acid concentrations

Table 4.4: Parameters obtained from X-ray diffractogram analysis for synthesized hydrogels with varied citric acid concentration

Citric acid %	2θ	d-spacing (Å)	Miller Indices		
			h	k	l
2.75	11	7.98	0	0	3
	20	4.37	1	0	1
	21	4.17	1	0	2
20.00	12	7.24	1	0	1
	15	5.76	2	0	0
	19	4.66	0	0	2
	21	4.32	1	0	2
	24	3.64	3	1	0
	29	3.06	2	2	2
	33	2.66	4	1	0
	38	2.35	3	1	3

The hydrogel sample diffractograms display peaks that increase in size with an increase in the crosslinking agent ratio. Lower citric acid concentration (<5%) displays two peaks whereas a higher concentration (Figure 4.15) shows more than two peaks. The major and consistent peak observed at 2θ = 20° is because of the cellulose backbone. In Figure 4.15) show other additional peaks 2θ = 15°, 24°, 29°, 26°, 33°, and 38°, where peak intensities increased with the increase in crosslinker ratio (Wen *et al*., 2015). The peak at 2θ = 11°, 15°, and 26° are due to HEC and this indicates that HEC participated in the crosslinking process (Mukerabigwi *et al*., 2016). The indexing of the 2θ diffractogram peaks and the d-spacing from Bragg's equation (Equation 3.11) is shown in Table 4.4.

The calculated degree of crystallinity index was lower than that of the corresponding raw cellulose; this is a result of a breakdown of the hydrogen bonding. The decrease in the depth of 2θ = 18° shows an increase in the amorphous area in the hydrogels as compared to cellulose hence the observed reduction in the crystallinity index in hydrogels. The chemical reactions that occur during the crosslinking process result in the breaking and making of bonds, which influence the crystallinity of the hydrogel (Collazo-bigliardi *et al*., 2018). The formation of numerous irregular patterns when the CA concentration increases results in fewer void volumes unlike when CA is lower and they all actively

participate in crosslinking hence large void space thus can easily swell. A mixture of regular and irregular patterns may arise in the process, which make up irregular polymers that are amorphous (Akar and Altınıs, 2012). Moreover, hydroxyl groups in the cellulose structure are the active groups that participate in the crosslinking process hence reduce the interaction of CMC and HEC.

4.2.5 Hydrogel Swelling Studies

The hydrogel swelling behavior is much influenced by the external environment such as salinity, presence of initiator, pH, and temperature of the solvent. The effect of different metal initiators on the swelling capacity of different citric acid (2.75%, 3.75%, 5%, 10%, and 20%) concentrations synthesized hydrogel with standard deviations for 24 hours is illustrated in Figure 4.16 and 4.17 respectively all in non-saline distilled water at room temperature.
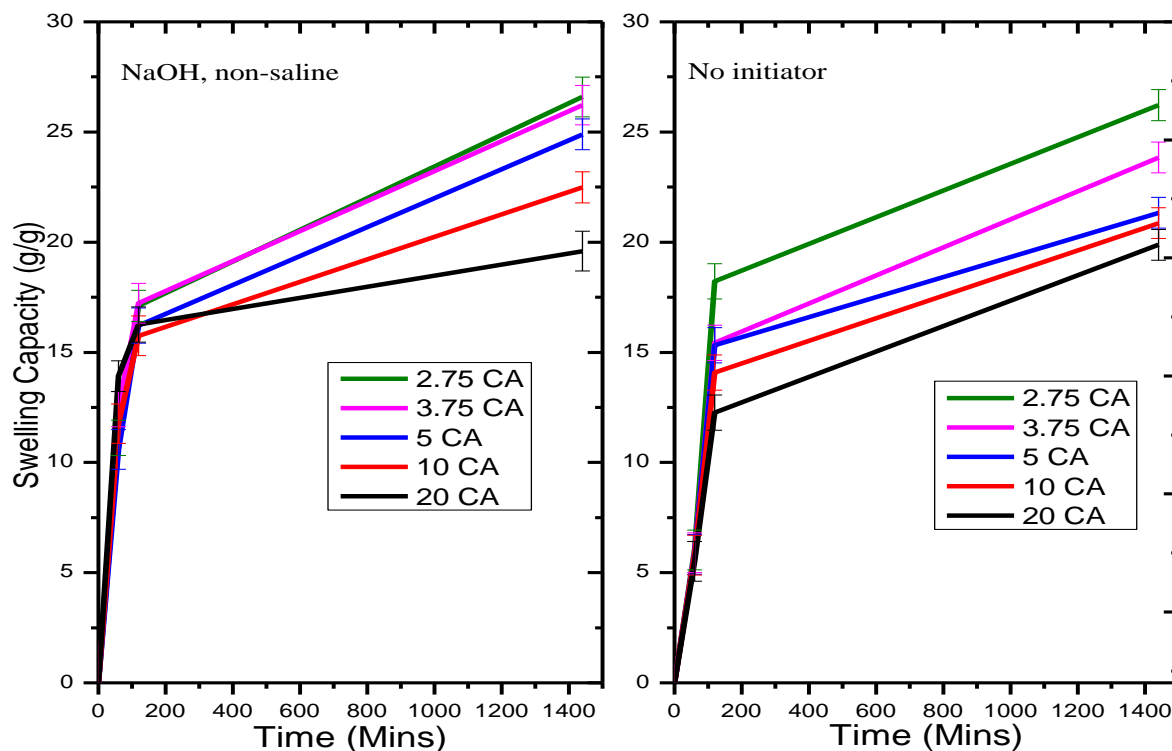
Figure 4.16: Swelling capacity for synthesized hydrogels using citric acid in distilled water at room temperature for 1440 minutes

The use of initiators such as sodium hydroxide and potassium hydroxide also affect the swelling of the resultant hydrogel as in Figure 4.16 and 4.17 and the action of the metal present shows an impact on the retention level (Omidian *et al*., 1998). When KOH was used the swelling capacity was 30 g/g, NaOH gave 27 g/g, and in the absence of initiator 26 g/g. Swelling capacity is one of the fundamental properties of hydrogels. The swelling capacity of the hydrogels is influenced by the monomer type, presence of initiator, reactivity, function groups present, and concentration of the crosslinker (Kowalski *et al*., 2019). Hydrophilic functional groups attached to the polymer backbone from crosslinking reactions determine the hydrogel's ability and amount of water absorbed. The water inside the hydrogel allows free diffusion of some solute molecules, while the polymer serves as a matrix to hold water together. The swelling and de-swelling can be altered by varying the external environment in the form of pH, temperature, and salinity (Saini, 2017).

Hydrogel synthesized in presence of potassium hydroxide as initiator was utilized in this study due to high swelling capacity.

The effect of both non-saline and saline solvent conditions was evaluated and the results are depicted in Figure 4.17respectively.
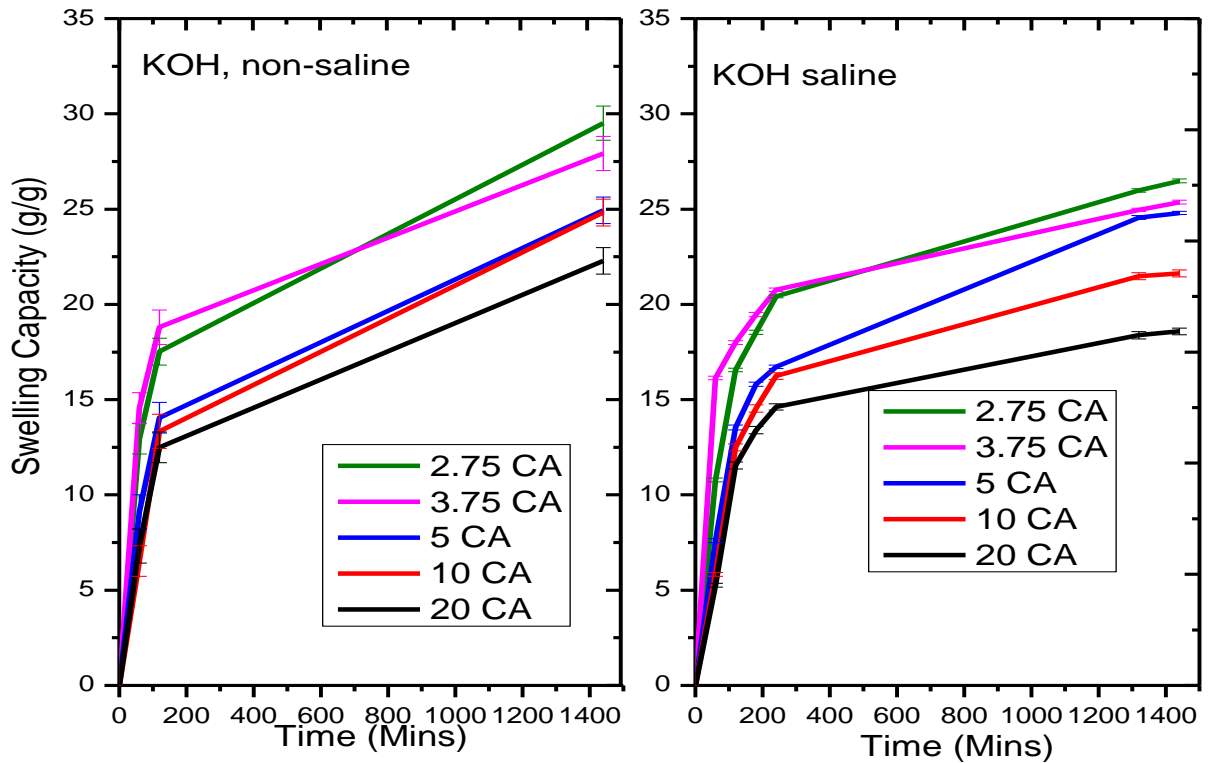
Figure 4.17: Swelling capacity synthesized hydrogel with citric acid in distilled water saline and non-saline at room temperature for 1440 minutes

The hydrogels formed in this study are chemically cross-linked resulting in a polymer chain network structure with better swelling capacity as compared to respective polymers (Das *et al*., 2018). Gun *et al*. (2017) established that water in the hydrogel structure is attached through hydrogen bonding or the free water molecules fill up the voids or spaces present in the structure. The solvent molecules attack the hydrogel surface allowing the solvents to penetrate the network structure; this causes more solvents to be bound because of the expansion of the network (Bouhendi and Bagheri-marandi, 2010). When the citric acid concentration is <5% the swelling capacity was high throughout the study for all

conditions. In the case of saline and non-saline condition to mimic body fluid (NaCl and CaCl$_2$ solution), the highest swelling was 30 g/g and 26 g/g for 2.75 % citric acid as in Figure 4.17. The hydrogel with a low CA concentration is known to be more hydrophilic as compared to the high CA concentration, which results in a rigid network that absorbs less fluids.

The swelling capacity of KOH initiator synthesized hydrogels effects on different pH (2.08 and 12.82) are illustrated in Figure 4.18.
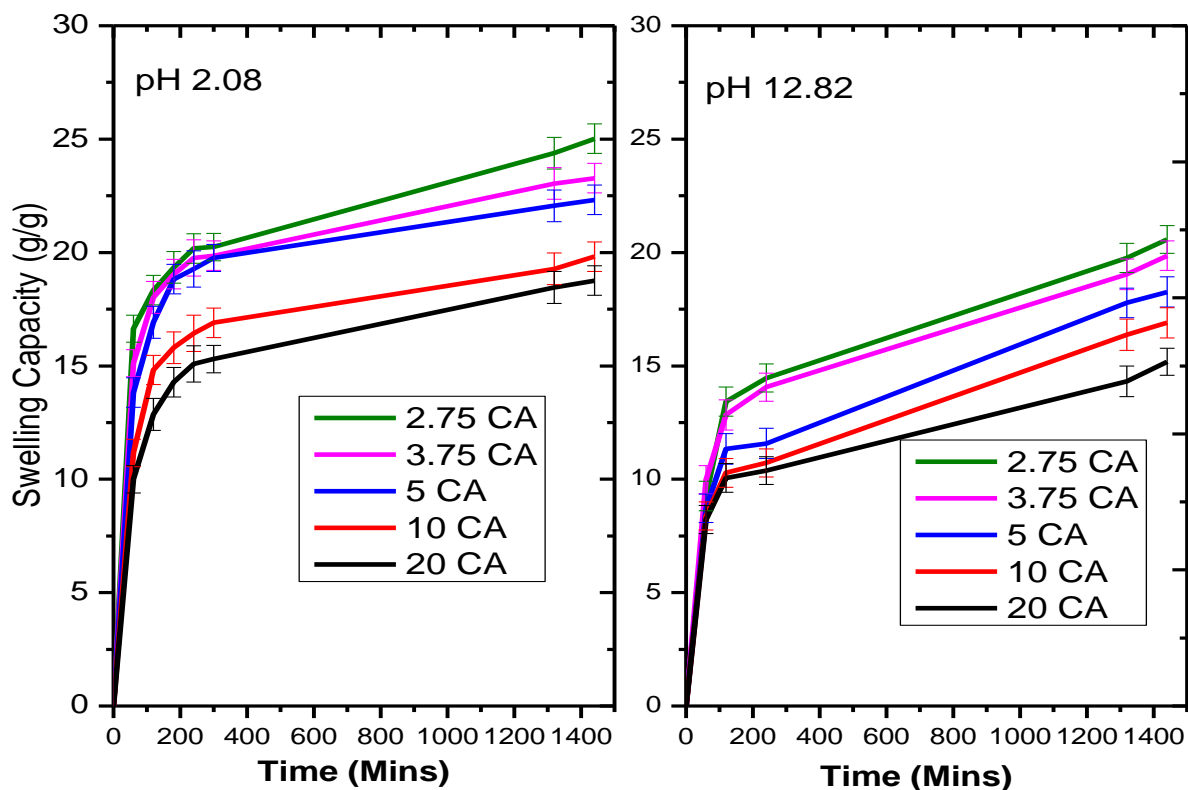
Figure 4.18: Swelling capacity synthesized hydrogel with citric acid in distilled water at pH 2.08 and 12.82 for 1440 minutes

The effect of pH was also determined at pH 7.0, 2.08, and 12.82 representing neutral, acidic, and basic conditions as in Figure 4.17 and 4.18 respectively. The swelling was high at lower CA concentration for all pH conditions, this increased from acidic media to a maximum at neutral and further decrease observed at the basic condition. At neutral pH, the hydrogel forms a network through hydrogen bonds with the water molecules, which

attack the surface causing swelling, thus water fills up the void spaces. In the case of an acidic medium, the presence of H^+ ions can be a protonated-causing attachment to the COO^- ion of the CA group or the CMC group (Tamura *et al.*, 2012). Repulsive forces cause less swelling of the hydrogel network as compared to the case of neutral pH where hydrogen bonding is prevalent. The force due to the rubbery elasticity of hydrogels varies with the degree of crosslinking hence a similarity in the swelling behavior. However, the basic medium contains Na^+ ions, which can cause deprotonation of attachment to COO^- group forming a stable compound, hence a decrease in the flexibility of the network (Kaith *et al.*, 2010). Consequently, the presence of -OH can also be attached chain network thus, result in less swelling ratio.

The effect of temperature on swelling capacity is displayed in Figure 4.19 for the synthesized hydrogel.
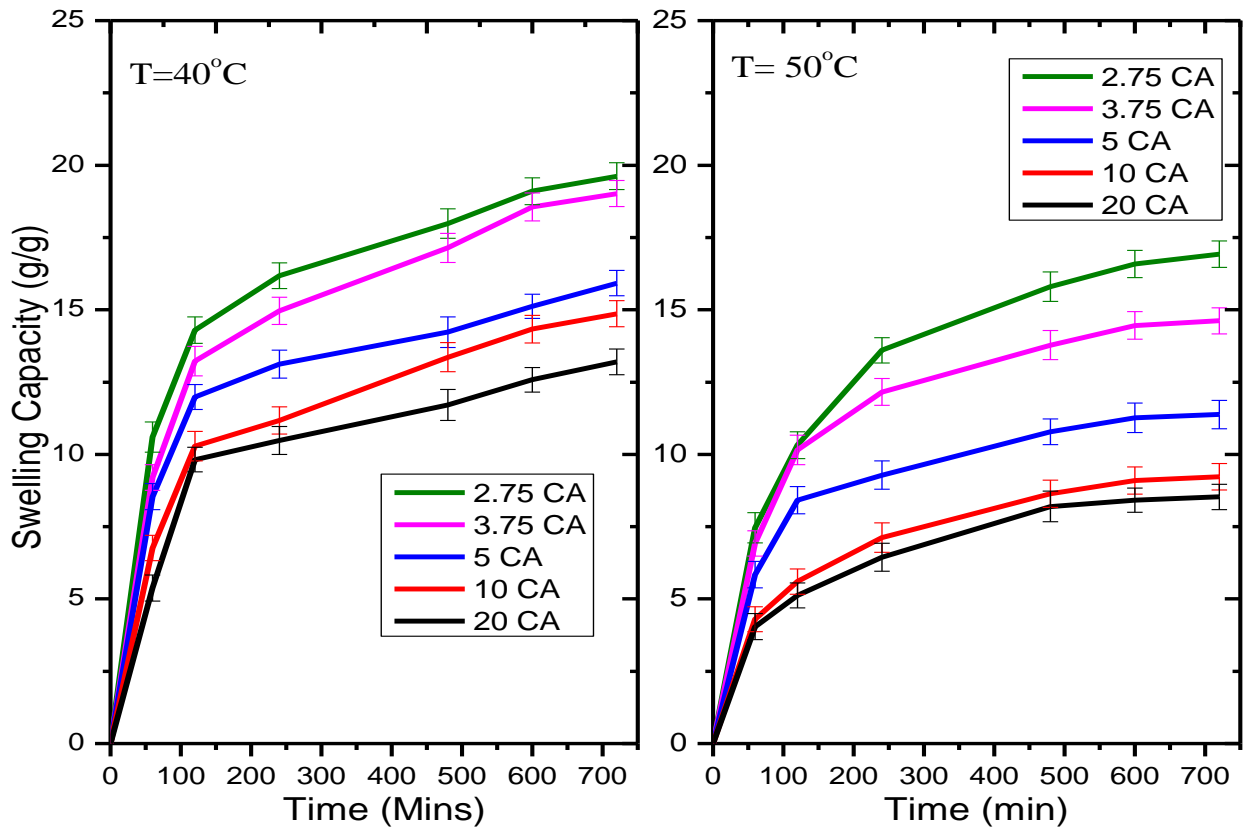
Figure 4.19: Swelling capacity of synthesized hydrogel with citric acid in distilled water at 40°C and 50°C for 700 minutes

The results displayed in Figure 4.19 show a similar trend whereby the low concentration CA hydrogels swell more than the high concentration. However, hydrogels are temperature sensitive; swelling capacity decrease with the increase in temperature and maximum swelling was at room temperature ((Figure 4.17) this was at room temperature. Therefore, these hydrogels are said to be thermo-responsive as the elasticity is affected by temperature (Dilaver, 2011). The polymer chain contract causing the pore network to shrink and this then limits the hydrogen bond formation with water molecules (del Valle *et al*., 2017). Generally, the swelling decreases with an increase in crosslinking agent ratio, caused by a rise in the cross-linked points, which yield short-chain networks. This causes the hydrogel to lose flexibility resulting in low swelling capacity (Saini, 2017).

4.2.6 Degradation Studies of Hydrogels

The degradation studies in distilled water of the synthesized hydrogels with varying citric acid concentrations are depicted in Figure 4.20.
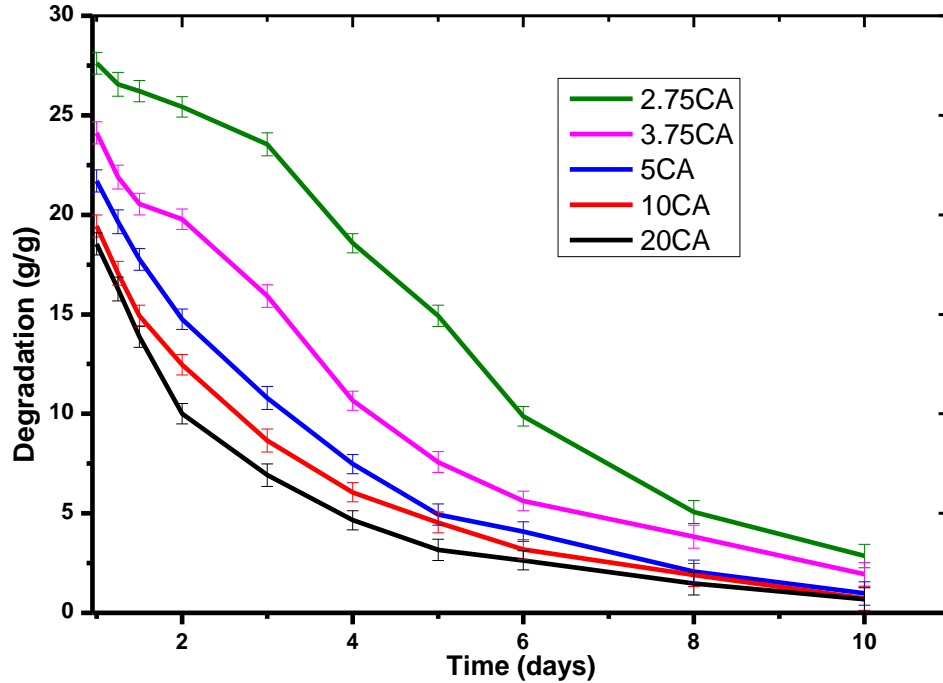
Figure 4.20: Degradation of synthesized hydrogel with varying citric acid concentrations for 10 days period

Degradation of swollen hydrogels was carried out after 24 hours of swelling in a non-saline solution at room temperature for ten days. The samples were kept in the same solution and mass measurement done after 24 hours. In Figure 4.20 when the concentration of the crosslinker was higher, the degradation was higher as compared to that with low concentration. When the citric acid concentration was greater than 5%, degradation was much faster due to the less stiff crosslinking networks that exist. Natural and synthetic hydrogels can be either bi-functional or multifunctional hence find application in different areas depending on their crosslinking nature (Zohuriaan-mehr and Kabiri, 2008). The ability of the hydrogel to release fluids after absorbing makes it an

important material that can help maintain the moisture of the soil in agriculture as well as in drug delivery provided the release rate is controlled (Hüttermann *et al*., 2009; Tamura *et al*., 2012). Furthermore, the aspect of degradation makes it environmentally friendly and therefore has no major impact on the environment (Mcbath and Shipp, 2010).

4.3 Application of Hydrogels

The quality of the soil under study was determined to obtain the favorable properties effective for tomato growth. The application studies were carried out in using hydrogel synthesized with 2.75% citric acid concentration, which exhibited the highest swelling capacity and slow degradation.

4.3.1 Soil Properties

The forest soil properties are displayed in Table 4.5.

Table 4.5: Summary of forest soil properties used for the growth of tomatoes

Parameter	Quantity (n=3) Mean ±SD
pH	4.4 ±0.02
Electrical Conductivity (dSm^{-1})	0.10 ±0.01
Total Nitrogen, (%N)	1.02 ±0.03
Phosphorus content, (mg/kg)	2.75 ±0.21
Potassium content, (mg/kg)	0.27 ±0.02

The nutrients present in soil depend upon the elemental nature of the soil and the organic material content (Brandy and Weil, 2004). Soil nutrients exist both as complex insoluble compounds and as simple soluble forms. Simple elements in the soil are readily available for plant uptake through the roots. The organic materials need to be broken down through decomposition to simpler, more available forms to benefit the plants (Ayilara *et al*., 2020).

The soil pH directly affects the availability of essential nutrients. In the case of acidic soils, minerals such as copper, manganese, and zinc become more available for plants' uptake. On the other hand, alkaline soil contains many bicarbonate ions which inhibit the normal uptake of other ions, thus influencing plant growth (Yimer and Chimdi, 2019). The tomato plant does well in the soil with a pH range of 5.5 - 6.8 which is slightly acidic. In Table 4.5 the soil was acidic hence some manure was added to all the soil media to regulate the acidity. According to Naika *et al*., (2005) the acidity can be managed by the addition of organic fertilizers. The number of soluble salts was determined as the electrical conductivity (EC) of soil. The soil electrical conductivity was found to be 0.10 dSm^{-1}, which was sufficient for the growth of tomatoes as they are tolerant to 2.5 dSm^{-1} according to the United States Department of Agriculture, (2014). The acceptable limit depends on the salt tolerance of the plants grown (Debnath and Pachauri, 2014). The EC levels can be used to infer the amount of water and water-soluble nutrients that are required for plant uptakes such as nitrates and potassium. Irrigation can however be used as a way of managing the EC levels tolerant to the plant as excess water flushes excess salts below the root zone.

Soil total nitrogen was found to be 1.02% and this was generally sufficient to support the growth of the tomato plant as they require nitrogen for chlorophyll. According to Landon, (2014) soil can be classified per the total nitrogen content, greater than 1.0% very high, 0.5 - 1.0% high, 0.2 - 0.5% medium, 0.1- 0.2% low, less than 0.1% as very low. In this case, the nitrogen concentration was very high which is influenced by the high carbon content present.

The total potassium and phosphorous (Table 4.5) present were found to be high for the forest soil. However, this potassium may not be readily available for plant use as they exist in various form. The potassium content of the soil can be described as adequate, high, and very high (Yimer and Chimdi, 2019). The soil pH affects the availability of the phosphorous to the plant as acidic soil has high iron or aluminum that can easily bind the phosphate group. Thus, the addition of organic fertilizer increases the availability of

phosphorous. The availability of phosphorous is influenced by the site conditions, such as moisture, temperature, aeration, and salinity which regulate its mineralization from organic matter decay (Prasad, 2019).

4.3.2 Tomato Plant Height Grown in Hydrogel Modified Soil

Figure 4.21 represents tomato plant height grown in hydrogel modified soil media with standard deviations in different water regimes; twice a week, after two days, and once a week respectively for 54 days. The soil media comprise of soil with hydrogel 2% and 1%, CMC 1%, 1% CMC + 1% hydrogel, and soil only as control.
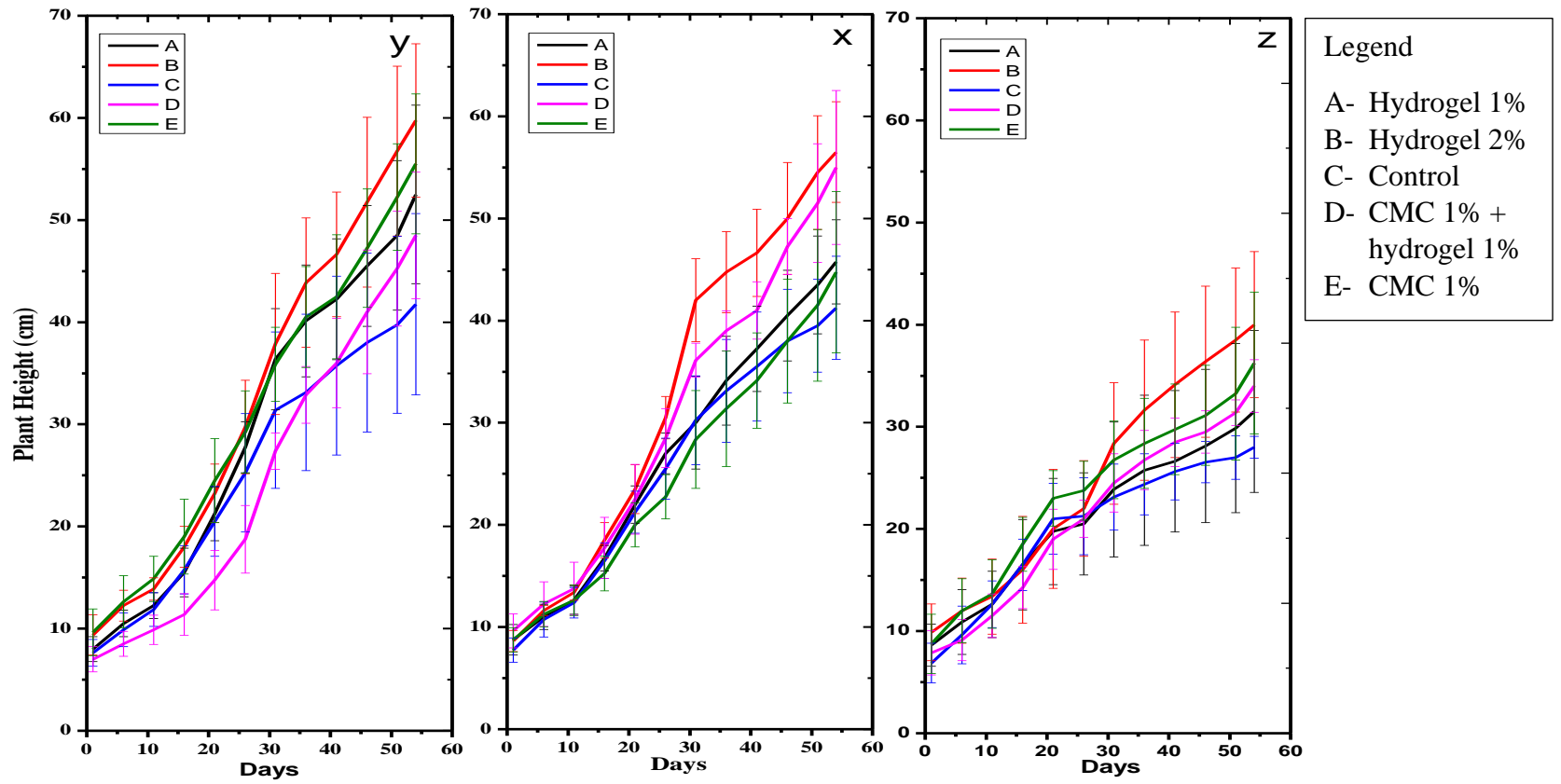
Figure 4.21: Tomato plant height grown in hydrogel modified soil at different water regimes

The plant height was measured from the base to the tip of the plant using a tape measure. The plant height growth rate was almost similar for the first 21 days in all treatments (Figure 4.21). The control sample showed a general low trend in the height for all the water regimes, whereas 2% of hydrogel media displayed a higher trend. However, for once per week water regime the plant height was generally low as compared to other regimes and this could be due to the water stress hence slow growth. The 1% CMC + 1% hydrogel displayed a higher height in watering twice a week as compared to after two days and once a week. When the hydrogel 1% was used the height was lower as compared to 2% hydrogel and with 1% CMC + 1% hydrogel. The lower height of the control sample can be ascribed to high infiltration of water through the soil, unlike the amended soil that retains moisture for longer periods.

Statistical analysis of the data obtained (Appendix C and D) revealed that there is a significant difference ($p \leq 0.05$) in the tomato plant height in the different water regimes and soil media composition, P= 5.3E-09 and P= 0.00535 respectively. Analysis with ANOVA (Appendix Q and R) showed that a rise in hydrogel concentration suggestively increases the amount of water available in the soil hence more growth. There existed some similarity on watering after two days and twice a week, whereas once a week showed some variation.

4.3.3 Tomato Plant Leaf Length Grown in Hydrogel Modified Soil

Figure 4.22 represents tomato plants' leaf length grown in hydrogel modified soil media with standard deviations in different water regimes; twice a week, after two days, and once a week respectively for 54 days.
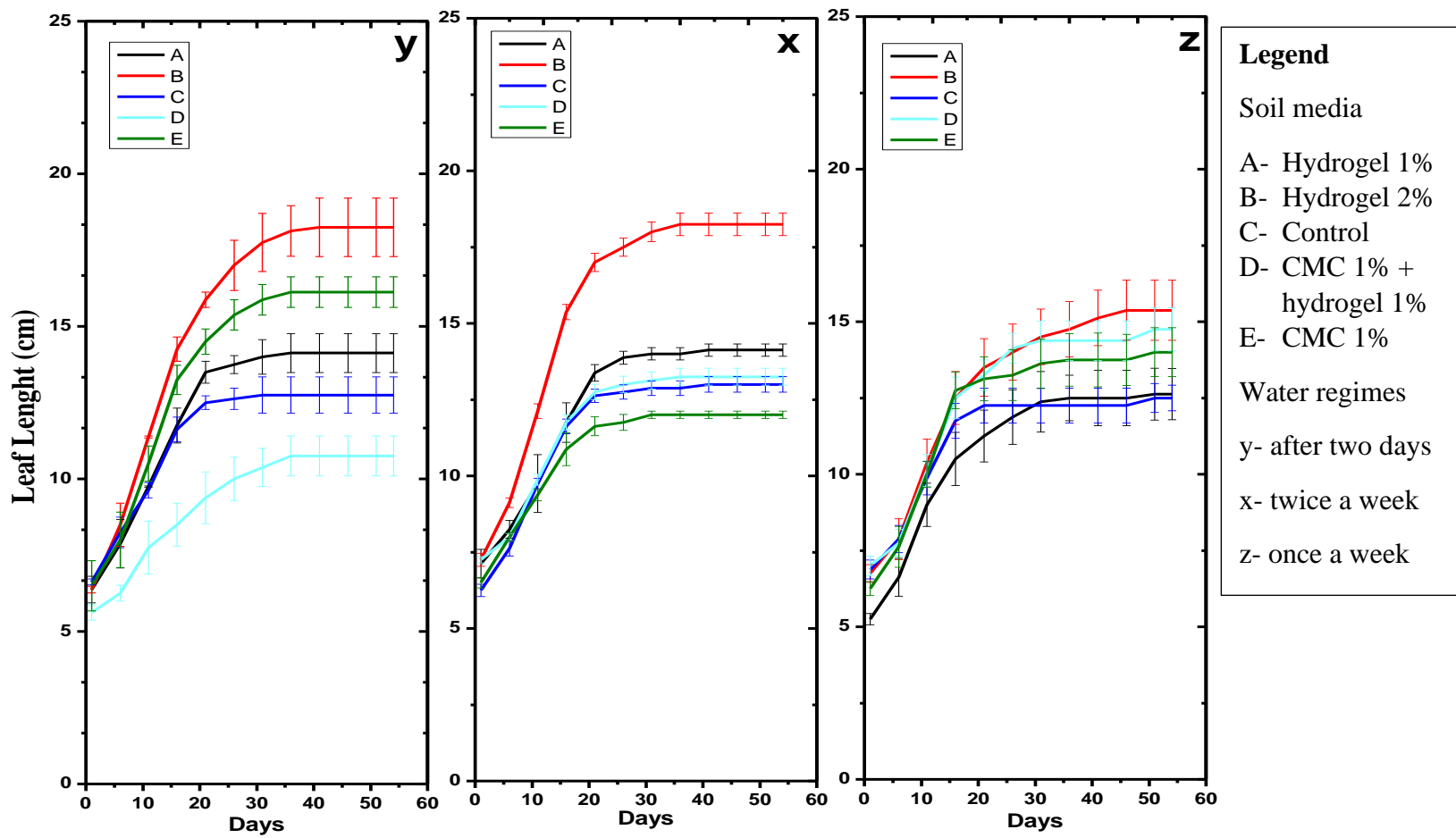
Figure 4.22: Tomato plant leaf length grown in hydrogel modified soil at different water regimes for 54 days

The length of the leaf was measured from the stem to the tip of the leaf that was chosen randomly and mapped for identification and the length monitored. Generally, the leaf chosen during the transplanting day reached a maximum growth length after 21 days (Figure 4.22). Plants with 2% hydrogel had the highest growth length in all the water regimes. A rapid increase in the leaf length was observed between day 6 and day 21 in all treatments. The leaves displayed a changing color to yellow on day 41 and most of them wilted. Wilting was observed more on watering once a week, as shown in Plate 4.1. The presence of moisture in the soil results in the growth of the leaves thus increase in length was higher in 2% hydrogel amended soils and lower in control (Agaba *et al*., 2011).

Plate 4.1: Side-view of tomato plants for once a week water regime at week 6 after transplanting for the different hydrogel modified soil

Statistical analysis of the data obtained (Appendix E and F) revealed that there was no significant difference ($p \leq 0.05$) in the tomato leaf length in the different water regimes, ($p = 0.317$). However, there was a significant difference ($p \leq 0.05$) in the tomato leaf length in the different soil media compositions, ($p = 2.75E-15$). ANOVA showed that a rise in hydrogel concentration resulted in increased growth of the leaf length. The high concentration of hydrogel renders an increase in soil moisture hence the growth of the

plant is more compared to low moisture in the soil. According to (Appendix Q), the soil treatment 2% hydrogel composition indicated was significantly different as compared to the other soil media that displayed some similarity.

4.3.4 Number of Leaves of Tomato Plants Grown in Hydrogel Modified Soil

The number of leaves of tomato plants is shown in Figure 4.23 grown in hydrogel-modified soil media with standard deviations in different water regimes; twice a week, after two days, and once a week respectively for 54 days.

Figure 4.23: Number of leaves for tomato plant grown in hydrogel modified soil at different water regimes for 54 days

The number of leaves was below 10 by the 26th day for both after two days and once a week for all treatments as shown in Figure 4.23. The water regime after two days had more leaves as compared to the other regimes. The hydrogel-amended soil had a higher number of leaves both once a week and after two days of watering regimes. When watering twice a week the control sample had a greater number of leaves, whereas 2% hydrogel amended soil was similar to that of CMC + hydrogel amended soil. Generally, CMC only amended soil had the lowest number of leaves.

Statistical analysis of the data obtained (Appendix G and H) revealed that there was no significant difference ($p \leq 0.05$) in the number of leaves in tomato plants in the different water regimes and soil media composition, p=0.474 and p=0.123 respectively. ANOVA test revealed there was no significant difference in the number of leaves in both treatment variables.

4.3.5 Number of Branches of Tomato Plants Grown in Hydrogel Modified Soil

The number of branches for the tomato plant is shown in Figure 4.24 grown in hydrogel-modified soil media with standard deviations in different water regimes; twice a week, after two days, and once a week respectively for 54 days.
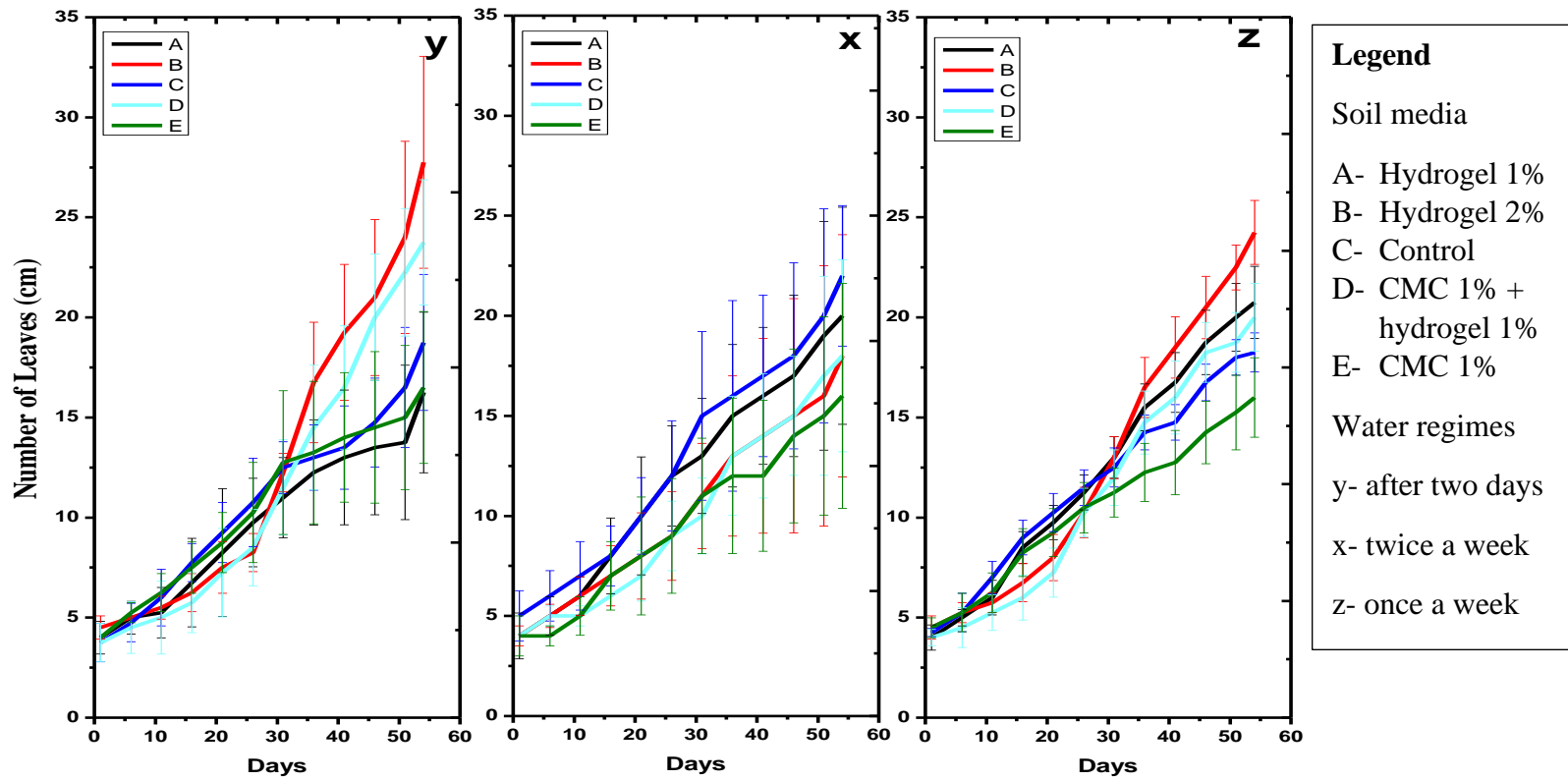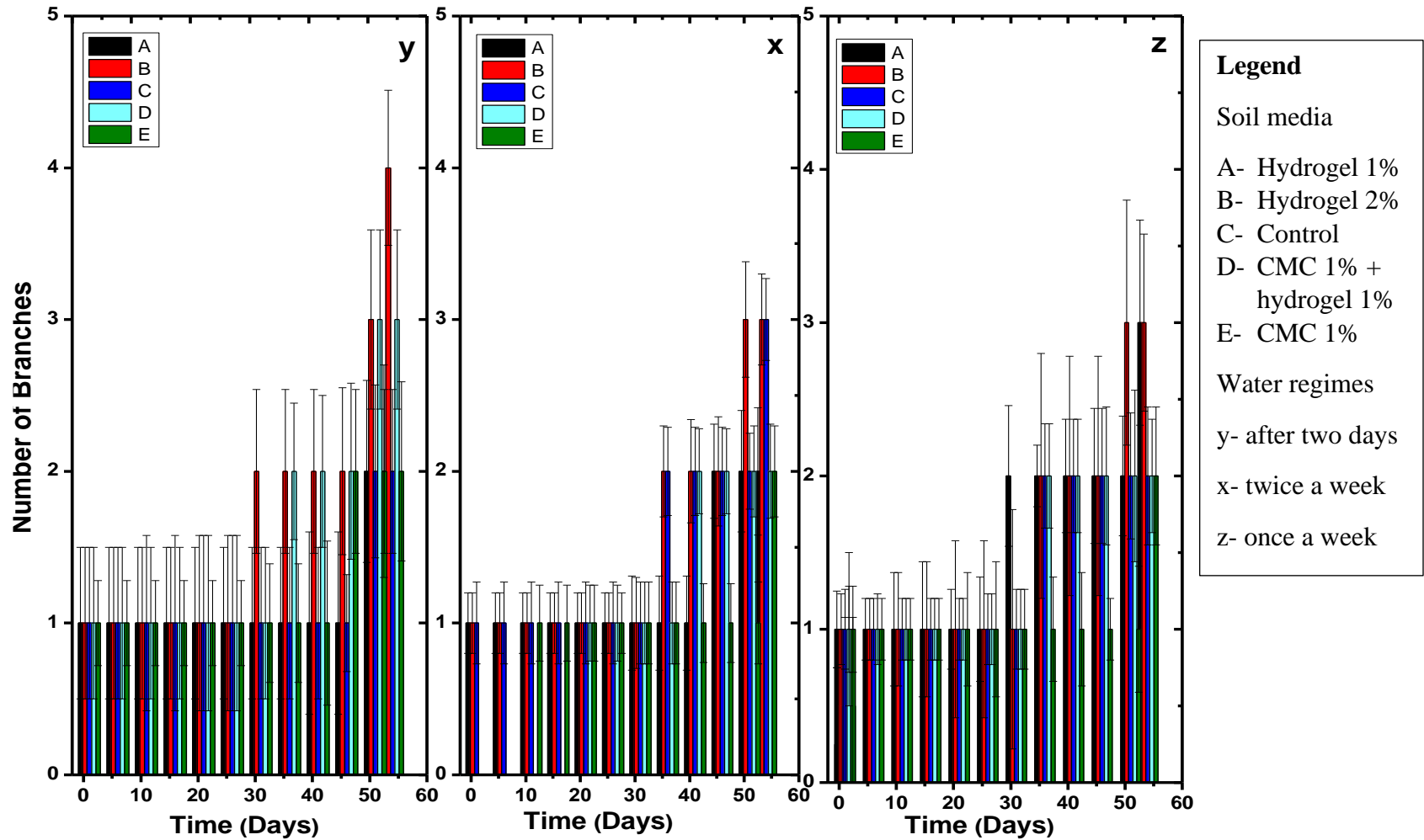
Figure 4.24: Number of branches of tomato plant grown in hydrogel modified soil at different water regimes for 54 days

The number of branches in all treatments was generally low, all below 5. The 2% hydrogel amended soil had more branches all through, 3, 4, and 3 twice a week, after two days and once a week respectively by the end of 8 weeks. In Figure 4.24 the control sample and 1% hydrogel amended soil had a maximum of 2, whereas the CMC amended soil had a lower number of branches in all water regimes displaying a maximum of 2 as compared to 2% hydrogel. In the case of 1% hydrogel amended soil, a high number of branches was observed while watering once a week (Figure 4.24).

Statistical analysis of the data obtained (Appendix I and J) revealed that there was a significant difference ($p \leq 0.05$) in the number of branches in tomato plants in the different water regimes and soil media composition. ANOVA test revealed that high hydrogel concentration translates to a rise in the water available in the soil thus its moisture, which promotes plant growth. According to (Appendix Q and R), there was some notable significant difference between watering once a week and after two days. Furthermore, on soil media composition, the control sample and 1% CMC amended soil exhibited some significant differences, whereas 2%, 1% hydrogel, and the 1% CMC + 1% hydrogel indicated similarities.

4.3.6 Root Growth of Tomato Plants Grown in Hydrogel Modified Soil

4.3.6.1 Root Score of Tomato Plants

Figure 4.25 displays the root score for tomato plants for different water regimes (twice a week, after two days, and once a week) with standard deviations grown in hydrogel modified soil media; hydrogel 1%, hydrogel 2%, control, CMC 1% + hydrogel 1% and CMC 1% for 54 days.
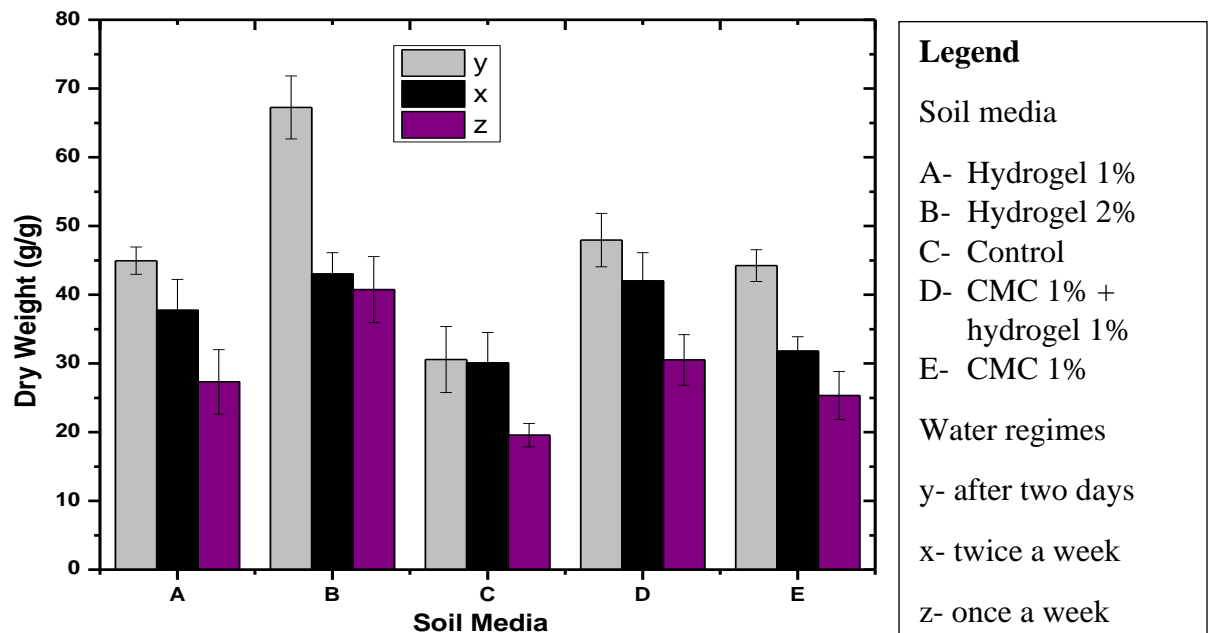
Figure 4.25: Root score for different water regimes for tomato plant grown in hydrogel modified soil for 54 days period.

Roots play a substantial role in the growth of plants beyond the support role. However, less focus is put on this part of the plants compared to the other parts. According to Aragao *et al*. (2008), the decline in plant root mass can be associated with low soil moisture. The root score was observed for the dry roots on a scale of 1, 3, and 5 designated as less dense, dense, highly dense root networks respectively. The 2% hydrogel containing soil (media B) had a generally high dense root network in all water regimes (Figure 4.25). When watering was after two days, the tomato had a high root network as compared to other water regimes as seen in Figure 4.25. Whereas watering once a week showed low root density for all the modified soil media. The roots play an important role in the growth of plants in that it aids in nutrient and water acquisition. The development of lateral roots increases the strength of roots (Ogbuehi *et al*., 2014). Plate 4.2 shows the various root network for the tomato plant before and after drying.
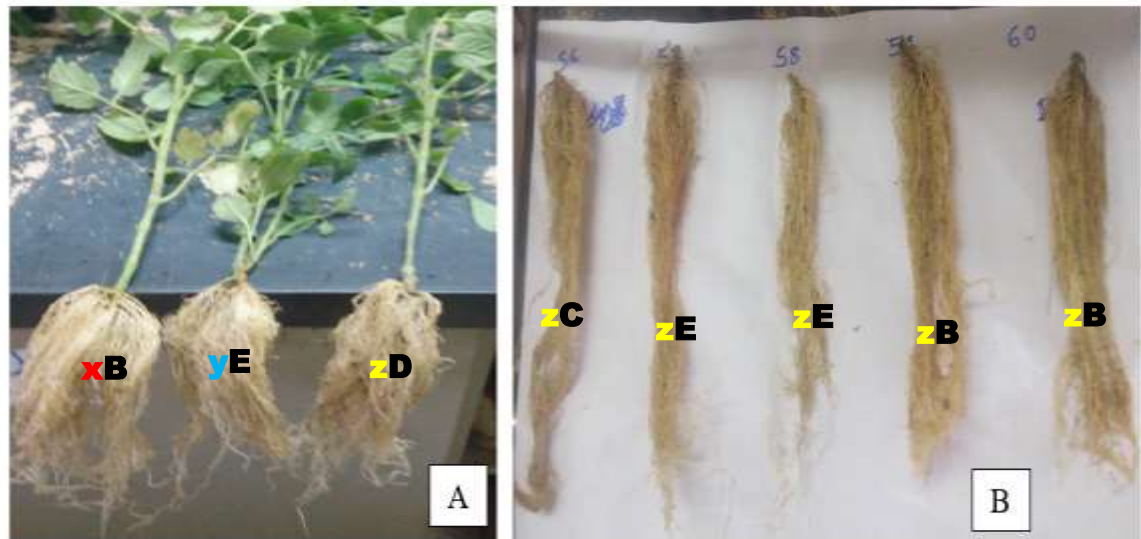
Plate 4.2: Root network development for wet tomato roots (A) and dry tomato plant roots (B)

Statistical analysis of the data obtained (Appendix K and L) revealed that there was a significant difference ($p \leq 0.05$) in the root score for tomato plant roots in the different water regimes and soil media composition. The root development is influenced by moisture content in the soil, thus the difference in the root network. In this case, the ANOVA test revealed that with 2% hydrogel modified soil and control plants were significantly different, whereas the other media displayed a similarity (Appendix Q). ANOVA test revealed no significant difference in the root score in terms of the three water regimes.

4.3.6.2 Root and Shoot Dry Mass

Figure 4.26 displays the tomato plants dry mass for root to shoot ratio for different water regimes (twice a week, after two days, and once a week) with standard deviations grown in hydrogel modified soil media; hydrogel 1%, hydrogel 2%, control, CMC 1% + hydrogel 1% and CMC 1% for 54 days. The dry mass root to shoot ratio was calculated according to Equation 3.12.
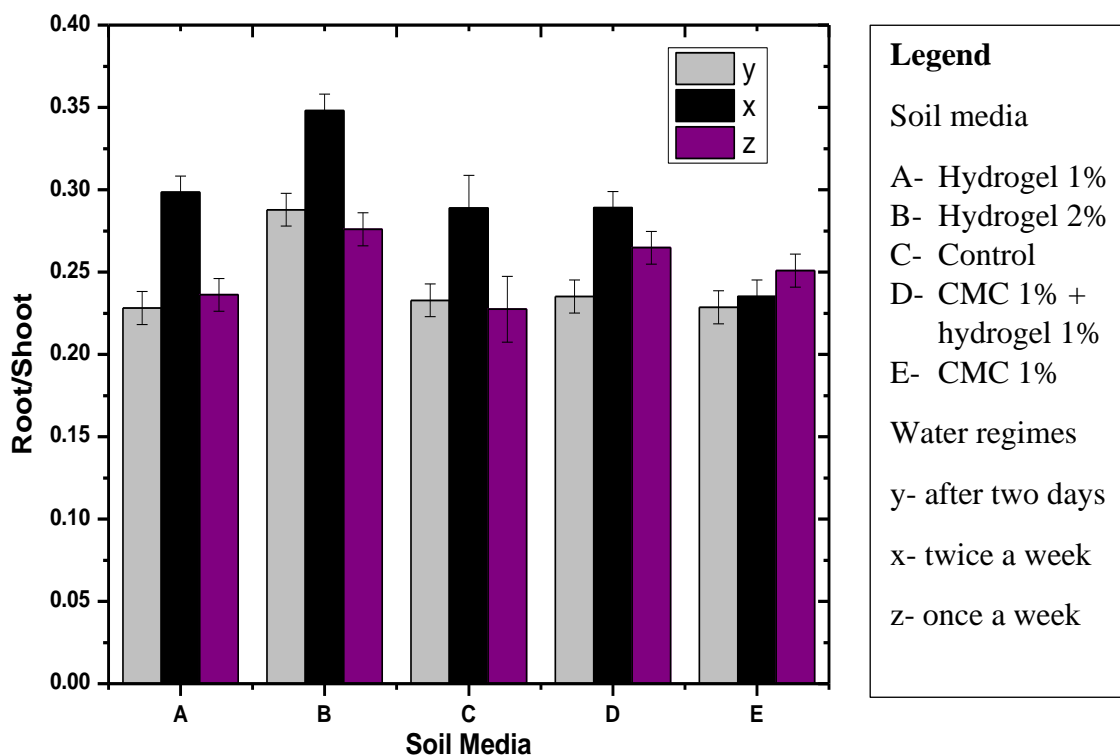
Figure 4.26: Root and shoot dry mass ratio for different water regimes for tomato plant grown in hydrogel modified soil for 54 days period

The health of a plant is influenced much by the root system as the roots permit water and nutrients absorption from the surrounding soil (Basirat *et al.*, 2011). In this experiment, the root to shoot ratio for the control sample will provide the normal for all soil media composition. Therefore, from Figure 4.26, when watering twice a week the plant growth was good for 2% and 1% hydrogel soil media as their ratio was higher than control media. The 1% CMC + 1% hydrogel media had similar characteristics as the control. Finally, the 1% CMC had poor plant health as it was below the control. Then after two days of water regime, 2% hydrogel and 1% hydrogel + 1% CMC media indicate good plant health, whereas 1% hydrogel and 1% CMC soil media being slightly below the control media had poor health. All the soil media display good plant growth when watering once a week, as their ratios are above the control media. In general, the 2% hydrogel-modified soil media had good plant growth. The health of a plant is influenced by factors such as nutrient

availability, moisture levels, temperature, pH and salinity among others. The development of the root affects the growth of the shoot as when there are fewer root hairs there is minimal growth. The 2% hydrogel amended soil led to the development of a condensed root network leading to aggregation, which generates good interaction with the soil moisture thus better utilization of the water by the plant for growth (Agaba *et al*., 2011).

Statistical analysis of the data obtained (Appendix M and N) revealed that there was a significant difference ($p \leq 0.05$) in the root to shoot ratio for tomato plants in the different water regimes and soil media composition. The root to shoot ratio is influenced by moisture content and nutrients in the soil, thus the difference in the root growth and shoot development. In this case, the ANOVA test revealed that 2% hydrogel modified soil and 1% hydrogel modified soil, control and CMC 1% plants were significantly different. Although, control and 1% hydrogel show similarity. However, the CMC 1% + hydrogel 1% was not significantly different (Appendix Q). Similarly, there was a significant difference in the root to shoot for the after two days and then twice a week water regime. Once a week was not significantly different from the other two water regimes (Appendix R).

4.3.7 Plant Moisture of Tomato Plants Grown in Hydrogel Modified Soil

Figure 4.27 displays the difference in tomato plant mass for different water regimes (twice a week, after two days, and once a week) with standard deviations grown in hydrogel modified soil media; hydrogel 1%, hydrogel 2%, control, CMC 1% + hydrogel 1% and CMC 1% for 54 days. The plant moisture refers to the difference in mass of the fresh plant and that of the dried plant calculated using Equation 3.13.

Figure 4.27: Plant moisture for different water regimes for tomato plant grown in hydrogel modified soil for 54 days period
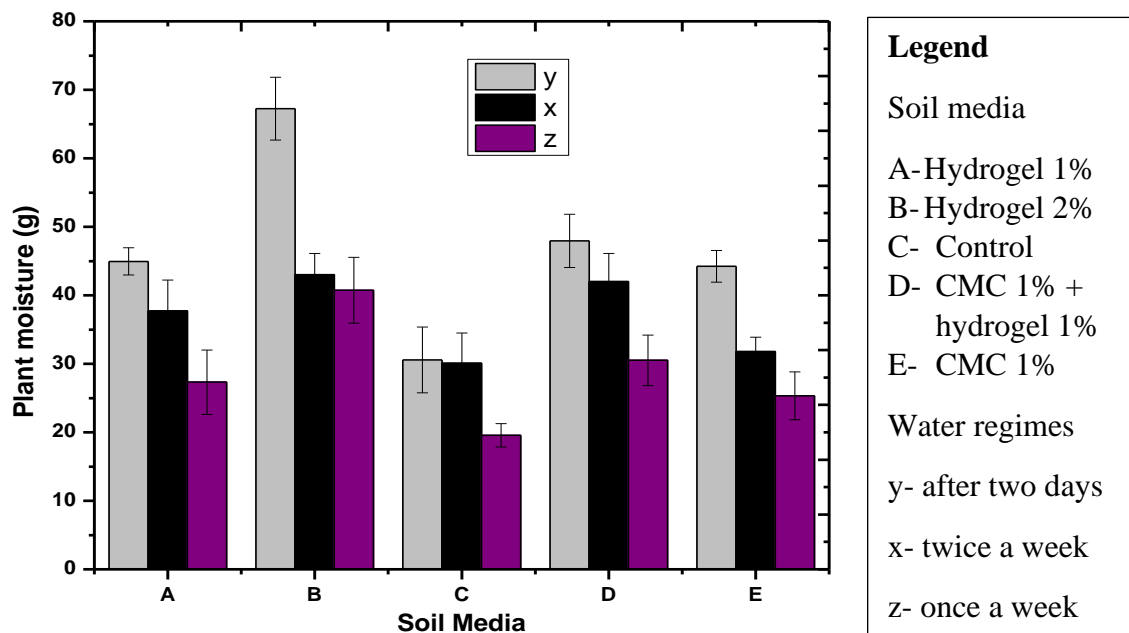
In this experiment, the after two days water regime had high plant moisture in all modified soil media, followed by twice a week with the lowest being a once-a-week water regime. In terms of the modified soil media composition, the plant moisture displays a decreasing pattern in the order media B, D, A, E then C as in Figure 4.27. The control sample had the lowest mass in all cases; this is because the water loss rate through percolation was higher in the soil alone. Unlike modified soil media that contain hydrogel and CMC that have water retention abilities; hence, plant moisture is affected. The plant moisture provides information on the amount of water that is available in the plant and this can vary depending on the soil moisture and other factors. Othmani *et al.* (2015) suggested that plants under water stress or deficit tend to store less water in their stem and leaves, thus giving a lower yield. Watering frequency influences the amount of water stored in the plant system thus hydrogels' presence acted as a water reservoir making it available for the plant during the watering cycles. Therefore, this enhanced growth in media B plants,

thus high dry mass. This confirms the previous results for root development that a dense root network increases the dry mass.

Statistical analysis of the data obtained (Appendix O and P) revealed that there was a significant difference ($p \leq 0.05$) in the plant moisture in tomato plants in the different water regimes and soil media composition. The p-value for water regimes and soil media composition were 2.41E-06 and 7.14E-05 respectively. The plant mass is a result of moisture content in the plant, thus influenced by the amount of water uptake. In this case, the ANOVA test (Appendix Q) revealed that % hydrogel modified soil and 1% hydrogel modified soil, control and CMC 1% plants were significantly different. Although, control and 1% hydrogel show similarity. However, the CMC 1% + hydrogel 1% was not significantly different. Consequently, after two days and twice a week water regime were significantly different while for once a week water regime the results were significantly different as indicated in Appendix R.

In general, the control sample growth was almost similar to the amended soils in the first 21 days as not much difference was noted. In the fourth week, however, changes were evident as signs of wilting were observed in some treatments for the various water regimes. This resulted in a variation in growth of the plant height, leaf length, number of branches, and the number of leaves. The tomato plant was selected because it is resilient to agronutrients, resulting in substantial growth after irrigation (Hunter, 2010). Any minimal changes that can subject stress to the plant are easily noted with the tomato plant.

The control soil sample depleted its maximum water content after three days and around the third day, the plant had begun to wilt, and there was cohesion in the soil, indicating that the sample needed to be re-irrigated. During this time, the plant was subjected to leaf damage and a reduction in the number of leaves, as well as a decrease in the sample's height. Upon irrigation, the plant grew and increased in the number of leaves, height, and thickness. However, for the case of hydrogel and CMC modified soil growth was almost similar for the 1% CMC + 1% hydrogel and the 1% CMC, whereas 2% hydrogel growth

78

was the highest. The wilting signs for higher hydrogel percentages were observed after the fifth or sixth day after irrigation.

An increase in water volume from 250 mL to 300 mL on day 26 showed a rise in growth in all samples, therefore, higher plants require more water for survival and growth. The use of hydrogel to amend soil moisture in the once-a-week water regime was effective as the general plant growth was high throughout (Demitri *et al*., 2013). Thus, hydrogel can be utilized to reduce irrigation frequency. The use of high percentage hydrogel was effective as compared to a lower percentage or CMC + hydrogel. The optimum plant growth was observed when watering regime was after two days followed by twice a week and then once a week. The tomato plant performance and growth effects during the 54 days of study are displayed in Plate 4.3 and Appendix T and U.

Plate 4.3: Tomato plant growth performance in hydrogel modified soil observed from front view at different weeks for different water regimes

The plant growth in all the treatments was almost uniform until week 4. All treatments were irrigated according to their regime. The wilting experience was mild as the plants were not completely dry, once a week water regime experienced wilting by day 3 for control and by day 5 or 6 with the hydrogel amended soil as observed in Plate 4.3 and Appendix U. The irregular growth patterns observed were caused by wilting and after irrigation, the plants returned to growth. It was evident that the higher hydrogel in soil increased water retention hence the plant sample was resistant to drought-like conditions thus more growth (Cannazza *et al*., 2014). There is need to upscale on water conservation practices making it operative and affordable, reducing water wastage while capitalizing on crop yield. This will meet the rising population demand for food as production increases as result of efficient use of water in irrigation.

The tomato plant is not drought-resistant thus requires watering frequently for better quality yields. The amount of water required is dependent on the type of soil, as different soils have differing irrigation patterns. The addition of hydrogel to the soil improves the water retention capacity of the soil (Amend, 2005). Good soil aeration provides a good environment for root development thus improved yield. By observation, the plants in hydrogel-modified soil maintained a fresh growth for a longer period while control almost wilted before irrigation again especially in the once per week water regime (Plate 4.3 and Appendix U). Hydrogels have provided a solution to the reduction of irrigation frequency. An effective schedule of irrigation time is important as water is administered only when needed (Alhammadi and Al-shrouf, 2013). Hydrogels can swell, shrink, and re-swell, thus, reducing percolation and runoff by retaining water and releasing it later (Ghyadah *et al*., 2018).

CHAPTER FIVE

CONCLUSION AND RECOMMENDATIONS

5.1 Conclusion

Agricultural waste can be utilized through value addition to produce other products. In the case of unpredictable climatic changes resulting in scarcity of water in both arid and semi-arid areas use of hydrogels can be used to curb the situation. The following conclusion can be drawn from the study;

i. Coir fibers constituted 42.1 ±1.5% cellulose thus making it a potential source of cellulose adding value to this waste material. The cellulose extracted was characterized with functional groups of typical cellulose material with good thermal properties. The swelling capacity of the extracted cellulose was low and the presence of OH groups create an amicable environment for modification.

ii. The derivatization of cellulose was done by esterification in an alkaline medium. The CMC from coir fiber exhibited a moderate swelling ratio and a high degree of substitution making it efficient for further surface modification. The resultant CMC displayed typical functional groups as that of standard CMC material. Compared to the precursor they exhibit good thermal properties and high ash content due to sodium metal presence.

iii. Synthesis of CMC/HEC hydrogels using citric acid as a crosslinking agent produced superabsorbent hydrogels that are swellable, thermally stable, and degradable. The synthesized hydrogel with low citric concentration exhibited a high swelling ratio and slow degradation. These hydrogels displayed characteristics similar to cellulose as this is the major backbone of the resultant product. The improvement of the properties of HEC-CMC hydrogel was a result of the good characteristics of derivatized CMC, particularly having accessible functional groups for modification.

iv. The ability to absorb and retain large water volumes has proven hydrogels ideal for use in crop production as a water reservoir. This has led to improved water retention of soils and the water supply to plants.

v. The hydrogels developed had a good swelling capacity and good retention thus can be said to be viable for use in crop production reducing the irrigation efficiency while maximizing the water available for the plant. In this study, the optimum watering pattern was after two days.

5.2 Recommendations

The following recommendations can be made from this study and future works.

5.2.1 Recommendation from this Study

i. HEC-CMC hydrogels' ability to retain water for long periods could be explored as a material for the fabrication of biodegradable hygiene products.

ii. There is a need to explore the impact of using different crosslinking agents such as maleic acid, epichlorhydrin on the swelling capacity of hydrogels

iii. The characterization and utilization of lignin, which is a byproduct of cellulose extraction should be explored.

iv. The use of hydrogel as a delivery system for fertilizer or nutrient delivery should be explored.

5.2.2 Recommendation for Further Works

i. There is need to synthesize hydrogels using other agricultural biomass and compare their activity with others.

ii. Raising awareness to the general public on the availability of natural hydrogels emphasizing on the merits.

REFERENCES

Abdel-Halim, E. S. (2014). Chemical Modification of Cellulose Extracted from Sugarcane Bagasse: Preparation of Hydroxyethyl Cellulose. *Arabian Journal of Chemistry*, *7*(3), 362–371.

Agaba, H., Justus, L., Orikiriza, B., Obua, J., and Kabasa, J. D. (2011). Hydrogel Amendment to Sandy Soil Reduces Irrigation Frequency and Improves the Biomass of Agrostis stolonifera. *Agricultural Sciences*, *2*(4), 544–550.

Agrawal, A., Allen, J. J., Fei, H., Fisher, E., Boyd, T., and Bovet, C. (2019). Physical and Thermal Analysis. In *Physical Methods in Chemistry and Nano Science,* 141–336. Rhaptos.

Ahmed, E. M. (2015). Hydrogel: Preparation, Characterization, and Applications: A Review. *Journal of Advanced Research*, *6*(2), 105–121.

Ahorsu, R., Medina, F., and Constanti, M. (2018). Significance and Challenges of Biomass as a Suitable Feedstock for Bioenergy and Biochemical Production: A Review. *Energies*, *11*(3366), 1–19.

Akar, E., and Altınıs, A. (2012). Preparation of pH- and Ionic-Strength Responsive Biodegradable Fumaric Acid Crosslinked Carboxymethyl Cellulose. *Carbohydrate Polymers*, *90*(4), 1634–1641.

Alhammadi, M. S., and Al-shrouf, A. M. (2013). Irrigation of Sandy Soils, Basics and Scheduling. In *Crop Production*, 49–67. IntechOpen.

Allen, J. J., Fei, H., Fisher, E., Boyd, T., Bovet, C., and Agrawal, A. (2012). *Physical Methods in Chemistry and Nano Science*. Rice University Texas: Connexions.

Amen-Chen, C., Pakdel, H., and Roy, C. (2001). Production of Monomeric Phenols by Thermochemical Conversion of Biomass: A Review. *Bioresource Technology*, *79*(3), 277–299.

Amend, I. (2005). Irrigation Water Management. In *National Irrigation Guide,* 1–754.

Aragao, L. E., Goncalves, P. H., Silva, J. de A., and Dawson, L. A. (2008). The Effects of Water Availability on Root Growth and Morphology in an Amazon Rainforest. *Plant Soil*, *311*(1), 189–199.

Asl, S. A., Mousavi, M., and Labbafi, M. (2017). Synthesis and Characterization of Carboxymethyl Cellulose from Sugarcane. *Journal of Food Processing and Technology*, *8*(8), 1–6.

Astrini, N., Anah, L., and Haryono, A. (2012). Crosslinking Parameter on the Preparation of Cellulose Based Hydrogel with Divynilsulfone. *Procedia Chemistry*, *4*, 275–281.

Ayilara, M. S., Olanrewaju, O. S., Babalola, O. O., and Odeyemi, O. (2020). Waste Management through Composting: Challenges and Potentials. *Sustainability*, *12*(4456), 1–23.

Azadfar, M., Gao, A. H., and Chen, S. (2015). Structural Characterization of Lignin: A Potential Source of Antioxidants Guaiacol and 4-Vinylguaiacol. *International Journal of Biological Macromolecules*, *75*, 58–66.

Azubuike, C., Odulaja, J., and Okhamafe, A. (2012). Physicotechnical, Spectroscopic and Thermogravimetric Properties of Powdered Cellulose and Microcrystalline Cellulose Derived from Groundnut Shells. *International Pharmaceutical Excipients Council*, *3*(3), 106–115.

Azubuike, C. P., and Esiaba, J. (2012). Investigation Into Some Physico-Technical and Tableting Properties of Low-Crystallinity Powdered Cellulose Prepared from Corn Residues. *Journal of Pharmaceutical Research and Opinion*, *2*(8), 94–98.

Barba, C., Montané, D., Farriol, X., Desbrières, J., and Rinaudo, M. (2002). Synthesis and Characterization of Carboxymethyl Cellulose from Non-wood Pulps II. Rheological Behavior of CMC in Aqueous Solution. *Cellulose*, *9*(3–4), 327–335.

Basirat, M., Malboobi, M. A., Mousavi, A., Asgharzadeh, A., and Samavat, S. (2011). Effects of Phosphorous Supply on Growth, Phosphate Distribution and Expression of Transporter Genes in Tomato Plants. *Australian Journal of Crop Science*, *5*(5), 537–543.

Beena, K. S. (2013). Case Studies on Application of Coir Geotextiles for Soil Stabilization. *International Conference on Case Histories in Geotechnical Engineering*, 1–7.

Berglund, J., Mikkelsen, D., Flanagan, B. M., Dhital, S., Gaunitz, S., Henriksson, G.,

Lindström, M. E., Yakubov, G. E., Gidley, M. J., and Vilaplana, F. (2020). Wood Hemicelluloses Exert Distinct Biomechanical Contributions to Cellulose Fibrillar Networks. *Nature Communications*, *11*(4262), 1–16.

Beuther, P. D., Veith, M. W., and Zwick, K. J. (2010). Characterization of Absorbent Flow Rate in Towel and Tissue. *Journal of Engineered Fibers and Fabrics*, *5*(2), 1–7.

Bharadwaj, S., and Patkar, A. (2004). Menstrual Hygiene and Management in Developing Countries: Taking Stock. In *Junction Social*.

Bhardwaj, A. K., Shainberg, I., Warrington, D. N., and Levy, G. (2007). Water Retention and Hydraulic Conductivity of Cross-Linked Polyacrylamides in Sandy Soils. *Soil Science Society of American Journal*, *71*(2), 406–412.

Bista, P., Ghimire, R., Machado, S., and Pritchett, L. (2020). Response of Ancient and Modern Wheat Varieties to Biochar Application: Effect on Hormone and Gene Expression Involved in Germination and Growth. *Agronomy*, *10*(5), 1–11.

Bouhendi, H., and Bagheri-marandi, G. (2010). Cross-Linked Poly (Acrylic Acid) Microgels from Precipitation Polymerization. *Polymer-Plastics Technology and Engineering*, *49*, 1257–1264.

Brandy, N., and Weil, R. (2004). *Elements of the Nature and Properties of Soils* (2nd ed.). Pearson College Div.

Cannazza, G., Cataldo, A., Benedetto, E. De, Demitri, C., Madaghiele, M., and Sannino, A. (2014). Experimental Assessment of the Use of a Novel Superabsorbent polymer (SAP) for the Optimization of Water Consumption in Agricultural Irrigation Process. *Water*, *6*(7), 2056–2069.

Capanema, N. S. V, Mansur, A. A. P., Jesus, A. C. De, Carvalho, S. M., Oliveira, L. C. De, and Mansur, H. S. (2018). Superabsorbent Crosslinked Carboxymethyl Cellulose-PEG Hydrogels for Potential Wound Dressing Applications. *International Journal of Biological Macromolecules*, *106*, 1218–1234.

Cavka, A., Guo, X., Tang, S., Winestrand, S., Jönsson, L. J., and Hong, F. (2013). Production of Bacterial Cellulose and Enzyme from Waste Fiber Sludge. *Biotechnology for Biofuels*, *6*(25), 1–10.

Chan, E. W. C., Huang, C. M. Y., Chia, P. X., Lim, C. S. S., Nai, J. Q., Ding, D. Y., Seow, P. B., and Wong, C. W. (2017). Synthesis and Characterisation of Carboxymethyl Cellulose from Various Agricultural Wastes. *Cellulose Chemistry and Technology*, *51*(7–8), 665–672.

Chen, P., Zhang, W., Luo, W., and Fang, Y. (2004). Synthesis of Superabsorbent Polymers by Irradiation and Their Applications in Agriculture. *Journal of Applied Polymer Science*, *93*, 1748–1755.

Chen, Y., Zou, C., Mastalerz, M., Hu, S., and Gasaway, C. (2015). Applications of Micro-Fourier Transform Infrared Spectroscopy (FTIR) in the Geological Sciences - A Review. *International Journal of Molecular Science*, *16*, 30223–30250.

Ciolacu, D., Ciolacu, F., and Popa, V. I. (2011). Amorphous Cellulose – Structure and Characterization. *Cellulose Chemistry and Technology*, *45*(1–2), 13–21.

Collazo-bigliardi, S., Ortega-toro, R., and Chiralt, A. (2018). Isolation and Characterisation of Microcrystalline Cellulose and Cellulose Nanocrystals from Coffee Husk and Comparative Study with Rice Husk. *Carbohydrate Polymers*, *191*, 205–215.

Das, S., Kumar, V., Tiwari, R., Singh, L., and Singh, S. (2018). Recent Advances in Hydrogels for Biomedical Applications. *Asian Journal of Pharmaceutical and Clinical Research*, *11*(11), 62–68.

Debnath, S., and Pachauri, S. (2014). *Soil Sampling in Horticultural Crops and Routine Soil Testing*.

del Valle, L., Diaz, A., and Puiggali, J. (2017). Hydrogels for Biomedical Applications: Cellulose, Chitosan, and Protein/Peptide Derivatives. *Gels*, *3*(3), 1–28. 7

Demitri, C, Scalera, F., Madaghiele, M., Sannino, A., and Maffezzoli, A. (2013). Potential of Cellulose-Based Superabsorbent Hydrogels as Water Reservoir in Agriculture. *International Journal of Polymer Science*, *2013*(435073), 1–6.

Demitri, Christian, Del Sole, R., Scalera, F., Sannino, A., Vasapollo, G., Maffezzoli, A., Ambrosio, L., and Nicolais, L. (2008). Novel Superabsorbent Cellulose-Based Hydrogels Crosslinked with Citric Acid. *Journal of Applied Polymer Science*,

110(4), 2453–2460.

Dilaver, M. (2011). *Preparation and Characterization of Carboxymethylcellulose Based Hydrogels*. Dokuz Eylül University.

Ferdus, A. (2014). *Coconut or Coir Fiber: Properties, Manufacturing Process and Applications*.

Ferreira, R. L., Furtado, C. R. G., Visconte, L. L. Y., and Leblanc, J. L. (2006). Optimized Preparation Techniques for PVC-Green Coconut Fiber Composites. *International Journal of Polymeric Materials and Polymeric Biomaterials*, *55*(12), 1055–1064.

Garside, P., and Wyeth, P. (2003). Identification of Cellulosic Fibres by FTIR Spectroscopy. *International Institute for Conservation of Historic and Artistic Works, Taylor and Francis*, *48*(4), 269–275.

Geocon Surveys Limited. (2021). *Location Map of Kocos Kenya Limited*.

Ghadi, R., Jain, A., Khan, W., and Domb, A. J. (2016). Microparticulate Polymers and Hydrogels for Wound Healing. *Wound Healing Biomaterials*, *2*, 203–225.

Ghorpade, V. S., Vyankatrao, A., and Jacky, R. (2017). Citric Acid Crosslinked β-Cyclodextrin/ Carboxymethylcellulose Hydrogel Films for Controlled Delivery of Poorly Soluble Drugs. *Carbohydrate Polymers*, *164*, 339–348.

Ghyadah, R. A., Alokely, R., and Jabari, M. Al. (2018). *Utilizing Hydrogel for Improving Irrigation Management*. Palestine Polytechnic University.

Gigac, J., and Fišerová, M. (2008). Influence of Pulp Refining on Tissue Paper Properties. *Tappi Journal*, *7*(8), 27–32.

Gill, P., Moghadam, T. T., and Ranjbar, B. (2010). Differential Scanning Calorimetry Techniques: Applications in Biology and Nanoscience. *Journal of Biomolecular Techniques*, *21*(4), 167–193.

Golzarian, M. R., Frick, R. A., Rajendran, K., Berger, B., Roy, S., Tester, M., and Lun, D. S. (2011). Accurate Inference of Shoot Biomass from High-throughput Images of Cereal Plants. *Plant Methods*, *7*(2), 1–11.

Gun, V. M., Savina, I. N., and Mikhalovsky, S. V. (2017). Properties of Water Bound in Hydrogels. *Gels*, *3*(37), 1–30.

Gupta, A., and Prakash, J. (2015). Sustainable Bio-ethanol Production from Agro-residues: A Review. *Renewable and Sustainable Energy Reviews*, *41*, 550–567.

Hadi, N. A., Wiege, B., Stabenau, S., Marefati, A., and Rayner, M. (2020). Comparison of Three Methods to Determine the Degree of Substitution of Quinoa and Rice Starch Acetates, Propionates, and Butyrates: Direct Stoichiometry, FTIR, and 1H-NMR. *Foods*, *9*(83), 1–14.

Haleem, N., Arshad, M., Shahid, M., and Tahir, M. A. (2014). Synthesis of Carboxymethyl Cellulose from Waste of Cotton Ginning Industry. *Carbohydrate Polymers*, *113*, 249–255.

Hashem, M., Sharaf, S., Abd El-Hady, M. M., and Hebeish, A. (2013). Synthesis and Characterization of Novel Carboxymethylcellulose Hydrogels and Carboxymethylcellulolse-Hydrogel-ZnO-Nanocomposites. *Carbohydrate Polymers*, *95*(1), 421–427.

Holder, C., and Schaak, R. (2019). Tutorial on Powder X-ray Diffraction for Characterizing Nanoscale Materials. *American Chemical Society*, *13*(7), 7359–7365.

Hubbe, M. A., Ayoub, A., Daystar, J. S., Venditti, R. A., and Pawlak, J. J. (2013). Enhanced Absorbent Products Incorporating Cellulose and its Derivatives: A Review. *BioResources*, *8*(4), 6556–6629.

Hubbe, M., Venditti, R., and Rojas, O. J. (2007). What Happens to Cellulosic Fibers During Papermaking and Recycling? A Review. *BioResources*, *2*(4), 739–788.

Hunter, B. L. (2010). *Enhancing Out-of-Season Production of Tomatoes and Lettuce Using High Tunnels*. Utah State University.

Hüttermann, A., Orikiriza, L. J. B., and Agaba, H. (2009). Application of Superabsorbent Polymers for Improving the Ecological Chemistry of Degraded or Polluted Lands. *Clean-Soil, Air, Water*, *37*(7), 517–526.

Ibrahim, M. M., Koschella, A., Kadry, G., and Heinze, T. (2013). Evaluation of Cellulose and Carboxymethyl Cellulose/Poly(Vinyl Alcohol) Membranes. *Carbohydrate Polymers*, *95*(1), 414–420.

Ji, X., Wu, R. T., Long, L., Guo, C., Khashab, N. M., Huang, F., and Sessler, J. L. (2018).

Physical Removal of Anions from Aqueous Media by Means of a Macrocycle-Containing Polymeric Network. *Journal of the American Chemical Society*, *140*(8), 2777–2780.

Joshi, M. K., Pant, H. R., Tiwari, A. P., Maharjan, B., Liao, N., Kim, H. J., Park, C. H., and Kim, C. S. (2016). Three-Dimensional Cellulose Sponge: Fabrication, Characterization, Biomimetic Mineralization, and In-vitro Cell Infiltration. *Carbohydrate Polymers*, *136*, 154–162.

Kaith, B. S., Jindal, R., Mittal, H., and Kumar, K. (2010). Temperature, pH and Electric Stimulus Responsive ydHrogels from Gum Ghatti and Polyacrylamide-Synthesis, Characterization and Swelling Studies. *Der Chemica Sinica*, *1*(2), 44–54.

Kargarzadeh, H., Ioelovich, M., Ahmad, I., Thomas, S., and Dufresne, A. (2017). Methods for Extraction of Nanocellulose from Various Sources. In *Handbook of Nanocellulose and Cellulose nanocomposites* (1st ed.). Wiley-VCH Verlag GmbH &Co. KGaA.

Katata-seru, L., Moremedi, T., Aremu, O. S., and Bahadur, I. (2017). Green Synthesis of Iron Nanoparticles Using Moringa Oleifera Extracts and their Applications: Removal of Nitrate from Water and Antibacterial Activity Against Escherichia coli. *Journal of Molecular Liquids*, *256*, 296–304.

KCDA. (2013). *Kenya Coconut Development Authority National Coconut Survey*.

Khai, D. M., Nhan, P. D., Hoanh, T. D., Academy, M. T., Giay, C., and Giay, C. (2017). An Investigation of the Structural Characteristics. *Vietnam Journal of Science and Technology*, *55*(4), 452–460.

Khalil, H. P. S. A., Alwani, M. S., and Omar, A. K. M. (2006). Chemical Composition, Anatomy, Lignin Distribution, and Cell Wall Structure of Malaysian Plant Waste Fibers. *BioResources*, *1*(2), 220–232.

Kia, L., Jawaid, M., Ariffin, H., and Alothman, O. Y. (2017). Isolation and Characterization of Microcrystalline Cellulose from Roselle Fibers. *International Journal of Biological Macromolecules*, *103*, 931–940.

Kiatkamjornwong, S. (2007). Superabsorbent Polymers and Superabsorbent Polymer

Composites. *Science Asia*, *1*(33), 39–43.

Kim, J., and Yun, S. (2006). Discovery of Cellulose as a Smart Material. *Macromolecules*, *39*(12), 4202–4206.

Kimani, P. K., Kareru, P. G., Madivoli, S. E., Kairigo, P. K., and Maina, E. G. (2016). Comparative Study of Carboxymethyl Cellulose Synthesis from Selected Kenyan Biomass. *Chemical Science International Journal*, *17*(4), 1–8.

Kocherbitov, V., Ulvenlund, S., Kober, M., Jarring, K., and Arnebran, T. (2008). Hydration of Microcrystalline Cellulose and Milled Cellulose Studied by Sorption Calorimetry. *Journal of Physical Chemistry B*, *112*(12), 3728–3734.

Kowalski, G., Kijowska, K., Witczak, M., Kuterasinski, Ł., and Łukasiewicz, M. (2019). Synthesis and Effect of Structure on Swelling Properties of Hydrogels Based on High Methylated Pectin and Acrylic Polymers. *Polymers*, *11*(114), 1–16.

Landon, J. R. (2014). *Booker Tropical Soil Manual. A Handbook for Soil Survey and Agricultural Land Evaluation in the Tropics and Subtropics*. Routledge:Taylor and Francis.

Latif, A., Anwar, T., and Farrukh, M. A. (2006). Two-Step Synthesis and Characterization of Carboxymethylcellulose from Rayon Grade Wood Pulp and Cotton Linter. *Journal of Saudi Chemical Society*, *10*(1), 95–102.

Lomelí-Ramírez, M. G., Anda, R. R., Kestur, G., Graciela, I. B. de M., and Iwakiri, S. (2018). Comparative Study of the Characteristics of Green and Brown Coconut Fibers for the Development of Green Composites. *BioResources*, *13*(1), 1637–1660.

Madeleine, C., and Ruffinegngo, E. (2013). Textiles: Stop the Chemical Overdose! *European Environment and Health Initiative*, 1–98.

Maitra, J., and Shukla, V. K. (2014). Cross-linking in Hydrogels - A Review. *American Journal of Polymer Science*, *4*(2), 25–31.

Martins, D., Ferreira, H., Leite, R., Ferreira, H., Moretti, M., Silvia, R., and Gomes, E. (2011). Agroindustrial Wastes as Substrates for Microbial Enzymes Production and Source of Sugar for Bioethanol Production. In S. Kumar (Ed.), *Integrated Waste Management, 2*, 319–36).

Massah, A. R., Mosharafian, Masumeh Momeni, A. R., Aliyan, H., and Naghash, J. (2007). Solvent-Free Williamson Synthesis: An Efficient, Simple, and Convenient Method for Chemoselective Etherification of Phenols and Bisphenols. *Synthetic Communications*, *37*(11), 1807–1815.

Mcbath, R. A., and Shipp, D. A. (2010). Swelling and Degradation of Hydrogels Synthesized with Degradable Poly(b-amino ester) Crosslinkers. *Polymer Chemistry*, *1*, 860–865.

Mcgraw, J., Mcphail, L. T., Oschipok, L. W., Horie, H., Poirier, F., Steeves, J. D., Ramer, M. S., and Tetzlaff, W. (2004). Galectin-1 in Regenerating Motoneurons. *European Journal of Neuroscience*, *20*(11), 2872–2880.

Mudgal, S., Lockwood, S., Ding, H., Velickov, S., Commandeur, T., and Siek, M. (2014). *Study on Soil and Water in a Changing Environment*.

Mukerabigwi, J. F., Lei, S., Fan, L., Wang, H., Luo, S., Ma, X., Qin, J., Huang, X., and Cao, Y. (2016). Eco-friendly Nano-Hybrid Superabsorbent Composite from Hydroxyethyl. *RSC Advances*, *6*(38), 31607–31618.

Murigi, M. K., Madivoli, E. S., Mathenyu, M. M., Kareru, P. G., Gachanja, A. N., Njenga, P. K., Nowsheen, G., Githira, P. N., and Githua, M. (2014). Comparison of Physicochemical Characteristics of Microcrystalline Cellulose from Four Abundant Kenyan Biomasses. *IOSR Journal of Polymer and Textile Engineering*, *1*(2), 53–63.

Mussatto, S. I., and Roberto, I. C. (2004). Alternatives for Detoxification of Diluted-Acid Lignocellulosic Hydrolyzates for Use in Fermentative Processes: A Review. *Bioresource Technology*, *93*(1), 1–10.

Naika, S., Jeude, J., Goffau, M. de, Hilmi, M., and Dam, B. van. (2005). *Cultivation of Tomato* (4th ed.). Wageningen:PROTA.

Nazeer, A. (2014). To Study the Mechanical Properties of Coconut Coir Fiber Reinforced with Epoxy Resin AW 106 and HV 953 IN. *International Journal of Modern Engineering Research (IJMER)*, *4*(7), 38–47.

Ng, H. M., Saidi, N., Omar, F. S., and Kasi, R. (2018). Thermogravimetric Analysis of Polymers. *Encyclopedia of Polymer Science and Technology*, 1–29.

Ogali, R. E., Akaranta, O., and Obot, I. B. (2011). Extraction and Characterization of Coconut (Cocos nucifera L.) Coir Dust. *Songklanakarin Journal Science and Technology*, *33*(6), 717–724.

Ogbuehi, H. C., Ogbonnaya, C. I., and Ezeibekwe, I. O. (2014). Study of Root Growth Parameters of Plants (Glycine Max L., Vigna Subterranea L. and Zea Mays L.) in Diesel Oil Polluted Soil. *Global Journal of Biology, Agriculture and Health*, *3*(1), 287–293.

Oh, S. Y., Yoo, I., Shin, Y., Kim, C., and Kim, Y. (2005). Crystalline Structure Analysis of Cellulose Treated with Sodium Hydroxide and Carbon Dioxide by Means of X-ray Diffraction and FTIR Spectroscopy. *Carbohydrate Research*, *340*(15), 2376–2391.

Okon, O., Eduok, U., and Israel, A. (2012). Characterization and Phytochemical Screening of Coconut (Cocos nucifera L .) Coir Dust as a Low Cost Adsorbent for Waste Water Treatment. *Elixir Applied Chemistry*, *47*, 8961–8968.

Omidian, H., Hashemi, S. A., Sammes, P. G., and Meldrum, I. G. (1998). Modified acrylic-based superabsorbent polymers. Effect of temperature and initiator concentration. *Polymer*, *39*(15), 3459–3466.

Othmani, A., Mongi, M., Rezgui, M., Cherif, S., and Mouelhi, M. (2015). Effects of Water Regimes on Root and Shoot Growth Parameters and Agronomic Traits of Tunisian Durum Wheat (Triticum durumDesf.). *Journal of New Sciences*, *18*(7), 695–792.

Pearson, C., Cornish, K., Mcmahan, C., Whalen, M., Rath, D. J., Dong, N., and Wong, S. (2007). Using Peat Pellets in Liquid Media to Root Sunflower Tissue Culture Plants. *Proceedings Assoc for Advancement of Industrial Crops (AAIC) Annual Meeting*, 78–81.

Poletto, M., Heitor, O. J., and Zattera, A. J. (2014). Native Cellulose: Structure, Characterization and Thermal Properties. *Materials*, *7*(9), 6105–6119.

Ponce, C., Chanona, J., Garibay, V., Palacios, E., Calderon, G., and Sabo, R. (2013). Functionalization of Agave Cellulose Nanoparticles and its Characterization by Microscopy and Spectroscopy Techniques. *Microscopy and Microanalysis*, *19*(S2),

200–201.

Prasad, R. (2019). *Phosphorus Basic: Understanding Phosphorus Forms and their Cycling in the Soil*.

Qi, X., Chu, J., Jia, L., and Kumar, A. (2019). Influence of Different Pretreatments on the Structure and Hydrolysis Behavior of Bamboo: A Comparative study. *Materials*, *12*(16), 1–14.

Ramos, E., Calatrava, S. F., and Jimenez, L. (2008). Bleaching with Hydrogen Peroxide. A Review. *Afinidad*, *65*(537), 366–373.

Rosa, S. M. L., Rehman, N., Miranda, M. I. G. De, Nachtigall, S. M. B., and Bica, C. I. D. (2012). Chlorine-Free Extraction of Cellulose from Rice Husk and Whisker Isolation. *Carbohydrate Polymers*, *87*(2), 1131–1138.

Saini, K. (2017). Preparation Method, Properties and Crosslinking of Hydrogel: A Review. *Pharma Tutor*, *5*(1), 27–36.

Salve, A., Bhardwaj, D., and Tahkur, C. (2018). Soil Nutrient Study in Different Agroforestry Systems in North Western Himalayas. *Bulletin of Environment Pharmacology and Life Science*, *7*(2), 63–72.

Sannino, A., Demitri, C., and Madaghiele, M. (2009). Biodegradable Cellulose-Based Hydrogels: Design and Applications: Review. *Materials*, *2*(2), 353–373.

Sannino, A., Esposito, A., De Rosa, A., Cozzolino, A., Ambrosio, L., and Nicolais, L. (2003). Biomedical Application of a Superabsorbent Hydrogel for Body Water Elimination in the Treatment of Edemas. *Journal of Biomedical Materials Research*, *67*(3), 1016–1024.

Sannino, A., Esposito, A., Nicolais, L., Del Nobile, M. A., Giovane, A., Balestrieri, C., Esposito, R., and Agresti, M. (2000). Cellulose-Based Hydrogels as Body Water Retainers. *Journal of Materials Science: Materials in Medicine*, *11*(4), 247–253.

Seki, Y., Altinisik, A., Demircioglu, B., and Tetik, C. (2014). Carboxymethylcellulose (CMC)– Hydroxyethylcellulose (HEC) Based Hydrogels: Synthesis and Characterization. *Cellulose*, *21*(3), 1689–1698.

Sen, T., and Reddy, H. N. J. (2011). Application of Sisal, Bamboo, Coir and Jute Natural

Composites in Structural Upgradation. *International Journal of Innovation, Management and Technology*, *2*(3), 186–191.

Sethi, S., Kaith, B. S., and Kumar, V. (2019). Fabrication and Characterization of Microwave Assisted Carboxymethyl Cellulose-Gelatin Silver Nanoparticles Imbibed Hydrogel: Its Evaluation as Dye Degradation. *Reactive and Functional Polymers*, *142*, 134–146.

Shen, T., and Gnanakaran, S. (2009). The Stability of Cellulose: A Statistical Perspective from a Coarse-Grained Model of Hydrogen-Bond Networks. *Biophysical Journal*, *96*(8), 3032–3040.

Shogren, R. L., Peterson, S. C., Evans, K. O., and Kenar, J. A. (2011). Preparation and Characterization of Cellulose Gels from Corn Cobs. *Carbohydrate Polymers*, *86*(3), 1351–1357.

Shokri, J., and Adibkia, K. (2013). Application of Cellulose and Cellulose Derivatives in Pharmaceutical Industries. *Licensee InTech*, 1–20.

Sikdar, P., Uddin, M., Dip, T., Islam, S., Hoque, S., Dhar, A., and Wu, S. (2021). Materials Advances Recent Advances in the Synthesis of Smart Hydrogels. *Materials Advances*, *2*, 4532–4573.

Simončič, B., and Rozman, V. (2007). Wettability of Cotton Fabric by Aqueous Solutions of Surfactants with Different Structures. *Colloids and Surfaces A: Physicochemical and Engineering Aspects*, *292*(2–3), 236–245.

Singanusong, R., Tochampa, W., and Kongbangkerd, T. (2014). Extraction and Properties of Cellulose from Banana Peels. *Suranaree Journal of Science and Technology*, *21*(3), 201–213.

Strunk, P. (2012). *Characterization of Cellulose Pulps and the Influence of their Properties on the Process and Production of Viscose and Cellulose Ethers*. Umeå University, Sweden.

Su, W., Wang, R., Qian, C., Li, X., Tong, Q., and Jiao, T. (2020). Research Progress Review of Preparation and Applications of Fluorescent Hydrogels. *Journal of Chemistry*, *2020*(8246429), 1–17.

Takase, M., Owusu-Sekyere, J. D., and Sam-Amoah, L. K. (2010). Effects of Water of Different Quality on Tomato Growth and Development. *Asian Journal of Plant Science*, *9*(6), 380–384.

Tamura, G., Shinohara, Y., Tamura, A., Sanada, Y., Oishi, M., Akiba, I., Nagasaki, Y., Sakurai, K., and Amemiya, Y. (2012). Dependence of the Swelling Behavior of a pH-Responsive PEG-Modified Nanogel on the Cross-link Density. *Polymer Journal*, *44*, 240–244.

Tooy, D., Nelwan, L., and Pangkerego, F. (2014). Evaluation of Biomass Gasification Using Coconut Husks in Producing Energy to Generate Small-Scale Electricity. *International Conference on Artificial Intelligence, Energy and Manufacturing Engineering*, 87–91.

UNEP. (2009). *Converting Waste Agricultural Biomass into a Resource*.

United States Department of Agriculture. (2014). *Inherent Factors Affecting Soil EC*. Retrieved from https://www.nrcs.usda.gov › FSE_DOCUMENTS

Verma, D., Gope, P. C., Shandilya, A., Gupta, A., and Maheshwari, M. K. (2013). Coir Fibre Reinforcement and Application in Polymer Composites: A Review. *Journal of Materials and Environmental Science*, *4*(2), 263–276.

Vitta, S. B., Stahel, E. P., and Stannett, V. T. (1989). The Preparation and Properties of Acrylic and Methacrylic Acid Grafted Cellulose Prepared by Ceric Ion Initiation. III. Some Physical, Mechanical, and Ion Exchange Properties. *Journal of Applied Polymer Science*, *38*(3), 503–510.

Waifielate, A. A., and Abiola, B. O. (2008). *Mechanical Property Evaluation of Coconut Fibre*. Blekinge Institute of Technology, Karlskrona, Sweden.

Wei, J., Du, C., Liu, H., Chen, Y., Yu, H., and Zhou, Z. (2016). Preparation and Characterization of Aldehyde- Functionalized Cellulosic Fibers through Periodate Oxidization of Bamboo Pulp. *BioResources*, *11*(4), 8386–8395.

Wen, X., Bao, D., Chen, M., Zhang, A., Liu, C., and Sun, R. (2015). Preparation of CMC/HEC Crosslinked Hydrogels for Drug Delivery. *BioResources*, *10*(4), 8339–8351.

Yang, H., Yan, R., Chen, H., Lee, H. D., and Zheng, C. (2007). Characteristics of Hemicellulose, Cellulose and Lignin Pyrolysis. *Elsevier Limited*, *86*(12–13), 1781–1788.

Yang, M., Wu, J., Graham, G. M., Lin, J., and Huang, M. (2021). Hotspots, Frontiers, and Emerging Trends of Superabsorbent Polymer Research: A Comprehensive Review. *Frontiers in Chemistry*, *9*(688127), 1–18.

Yeng, L., Wahit, M. U., and Othman, N. (2015). Thermal and Flexural Properties of Regenerated Cellulose (Rc)/Poly(3-Hydroxybutyrate) (PHB) Biocomposites. *Jurnal Teknologi*, *75*(11), 107–112.

Yimer, S. M., and Chimdi, A. (2019). Soil Quality Analysis for Sustainability of Forest Ecosystem: The Case of Soil Quality Analysis for Sustainability of Forest Ecosystem: The Case of Chilimo-Gaji Forest, West Shewa Zone, Ethiopia. *Journal of Environmental and Earth Science*, *9*(3), 1–9.

Zhang, Q.-W., Lin, L.-G., and Ye, W.-C. (2018). Techniques for Extraction and Isolation of Natural Products: A Comprehensive Review. *Chinese Medicine*, *13*(20), 1–26.

Zhou, J., Chang, C., Zhang, R., and Zhang, L. (2007). Hydrogels Prepared from Unsubstituted Cellulose in NaOH/Urea Aqueous Solution. *Macromolecular Bioscience*, *7*(6), 804–809.

Zimmermann, M., de Macedo, V., Zattera, A. J., and Santana, R. M. C. (2016). Influence of Chemical Treatments on Cellulose Fibers for Use as Reinforcements in Poly(Ethylene-co-vinyl Acetate) Composites. *Polymer Composites*, *37*(7), 10–13.

Zohuriaan-mehr, M., and Kabiri, K. (2008). Superabsorbent Polymer Materials: A Review. *Iranian Polymer Journal*, *17*(6), 451–477.

APPENDICES

Appendix I: TCI, LOI, and HBI for cellulose, treated fibers (TCF), and untreated fibers (UCF)

Sample	TCI H1371/H2900	LOI A1429/A890	HBI A3400/A1320
UCF	0.46±0.02	2.25±0.01	1.35±0.01
TCF	0.17±0.03	1.93±0.01	1.10±0.02
Cellulose	0.35±0.01	3.32±0.02	1.52±0.02

Appendix II: Peak area and temperature maximum for DTGA curves for the synthesized hydrogels

Hydrogel	Peak$_1$ Area %	Peak$_2$ Area %	Peak$_3$ Area %	Temp. max (T_m)
2.75% CA	7.10	84.42	-	300°C
3.75% CA	5.88	90.78	-	293°C
5.00% CA	7.10	84.42	-	300°C
10.00% CA	4.61	7.42	84	300°C
20.00% CA	4.61	7.42	84	300°C

Appendix III: Tomato plant height P-value variation for different water regimes

	df	SS	MS	F	P-value	F crit
Water Regime	2	7292	3646	19.57	5.3E-09	3.321403
Residuals	717	133578	186			
Total	719	140870				

Appendix IV: Tomato plant height P-value variation for different hydrogel modified soil

	df	*SS*	*MS*	*F*	*P-value*	*F crit*
Soil Media	4	2864	716	3.709	0.00535	3.867522
Residuals	715	138007	193			
Total	719	140871				

Appendix V: Tomato plant leaf length P-value variation for different water regimes

	df	*SS*	*MS*	*F*	*P-value*	*F crit*
Water Regime	2	34	17.17	1.152	0.317	3.321403
Residuals	717	10686	14.90			
Total	719	10720				

Appendix VI: Tomato plant leaf length P-value variation for different hydrogel modified soil

	df	*SS*	*MS*	*F*	*P-value*	*F crit*
Soil Media	4	1057	264.31	19.56	2.75E-15	3.867522
Residuals	715	9664	13.52			
Total	719	10721				

Appendix VII: Number of leaves of tomato plant P-value variation for different water regimes

	df	*SS*	*MS*	*F*	*P-value*	*F crit*
Water Regime	2	55	27.53	0.747	0.474	3.321403
Residuals	717	26425	36.85			
Total	719	26480				

Appendix VIII: Number of leaves of tomato plant P-value variation for different hydrogel modified soil

	df	SS	MS	F	P-value	F crit
Soil Media	4	267	66.73	1.82	0.123	3.867522
Residuals	715	26213	36.66			
Total	719	10721				

Appendix IX: Number of branches of tomato plant P-value variation for different water regimes

	df	SS	MS	F	P-value	F crit
Water Regime	2	6.2	3.0889	3.363	0.0352	3.321403
Residuals	717	658.6	0.9185			
Total	719	664.8				

Appendix X: Number of branches of tomato plant P-value variation for different hydrogel modified soil

	df	SS	MS	F	P-value	F crit
Soil Media	4	11.7	2.9361	3.215	0.0125	3.867522
Residuals	715	653.0	0.9133			
Total	719	664.7				

Appendix XI: Tomato plant root score P-value variation for different water regimes

	df	SS	MS	F	P-value	F crit
Water Regime	2	17.2	8.600	4.481	0.0156	3.403189
Residuals	57	109.4	1.919			
Total	59	126.6				

Appendix XII: Tomato plant root score P-value variation for different hydrogel modified soil

	df	SS	MS	F	P-value	F crit
Soil Media	4	20.93	5.233	2.724	0.0385	3.988545
Residuals	55	105.67	1.921			
Total	59	12.6				

Appendix XIII: Tomato plant root to shoot ratio mass P-value variation for different water regimes

Source of Variation	SS	df	MS	F	P-value	F crit
Water Regime	0.006964	2	0.003482	3.9292	0.0487	3.8853
Residuals	0.010634	12	0.000886			
Total	0.017597	14				

Appendix XIV: Tomato plant root to shoot ratio mass P-value variation for different hydrogel modified soil

Source of Variation	SS	df	MS	F	P-value	F crit
Soil Media	0.007629	4	0.001907	1.913	0.1843	3.47805
Residuals	0.009968	10	0.000997			
Total	0.017597	14				

Appendix XV: Tomato plant moisture mass P-value variation for different water regimes

	df	SS	MS	F	P-value	F crit
Water Regime	2	2975	1487.3	16.37	2.41E-06	3.403189
Residuals	57	5179	90.9			
Total	59	8154				

Appendix XVI: Tomato plant moisture mass P-value variation for different hydrogel modified soil

	df	SS	MS	F	P-value	F crit
Soil Media	4	2867	716.7	7.456	7.14E-05	3.988545
Residuals	55	5287	96.1			
Total	59	8154				

Appendix XVII: The significant difference (shown as letters) and mean of the different tomato plant growth parameters for the different hydrogel modified soil

Source of Variation (Soil Media)	Mean Height	Mean Length of Leaves	Mean No. of Branches	Mean Root Score	Mean Root/Shoot Ratio	Mean Plant Moisture
Soil & Hydrogel 1%	26.26 ab	11.83 b	0.92 ab	3.17 ab	0.25 b	36.67 b
Soil & Hydrogel 2%	30.44 a	14.59 a	0.85 ab	4.33 a	0.31 a	48.51 a
Control	24.46 b	11.42 b	1.09 a	2.50 b	0.25 b	26.98 b
Soil & Hydrogel 1% + CMC 1%	25.91 b	11.26 b	0.92 ab	3.17 ab	0.26 ab	37.84 ab
Soil & CMC 1%	27.07 ab	12.23 b	0.69 b	3.33 ab	0.24 b	34.73 b

Treatments with the same letter are not significantly different.

Appendix XVIII: The significant difference (as letters) and mean (as digits) of the different tomato plant growth parameters for the different water regimes

Source of Variation (Water regime)	Mean Height	Mean Number of Branches	Mean Plant Moisture	Mean Root/Shoot Ratio
After 2 days	29.32 a	0.80 b	45.90 a	0.29 a
Twice a week	28.83 a	0.85 ab	36.25 b	0.24 b
Once a week	22.34 b	1.02 a	28.69 c	0.25 ab

Treatments with the same letter are not significantly different.

Appendix XIX: Greenhouse field design setup based on the water and modified soil media

|	**Water Regime**		Front View				
Side View	x	1	A1	C1	B1	E1	D1
		2	C2	E2	D2	A2	B2
	y	1	A1	C1	D1	B1	E1
		2	C2	D2	B2	E2	A2
	z	1	C1	B1	A1	D1	E1
		2	D2	A2	C2	E2	B2
			Back View				Wall

Where media A, B, C, D, and E represent hydrogel 1%, hydrogel 2%, control, CMC 1% + hydrogel 1% and CMC 1% soil media respectively. The water regimes are as follows twice a week (x), after two days (y) and once a week water regime (z).

Appendix XX: Tomato plant growth performance in hydrogel modified soil observed from side view at different and weeks for different water regimes

Week 1 Side view

Week 4 side view

Week 6 side view

Week 8 side view
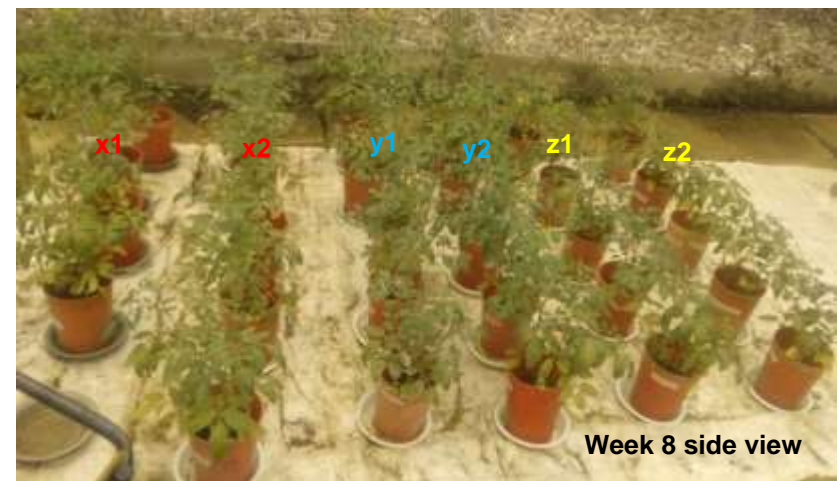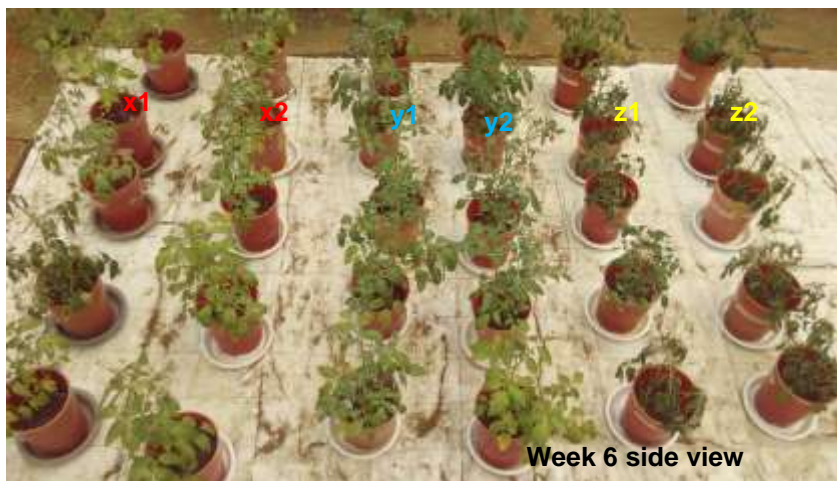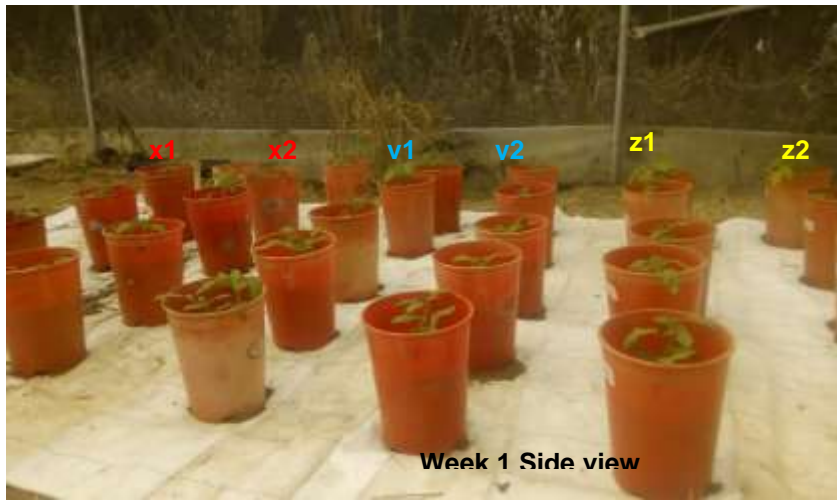
Appendix XXI: Tomato plant growth performance in hydrogel modified soil observed from back view at different weeks for different water regimes
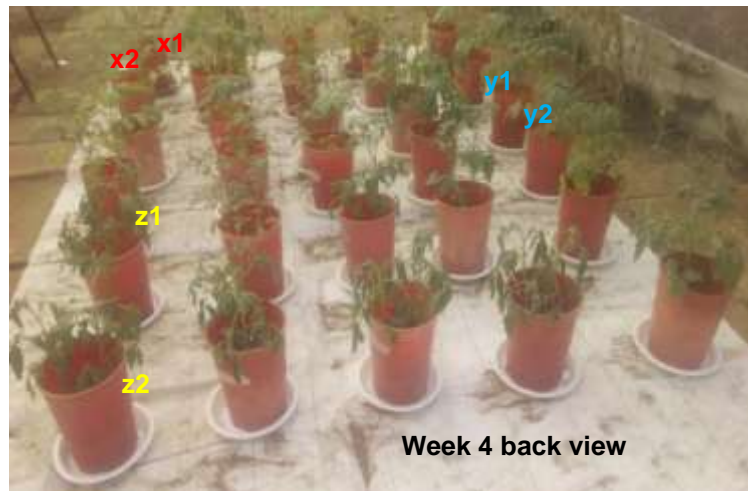
Appendix XXII: Publication

Journal of Natural Fibers

Characteristics of Microcrystalline Cellulose from Coir Fibers

Joyline Gichuki[a], Patrick Gachoki Kareru[a], Anthony Ngure Gachanja[a], and Catherine Ngamau[b]

[a]*Chemistry Department, Jomo Kenyatta University of Agriculture and Technology, Nairobi, Kenya;*

[b]*Horticulture and Food Security Department, Jomo, Kenyatta University of Agriculture and Technology, Nairobi, Kenya.*

ABSTRACT

This work aimed to extract and characterize microcrystalline cellulose from coir fibers. Extraction was achieved in a two-step process in which the coir fibers were treated with sodium hydroxide for 3 h at 100°C followed by bleaching with peracetic acid to remove residual lignin and hemicellulose. The microcrystalline cellulose powder characteristics such as the bulk density, tapped density, angle of repose and swelling ratio were found to be 0.08 ± 0.00 g/cm^3, 0.12 ± 0.0 g/cm^3, 38° and 8.15 ± 0.14 g/g, respectively. Fourier transform infrared spectroscopy exhibited characteristic microcrystalline cellulose peaks. The degree of crystallinity microcrystalline cellulose was found to be 39.5% as determined by X-ray diffraction analysis. The Differential scanning calorimetry and Thermogravimetric analysis revealed that the glass transition and onset of degradation temperature for microcrystalline cellulose were 206°C and 196°C, respectively. From the results, it was concluded that the coir fibers could be a good source of microcrystalline cellulose for applications in the binder, pharmaceutical, and paper making industries due to its powder properties, good swelling, and compressibility.